Royal Netherlands
Meteorological Institute
Ministry of Infrastructure and the Environment

On future Western European winters with applications to the energy sector

Hylke de Vries

De Bilt, 2012 | KNMI-publication 231

On future Western European winters with applications to the energy sector

Version 1.0

Date December 5, 2012
Status Final

ON FUTURE WESTERN EUROPEAN WINTERS

with applications to the energy sector

Hylke de Vries, Koninklijk Nederlands Meteorologisch Instituut
KNMI, POBOX 201, 3730 AE de Bilt, Nederland. **Version: December 5, 2012**

Contents

Executive Summary

This report summarizes research conducted at KNMI on request of GasTerra and NAM, to the future changes of western European winter temperatures and their relation to atmospheric blocking. It analyzes possible future changes and uncertainties of winter ***heating degreedays***, a key parameter in the gas and energy sector. A detailed comparison with the KNMI'06 scenarios is performed. Also discussed are the future changes of ***cold spells*** and the relation with ***atmospheric blocking***.

Data Two data sources have been used. Reanalysis data is used for the current climate. In a reanalysis, observations have been made consistent using a state-of-the art weather prediction model. For the future climate, global climate simulations are used from various climate centers. Climate models have insufficient resolution to reproduce weather exactly, yet are able to capture the historic mean state, its recent trend and the statistics of their fluctuations. Beyond the year 2000, additional external forcing is imposed, to simulate the future state. Note that the temperature response is not imposed, but generated internally by the climate model.

Uncertainties Three reasons can be given why not just one future state is generated by the climate models, but a range of possible future states. First of all, the external forcing is varied along different "Representative Concentration Pathways" (RCPs). Secondly, especially at short lead times, natural variability (i.e., the fluctuations generated by the internal dynamics) is important. Finally, different climate models respond differently to the same external forcing.

Scenarios Every few years KNMI issues climate scenarios for the Netherlands. These scenarios describe a range of possible future climates. No probabilities are assigned to them, but they are chosen to broadly cover the spread of the future climate projections in two key parameters for the Netherlands (temperature and circulation). Scenarios are meant to inform users and can be used to test robustness of adaptation measures. The upcoming scenarios (KNMI-next, autumn 2013) will be based on data used in the next IPCC report (IPCC-AR5).

Heating degreedays in winter will decrease in the Netherlands by 20% [10-30%] during the 21st century, thereby ranking current-climate "normal" winters among the "coldest" near the end of the century. The projected change for "cold" and "mild" winters (the 10% coldest and warmest respectively) is also on the order of 20% [10-30%], implying a stronger absolute reduction for the "cold" winters. The same reductions (20% [10-30%]) are found for a large part of Europe. The most important changes of the distribution are the reductions of the mean and the variability. Both factors reduce the frequency of very cold winters. The KNMI'06 scenarios cover $\sim$70% of the ensemble spread, and the W-scenario closely approximates the multi-model mean. The upcoming KNMI-next scenarios will cover more of the ensemble spread and may shift slightly towards a stronger future reduction. However, since no major changes in heating degreedays (compared to KNMI'06) are expected, there is presently no need for reconsidering the Wever (2008) report and its conclusions, although an update is recommended for the longer term (5 year).

Cold spells are periods in which the temperature stays below a certain threshold. They are strongly affected by climate change, because in addition to the projected increase of mean winter temperature, the variability decreases. Thus, the chances on cold spells reduce more strongly than expected on the base of a change of the winter mean temperature only (de Vries et al, 2012b). For cold spells that reach the 10% level (10 days per winter), future projections show that their minimum temperature may increase by 2°C in 2040 and by more than 4°C at the end of the 21st century. The average return time for a cold spell of ten days may increase by a factor 3-4 by 2040. Similar increases in return times are found for the annual minimum temperature. These quantitative results were shown for one climate model with a 'business as usual' emission scenario. While these results are qualitatively robust across models there is considerable uncertainty in the absolute changes.

Atmospheric blocking is a temporal interruption of the otherwise prevailing westerly circulation. Persistent atmospheric blocking increases the probability for having at least 5 cold days (10% coldest) in the Netherlands by a factor 75-150 compared to the random probability for such an event. However, the overall probability remains relatively low for the Netherlands (around 30-40%), indicating that even persistent blocking is not always associated with a series of cold days. Nevertheless, the mean circulation structure associated with cold days clearly resembles that of a blocking condition (easterly winds, high pressure above Scandinavia), and about 60-80% of the very cold days (1% coldest) in the Netherlands, nearby blocking is diagnosed. Thus cold days are a better predictor for blocking than blocking is for cold days. This holds for a large part of Europe.

An extended table of contents containing a summary of all major results is given on the following pages. Final remarks and recommendations can be found on page 40.

Extended contents

Chapter 1

Introduction

1.1 About this report

This report describes the main findings of the GasTerra/NAM/KNMI-project "Future changes of western European winter temperatures and the relation to atmospheric blocking". The report contains an introduction and three main parts. Each section examines a specific question or topic, and is started with a brief summary of the main conclusion. These conclusions are restated in the extended table of contents. Appendices have been added with further details on data, variables and methodology, as well as reprinted sections from several publications

1.2 Linking cold winter weather and atmospheric blocking

In the northern hemisphere, winds on average come from the west. These Westerlies are a direct consequence of fundamental physical balances. The large heat capacity of the ocean implies that south-westerly flow produces relatively warm weather in the winter, and that reversed wind conditions are necessary to produce low temperatures. Persistent reversed-wind conditions are referred as atmospheric "blocking"

At the mid-latitudes, the climatologically prevailing winds come from the West (called *Westerlies*). These Westerlies are a direct consequence of the fundamental balances that exist in the atmosphere-ocean system. Figure 1.1 shows the winter climatology of mean sea-level pressure and wind at 10m for the Euro-Atlantic region. There is a large-scale pressure pattern with low pressures in the North and high pressures near the Azores. The resulting winds are a consequence of on the one hand the tendency of the air to flow from high to low pressures and on the other hand the rotation of the Earth. The westerlies are responsible for transporting moist, relatively mild air towards Western Europe. As said above, the Westerlies are caused by fundamental physical balances. However, these balances do not prohibit the formation of large-scale temporal disturbances (referred to as 'anomalies'). These large-scale anomalies of the Westerly circulation are of vital importance to the atmosphere, as they (together with the Ocean

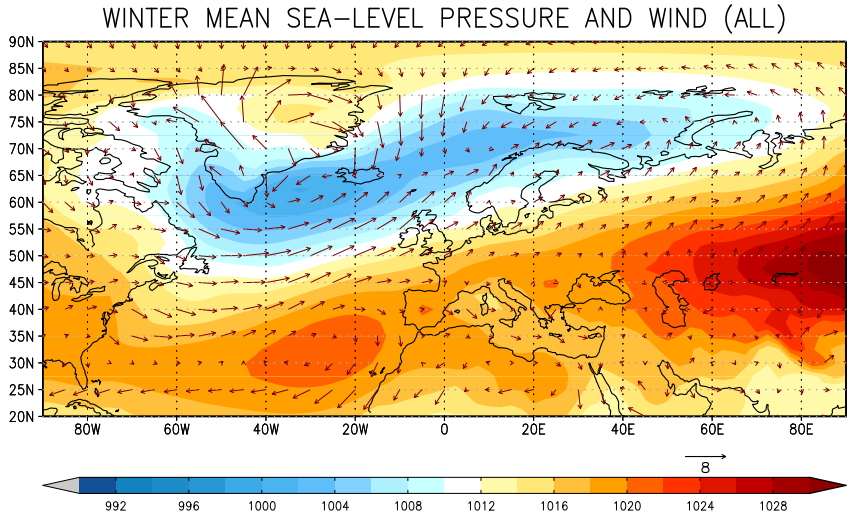

Figure 1.1: Mean sea-level pressure (shading, high pressure red, low pressure blue), and 10M wind (arrows) for the winter (October to March) climatology of ERA-40 reanalysis.

currents) play a crucial role in maintaining the net poleward heat transport. They are constantly being created and destroyed by a process called baroclinic instability (Holton, 1979; de Vries, 2007). Without such anomalies, the equator would get warmer and warmer, whereas the poles would get colder and colder.

Analyzed in terms of the mean sea-level pressure field, the anomalies take the form of so-called cyclones or storms (large-scale low-pressure systems), and anti-cyclones (high-pressure systems). The wind fields associated with such cyclones and anti-cyclones follow simple rules: counter-clockwise around a low-pressure system, and clockwise around a high-pressure system. It immediately follows from these rules that a high-pressure system to the North of the Netherlands will result in reduced, or even reversed Westerlies. In this sense, the high-pressure anti-cyclone leads to a 'blocking' of the climatologically prevailing Westerlies (Rex, 1950).

Relating temperatures to circulation

There is a strong link between (anomalous) circulation patterns and (anomalous) temperature distributions. Due to the lack of sunshine, the Northern Hemisphere (NH) cools significantly during the winter season. Since seas and oceans have a large heat capacity or 'memory' (they store a lot of heat inside their volume), it takes a long time to cool them. The land, on the other hand, has much shorter 'memory' and cools more rapidly. Therefore persistent easterlies will lead to colder than usual conditions in winter and warmer than usual conditions in summer. The large heat capacity of the sea also explains why in coastal regions of Western Europe the second half of the climatological winter is markedly colder than the first half.

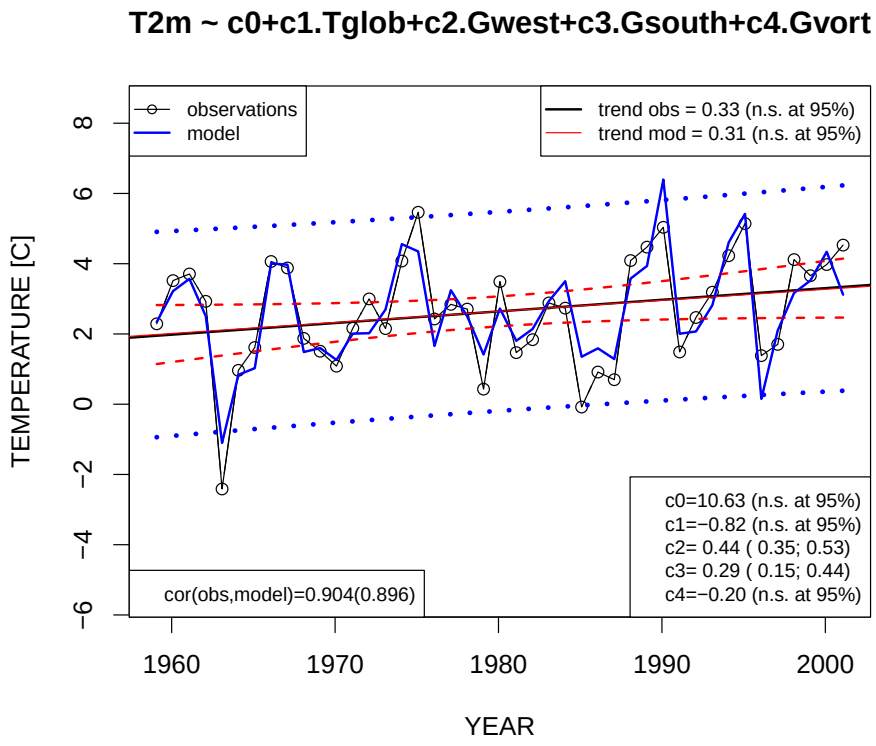

Figure 1.2: Multiple linear regression model of ERA40 (a) winter mean temperature; (b) monthly mean temperature. The components involved in the linear model are indicated. The dots denote observations (i.e. winter mean temperatures) and the lines indicate the fitted linear statistical model. There is a high correlation of 0.9. The trend is not significant at the 95% confidence level. For monthly data, the correlation reduces to 0.8.

The strong connection between circulation and associated temperature becomes most clear, if one tries to derive the observed temperature from the observed circulation. This can be done for instance by creating a multiple linear regression model for winter temperature. Figure 1.2 shows the result for the winter temperature in the Netherlands, obtained from ERA-40 reanalysis data (pseudo-observations, see Appendix A (p42)). The multiple linear regression model has the following components: global temperature, large-scale westerly wind, large-scale southerly wind, large-scale vorticty (whether a low or a high pressure field is nearby). The black line shows the observations, the blue line the fitted linear model. Trends have also been plotted for the two series (nearly identical), as well as uncertainty ranges for the linear model when it is used to predict the temperature ranges. Generally the statistical model and the observations agree well, and the correlation between the time-series is about 0.9. This correlation however strongly reduces (to 0.56) if one excludes the large-scale westerly wind component (Gwest) from the linear regression model. Extreme cold winter invariably have reduced westerly winds (Blocking situations), and ignoring

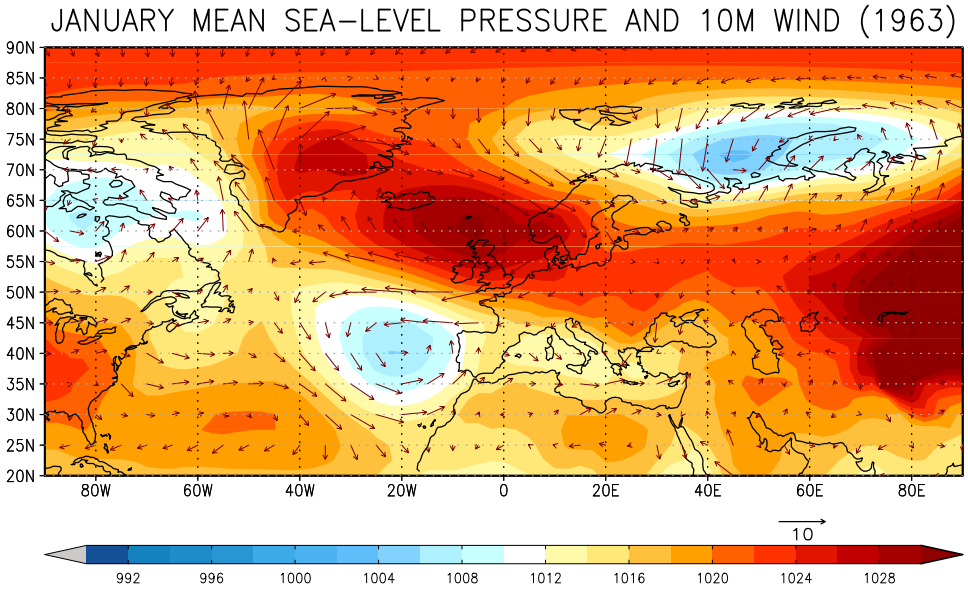

Figure 1.3: Mean sea-level pressure and 10M wind for January 1963.

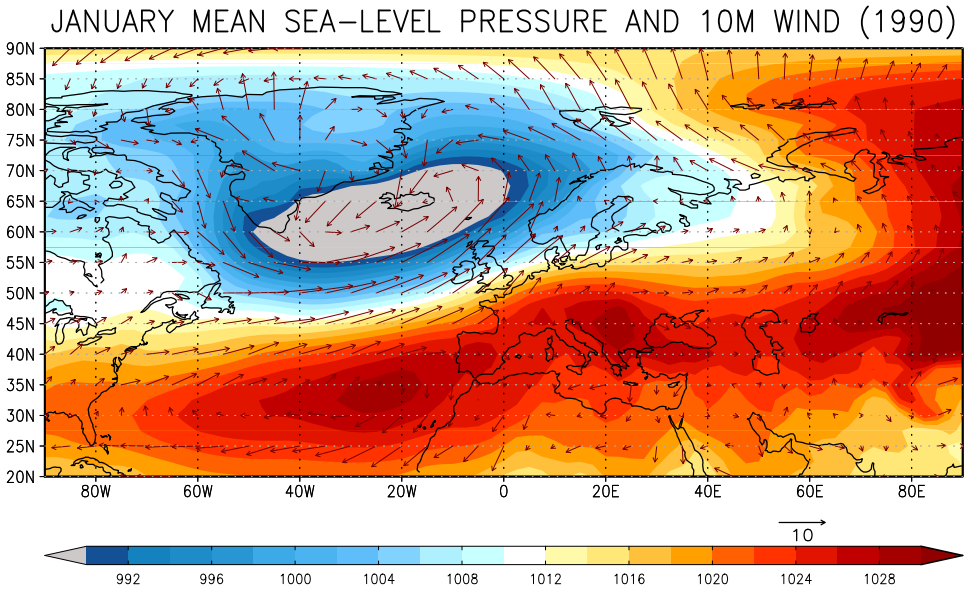

Figure 1.4: Mean sea-level pressure and 10M wind for January 1990.

this leaves out an important component. The southerly wind and vorticity contribute only slightly (without these two but with Tglob and Gwest included, the correlation remains high (0.85) for winter-mean temperature). Leaving out all circulation components (and only keep global temperature) leads to a decrease of the correlation over the historic period to near 0. Global mean temperature becomes only important for longer time series, when the trend becomes important.

Anomalous conditions

Two striking examples of how altered flow conditions influence the temperature are shown in Figure 1.3 and 1.4. These figures show the average mean sea-level pressure and 10m winds for January 1963 and 1990 respectively, which were respectively the coldest and warmest winters of the 1960-2000 period. Focusing on the January 1963 case, there are high pressures in the North and low pressures in the South. Contrast this flow state to January of the record mild winter 1990. In 1990 the Westerlies were (much) stronger than usual in our region, because the

North-South pressure differences are much stronger than those obtained for the climatology.

Although the above rationale is intuitively clear, on shorter time-scales reality is more complicated. Indeed, a high-pressure system over Northern Europe will set up a transport of air that originates in (cold) Siberia and hence will lead to colder than usual (climatological) conditions over Netherlands and Western Europe. Similarly, a large-scale cyclone (low-pressure system) at a similar location will lead to milder than usual conditions due to the transport of air that originated over the warm Atlantic. However, whether or not such a blocking anti-cyclone or cyclone (i.e., the anomaly) will lead to conditions that are significantly colder or warmer respectively, depends on more details of the meteorological conditions. Particularly important are the temperature patterns, that existed prior to the formation of the anomaly, and the duration or persistence (and near stationarity) of the anomalous flow conditions.

1.3 KNMI climate scenarios and climate model output

KNMI climate scenarios are consistent and plausible pictures of the future climate of the Netherlands. No probabilities are assigned to them. The scenarios that are currently being developed (KNMI-next) are based on data that will also be used in the next IPCC report (IPCC-AR5). The climate models that have generated this data were forced along different "Representative Concentration Pathways" (RCPs)

KNMI'06 scenarios

Every few years KNMI develops climate scenarios[1] for the Netherlands (van den Hurk et al, 2006; Klein Tank and Lenderink, 2009). Climate scenarios are consistent and plausible pictures of the future climate of the Netherlands. They have been realized using a combination of observations, and output from regional and global climate models. They provide information for vulnerability studies and adaptation planning.

Parameters that influence climate in the Netherlands the most, are temperature and circulation. Changes in just these two parameters only, lead to a two-dimensional space of all future climatic states in the Netherlands. The most recent scenarios (KNMI'06) are based on considering changes in these two steering variables, and their subsequent impact on other parameters like precipitation and wind. For temperature they consist of a mild (+1 degree) or

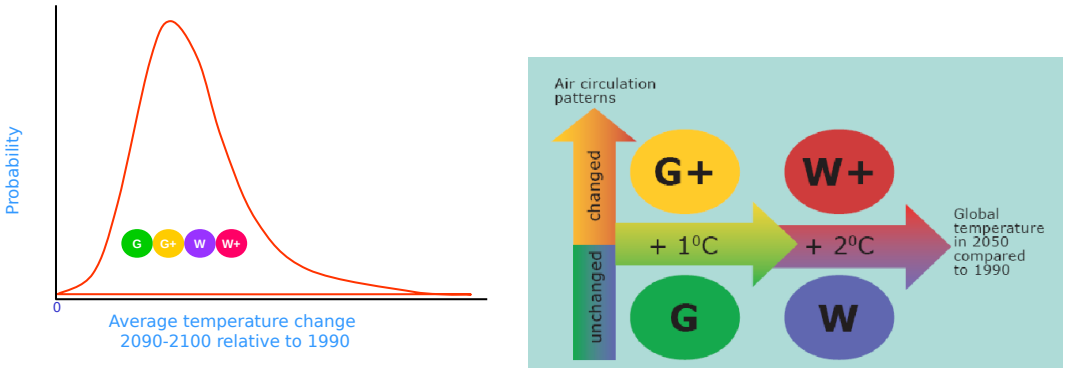

Figure 1.5: Schematic of the four KNMI'06 scenarios.

stronger (+2 degree) temperature increase (in 2050 compared to 1990), as graphically illustrated in Fig. 1.5. For circulation they consist of "no-change" or "change". An assumption in the scenarios is that regional (i.e., within the Netherlands) climatic differences in the future will be comparable to those differences in current climate. The left panel describes a cartoon of the relation between the four scenarios and the range of possible future temperature changes as simulated with global climate models around the world. The scenarios describe only four snapshots, and no intrinsic probability can be assigned to them.

[1] See `http://www.knmi.nl/klimaatscenarios/` for more information, and `http://climexp.knmi.nl/Scenarios_monthly/` for generating monthly timeseries.

Uncertainties

When global climate models are run forward in time to obtain information over the future climate, they depend on estimations of (rates of) greenhouse gas emissions and aerosols. These estimates in turn depend on hypotheses about the future development of world population, economy and technological development. In the 2007 report of the Intergovernmental Panel on Climate Change (IPCC-AR4, `http://www.ipcc.ch/`), different emission-scenarios are investigated. These lead to a predicted increase of global mean temperature in 2100 between 1 and 6 degrees Celsius by 2100. In order to sample the uncertainty as accurately as possible, many different climate models have been run assuming the same emission scenario. Up to 2050 the inter-model differences (with regard to e.g. global mean temperature) mostly exceed the predicted change resulting from the differences in the emission-scenarios. This emphasizes that the largest part of the uncertainty in 2050 still results from our limited understanding of the climate system. The KNMI'06 scenarios can not be mapped one to one to these IPCC emission-scenarios (Klein Tank and Lenderink, 2009) since the former were not based on the emission-scenarios, but on the changes in the global mean temperature. Therefore the global mean temperature provides an indirect link. For the period up to 2050, each of the four KNMI '06 scenarios can occur for each of the emission scenarios (Klein Tank and Lenderink, 2009).

Local differences

It is important to realize that an increase of global mean surface temperature of say one degree Celsius, does not imply that the temperature is increased uniformly and everywhere with one degree. There will be large geographical differences. Seas, for instance, will heat only very slowly, while the continents heat much faster. Poles are expected to heat faster than other regions. The geographical changes in the heat distribution will further impact on the circulation, which may in turn lead to changes in local processes. Following the KNMI'06 scenarios the winters in the Netherlands will get milder and wetter, although no major changes in the wind-climate (i.e. number of storms per winter) are expected.

KNMI-next scenarios

The next scenarios are expected to be published in 2013. The date of this publication is chosen such that it falls right after the publication of the next IPCC Assessment Report (IPCC-AR5). These KNMI-next scenarios will update the current KNMI'06 scenarios, and will be delivered in the form of a scientific report, a brochure and a website (and additionally, several scientific papers). Consistent with KNMI'06, the scenarios will take the form of a discrete matrix of possible future states, which, together, describe the bandwidth of likely future climates. This bandwidth is mainly provided by the range of climate model responses to external forcing in the Climate Model Intercomparison Project (CMIP5, `http://cmip-pcmdi-llnl.giv/cmip5/`). First analysis of the CMIP5 results, indicate that there is no need to changes the KNMI'06 approach drastically. The steering variables in KNMI-next will again be expressions of projected changes in the global mean temperature and the large-scale atmospheric circulation. However, their exact definition will differ from KNMI'06, in an attempt to optimize the explained local climate variability. Two further potentially relevant aspects are:

- Observations suggest that the Netherlands and surrounding countries are warming faster than expected from most climate model simulations (van Oldenborgh et al, 2009). Although the likely physical causes for the differences have been identified, the mechanisms underlying the changes are not fully understood. Observations like the ones above may indicate that the lowest temperature scenarios of CMIP5 should be discounted when constructing KNMI-next scenarios. Whether KNMI will do this is still an open question at time of writing this report (August 2012).

- KNMI'06 assumed that future regional climate differences within the Netherlands will remain as they are in the current climate. Since 2006 evidence for regional differences of climate changes has grown, and some regional differentiation is expected to be included in KNMI-next.

- Futher information from `http://www.knmi.nl/klimaatscenarios/future/index.php`.

1.4 Publications resulting from this project

In this study a considerable body of information on cold spells, cold winters and atmospheric blocking has been gathered. Part of the results have been published. The publications are listed here.

Publication	Type	Summary
de Vries (2011b)	Popular	Discusses cold spells in the Netherlands in the current and future climate. This paper has been reprinted in Appendix E (p49) of this report.
de Vries (2011a)	KNMI	Technical report describing main results of the project in the first year. Focuses on the large-scale character of cold spells and the circulation that causes them. Key results are also discussed in part 4 (p29) of this report.
de Vries et al (2012b)	Peer-reviewed	Discusses Western European cold spells in the current and future climate. The cold spells are shown to change mostly due to the change of mean and standard deviation. The standard deviation is shown to mostly change due to changes in the large-scale temperature gradient and the strength of the mean zonal wind.
Weijenborg et al (2012)	Peer-reviewed	Discusses atmospheric blocking interpreted as breaking of large-scale Rossby waves. The direction of breaking is shown to be linked closely to the location of breaking relative to the climatological storm track. Relevance to energy sector: Different breaking types have different impact on low-level temperature (discussed in Masato et al (2011)).
de Vries and van Westrhenen (2012)	Popular	Discusses the February 2012 cold spell, and the reasons why the "11-stedentocht" could not be held. Also discusses running heating degree days within a winter. The article has been reprinted in Appendix F (p54) of this report.
de Vries (2012b)	KNMI	Technical report describing main results of the project in the second year. It focuses on the cold spells in the Netherlands and western Europe. Key results are also discussed in part 3 (p17) of this report.
de Vries et al (2012a)	Peer-reviewed	Discusses the reduction of snowfall on the cold days of the future. This reduction occurs in addition to the already strong reduction of the number of Hellmann days (days with potential snowfall) in the future. It is shown that the origin for the change can be found in part in the circulation change. A few sections of this article have been reprinted in Appendix G (p59) of this report.
de Vries et al (2012c)	Peer-reviewed (submitted)	Discusses atmospheric blocking in a future climate and explains the changes in terms of changes of the mean and variance of the zonal circulation.
de Vries (2012a)	KNMI	This report

Table 1.1: Publications that have appeared in the literature, or that have been submitted for publication. Further information can be found on `http://www.knmi.nl/~vries`.

Chapter 2

Heating degreedays (HDD)

2.1 About this part

An important parameter for the gas and energy industry is winter heating degreedays. In this part, we extensively analyse this variable using climate model output that will also be used in the next IPCC report (IPCC-AR5). The results are compared to KNMI'06

2.2 Quality. Has the climate model output been calibrated to match observations?

Climate models do not reproduce observations exactly. In this part, all local (Netherlands) HDD time series are scaled such that their 1976-2005 median (P50) and P90-P10 difference are equal to the "1905-2007eqmean" series of Wever (2008)

Weather never repeats itself. Even in a stationary climate there will be small differences in long-term averages, and the long-term sample means will be approximately normally distributed along the true mean. In addition to natural variability, the climate models are not perfect. Because of their finite resolution, they rely on certain parameterizations to describe the influence of small-scale processes on the larger-scale dynamics. Different parameterizations can be used for similar processes, leading to small differences in dynamics and statistics.

In order to come to a meaningful comparison between observations and output from global climate model simulations, choices have to be made. In this part of the study, we have chosen to only calibrate the data when showing the local time-series of the Netherlands. In this scaling approach the median (P50) and standard deviation (approximated as the difference between the tail quantiles, $P90$-$P10$) for the period 1976-2005 are made equal to the values from the "1905-2007eqmean" series of Wever (2008), which are reproduced in Table 2.1. This approach guarantees that all members 'start' from the same reference conditions. However, they all exhibit (slightly) different future trends, and therefore give rise to different (but equally possible) future realizations. The trend biases appear to be uncorrelated to biases in the mean. For this reason we have not excluded any members because of their bias in mean of the control climate. In contrast to the local time-series results, the large-scale maps shown in the following sections, are mostly based on uncalibrated data, unless indicated otherwise. In some cases, calibration with respect

Series	**10%**	**50%**	**90%**
1905-2007,eqmean	2050	2252	2519
G, 2020	1970	2170	2434
G+, 2020	1944	2143	2404
W, 2020	1886	2085	2348
W+, 2020	1837	2032	2289
G, 2030	1940	2141	2405
G+, 2030	1908	2105	2365
W, 2030	1831	2030	2292
W+, 2030	1767	1960	2213

Table 2.1: The "1905-2007eqmean" heating degreedays values, as well as three important quantiles from the KNMI'06 scenarios. The climate model output has been calibrated to the 1905-2007 eqmean series. Reprinted from table 8 in Wever (2008).

to ERA-40 has been performed.

Approximated heating degreedays

The winter heating degreedays measure HDD is defined in (A.3 (p44)). For the Netherlands and most higher latitudes, the conditionality on the sign of $18 - \bar{T}$ is in practice nearly always satisfied in the winter half-year (Wever, 2008). Therefore, an alternative way to compute the winter HDD is based on simply using monthly-mean or seasonal-mean temperatures. In this approximation, winter HDD' is directly proportional to mean winter temperature. In this part of the study, the latter approach has been taken, and heating degreedays are computed as in (A.4 (p44)) from monthly-mean temperatures (October-March) using 30 days per month.

2.3 Heating degreedays. Climatology, extremes and the effect of the wind

In Europe, heating degreedays depend sensitively on latitude and the vicinity of the seas. It increases strongly over the continent where winters are much colder. It shows large interannual variability (10% of the mean). If the effect of the wind is included ('effective' heating degreedays), HDD increases by 10-30% in coastal regions, but much less further in land. Extreme years for the Netherlands are also extreme for a large part of Europe

Heating degreedays HDD, as defined in (A.3 (p44) is a commonly used variable for measuring the total 'intensity' of a winter, where anomalously high (low) values of HDD correspond to cold (mild) winters. Figure 2.1 shows the mean climatology of heating degreedays $HDD(\bar{T})$ computed using ERA-40 reanalysis data. There are large North to South and East to West differences in $HDD(\bar{T})$, with Siberia and the mountainous areas (Scandinavia, Alps, Turkish highland) clearly standing out. Due to the absence of significant topography, the gradient in the area around the Netherlands is mainly East to West (warmer near the sea). The largest values of $HDD(\bar{T})$ are found over Greenland, Northern Europe and Siberia. The interannual variability of HDD is large (right panel), in most regions more than 10% of the mean. In absolute numbers again the high latitude continental areas have the largest variability.

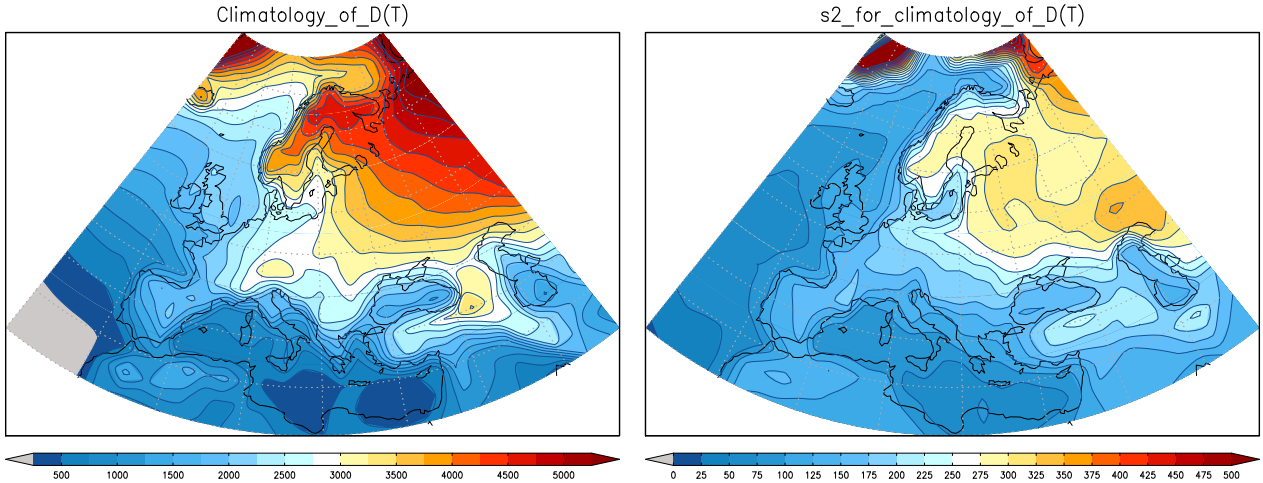

Figure 2.1: Heating degreedays HDD. (left) Climatology of $HDD(\bar{T})$ (colors show total $HDD(\bar{T})$ for climatological winter half year). The threshold $T_{threshold} = 18.0$ was used to determine HDD [see (A.3 (p44))]. (right) Interannual variability of heating degreedays HDD, shown as the sample standard deviation. Data: ERA-40.

Effect of the Wind

Heating degreedays can also be computed from effective temperature. If the same threshold is used, HDD increases by 10-30% in coastal areas, and by 1-10% further in land

It can be expected that the region Netherlands-France-British Isles is influenced significantly by the wind. This expectation is confirmed when we compare the climatology of $HDD(T_{eff})$ to the climatology of $HDD(\bar{T})$ as is done in Figure 2.2. The largest absolute differences occur in the Northern Atlantic, the largest relative differences in the Mediterranean (not shown). The Netherlands, and more generally all areas near the Atlantic coast show a strong increase. Further in land the differences quickly become small, typically on the order of 1-10% of $HDD(\bar{T})$. Note that due to the definition of T_{eff}, $HDD(T_{eff})$ will always be larger than $HDD(\bar{T})$.

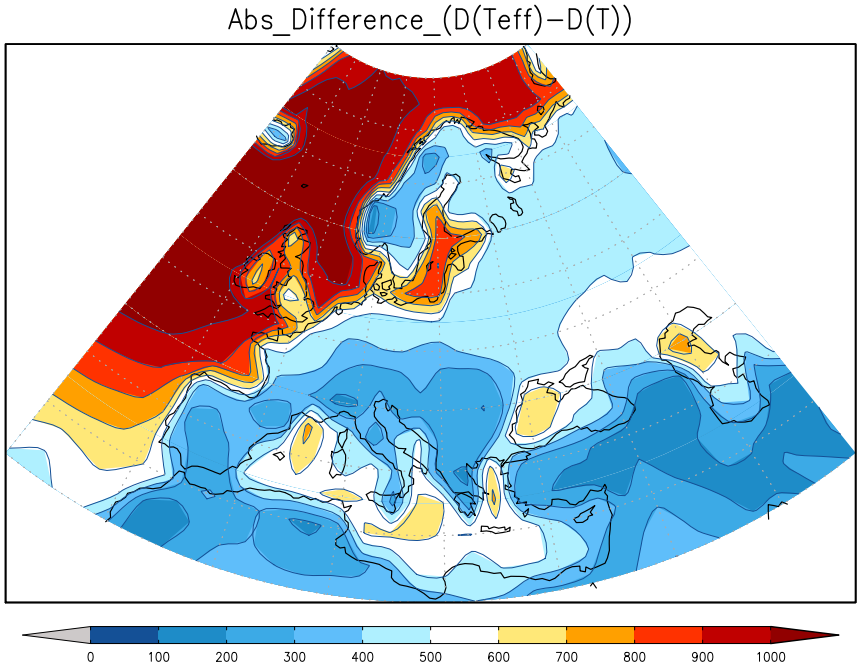

Figure 2.2: Difference between heating degreedays computed using effective temperature, or ordinary temperature: $HDD(T_{eff}) - HDD(\bar{T})$. Data: ERA-40.

Extremes

Winters that are exceptionally cold or mild in the Netherlands, are also exceptionally cold or mild in large regions

The total number of heating degreedays $HDD(\bar{T})$ computed for De Bilt shows large interannual variability (Fig 2.1b and de Vries (e.g. 2011a)). It is instructive to determine the spatial scale of anomalies $HDD_{anom} = HDD(\bar{T}) - HDD_{clim}(\bar{T})$ of the climatological mean $HDD_{clim}(\bar{T})$. To this aim we select the two years from the ERA-40 data set that produced the largest and smallest values of $HDD(\bar{T})$. The winters that were selected by this method are 1963 (largest $HDD(\bar{T})$) and 1990. Figure 2.3 contrasts these two extreme winters in terms of $D(\bar{T})$. Two features are directly apparent. First, the large spatial scale of the anomalies, both in case of the very cold, and the very mild winter. Second, the patterns observed for the two extreme winters look like the two 'phases' of a single pattern, with in case of the anomalously cold winter, a large positive anomaly in West and central Europe, and two accompanying negative anomalies at Greenland and the Turkish highland. The large scale in particular suggests that the atmospheric circulation plays an important role in determining the realized value of $HDD(\bar{T})$ for a single winter. In the introduction (Figs. 1.3-1.4, on page 3) we have shown that this is indeed the case.

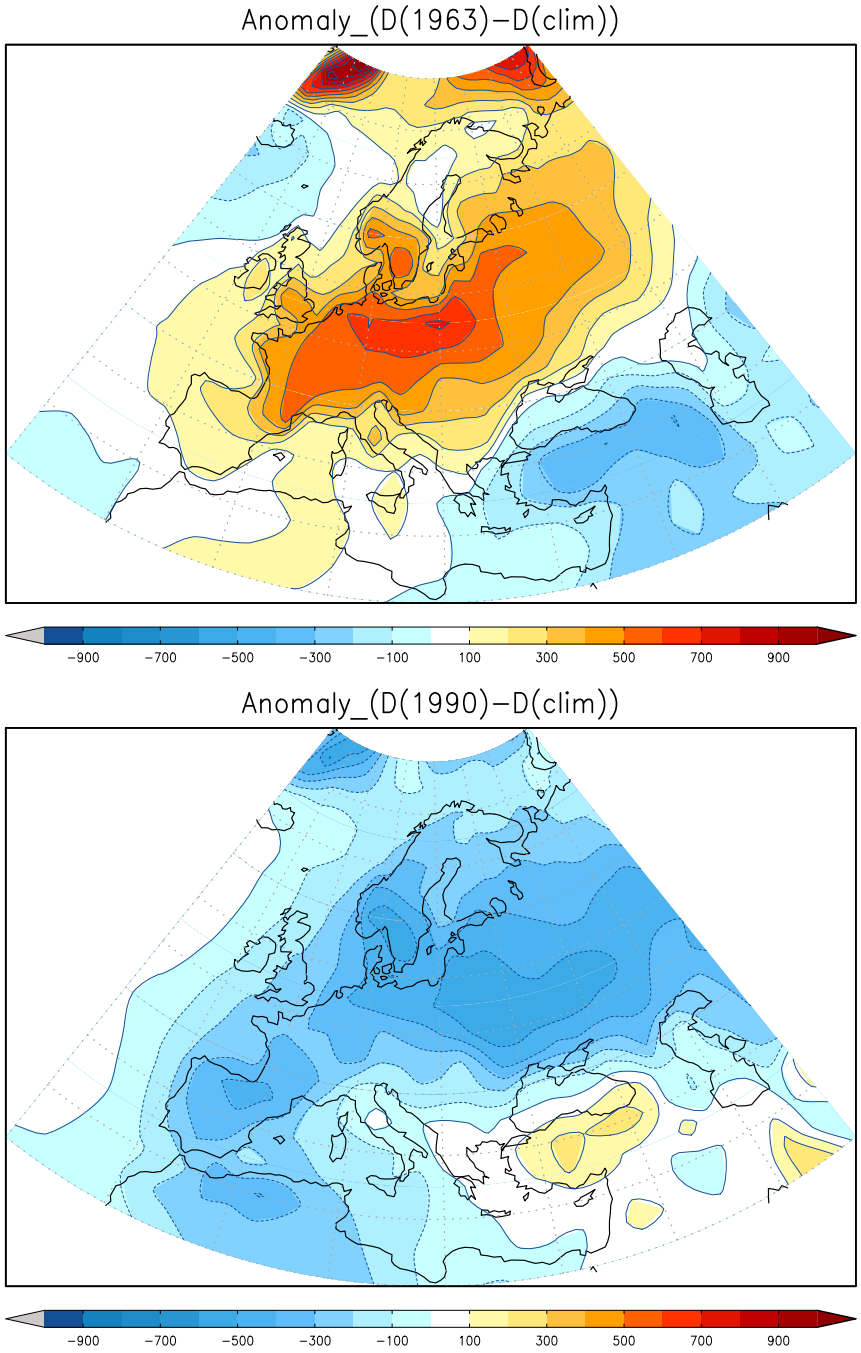

Figure 2.3: Heating degreedays $HDD(\bar{T})$. Anomalies from climatology, $HDD - HDD_{clim}$. (top) The winter with largest $HDD(\bar{T})$ at De Bilt (1963). (bottom) The winter with smallest $HDD(\bar{T})$ at De Bilt (1990). Data: ERA-40.

2.4 Future change. Projected changes for the Netherlands

The multi-model mean of all climate projections displays a 20% decrease over the 21st century, implying that "normal" winters in the current climate may be ranked among the 10% coldest winters beyond 2030. There is considerable spread in the results: RCP2.6 (strong mitigation) gives only a 10% decrease, while RCP8.5 (no mitigation) gives a 40% reduction

Figure 2.4 shows the evolution of winter degreedays for the Netherlands (multi-model ensemble mean, thick black line), obtained from all climate models that contributed to the CMIP5 archive. The dark grey area spans 80% of all ensemble members (excluding the 10% mildest/coldest members for each winter), the light grey band 98% of the members (excluding the 1% mildest/coldest members for each winter). The horizontal line denotes the reference climatological value of 2252 used to calibrate the climate model output (see also Table 2.1 (p7)). Therefore "normal" winters in the current climate may be ranked among the 10% coldest winters beyond 2030. The colored lines show the mean responses for the different RCP "forcing" scenarios (Meinshausen et al, 2011). While the scenario responses show considerable spread towards the end of the 21st century, they stay remarkably close together up to 2040-2050. Beyond 2040, either further reductions are found (in case of the RCP8.5 scenario), or a stabilization occurs (RCP2.6, strong mitigation), in which case the coldest winters might "pick up" again. In the next section we examine these results in more detail.

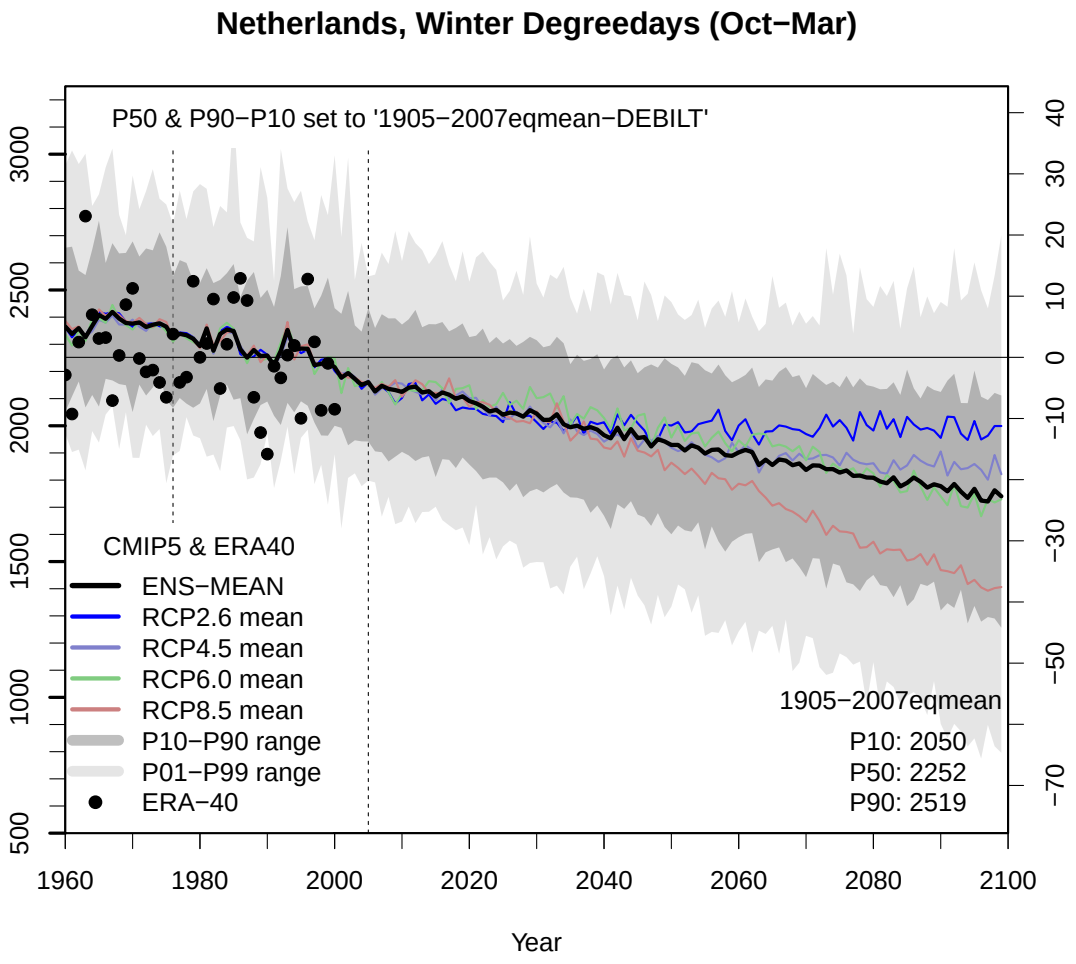

Figure 2.4: Winter heating degreedays in the Netherlands, computed using available CMIP5 data. The y-axis on the right denotes the percentage of change compared to 2252, the historic median from the observations (horizontal thin line). The colored lines denote the evolution of the ensemble mean for each RCP scenario. The thick black line denotes the multi-model mean. The vertical dashed lines mark the period used for calibrating (1976-2005). Data: CMIP5 and ERA-40.

2.5 Linking to KNMI'06. Projected changes of "normal", "cold" and "mild" winters

Percentually, the changes are almost independent of winter type (20% reduction). In absolute numbers the decrease is therefore largest for the coldest winters. The KNMI'06 scenarios cover about 70% of the ensemble spread for all three winter types. The W-scenario very well describes the multi-model mean. Based on these results, it is expected that the KNMI-next scenarios for winter heating degreedays will not be differing greatly from those of KNMI'06, although a slight shift towards a stronger future decrease is possible.

In this section, we focus on the changes of three characteristic winter types ("normal", "cold" and "mild"). The "normal" or average winter is defined for each year and ensemble member as the HDD median (P50) of a 30-year window centered around that year. In the same way, the "cold" winter is defined as the 30-year running 90% quantile (P90), while the "mild" winter is defined as the 30-year running 10% quantile (P10). This procedure results in an ensemble of medians and low- and high-tail quantiles for each year (other quantiles available on request by the author). The statistics (mean, trend, spread) of this ensemble can be compared to the KNMI'06 scenarios. Ideally the KNMI'06 scenarios broadly cover the spread of the ensemble. If not, this could be an indication that the upcoming KNMI-next scenarios (delivered in 2013) will be shifted somewhat with respect to the KNMI'06 scenarios. However, this shift will not necessarily happen, as the KNMI-scenarios are derived from other variables than winter heating degreedays.

Figure 2.5 shows the change of the "normal" winter (P50) including estimates of the uncertainty (dark and light shading correspond to one and two standard deviations around the mean respectively). This uncertainty, as will be discussed more rigorously in the next section, is caused by both natural variability, model differences, as well as the fundamental differences in forcing scenario (Meinshausen et al, 2011). Also shown are the KNMI'06 scenarios, as well as the uncertainty estimate of Wever (2008) for the current climate, which was based on observations of 1976-2005 and augmented with the observations from 1905-1975 with modified mean (horizontal dashed lines). Three conclusions can be drawn from the figure. First, despite the fact that the spread increases strongly with time, the future "normal" winter is warmer than in the present climate in almost all climate model simulations. The multi-model mean reduces by about 20% over the 21st century, with a standard deviation of about 10% on either side. Second, the KNMI'06 scenarios cover about 70% of the ensemble spread (the dark grey area). Third, the multi-model mean falls almost on top of the W-scenario of KNMI'06. Note that the W+ scenario of KNMI'06 falls

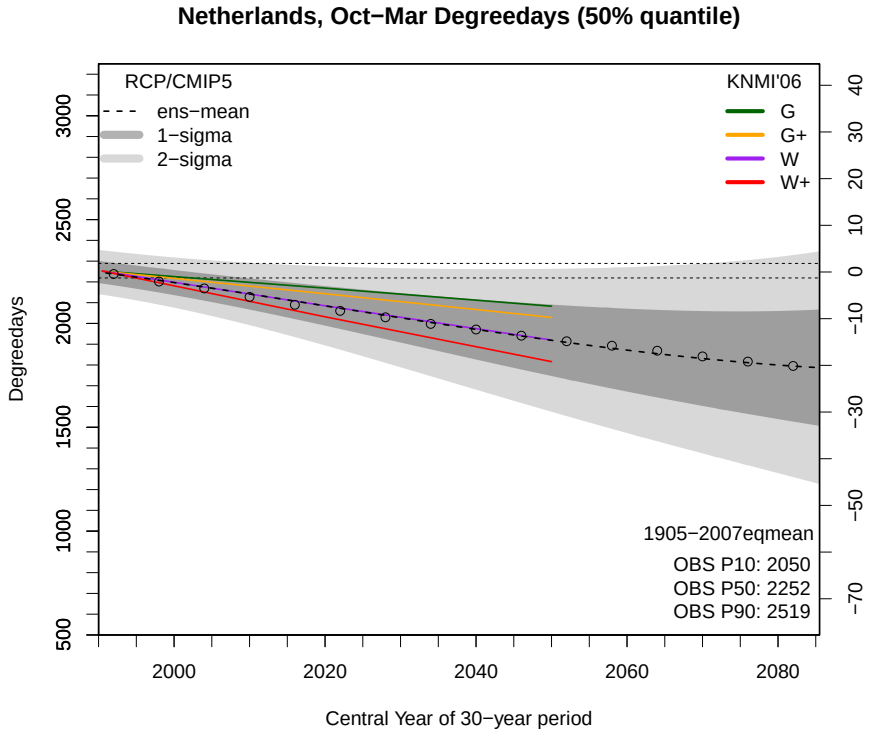

Figure 2.5: Heating degreedays for "normal" winters (P50). The x-axis denotes the central year of a 30-year period. The horizontal lines indicate the confidence interval for P50 obtained from Wever (2008). The dots denote the ensemble mean of 30-year running P50 values, the dashed line the ensemble mean of the polynomial fits [see (A.7 (p46))]. The light/dark shaded areas denote confidence intervals, computed as one and two standard deviations around the mean, computed using (A.11 (p46)). The colored lines denote the four KNMI'06 scenarios. Vertical axis on the right denotes percentage of change compared to 1990. Data: CMIP5.

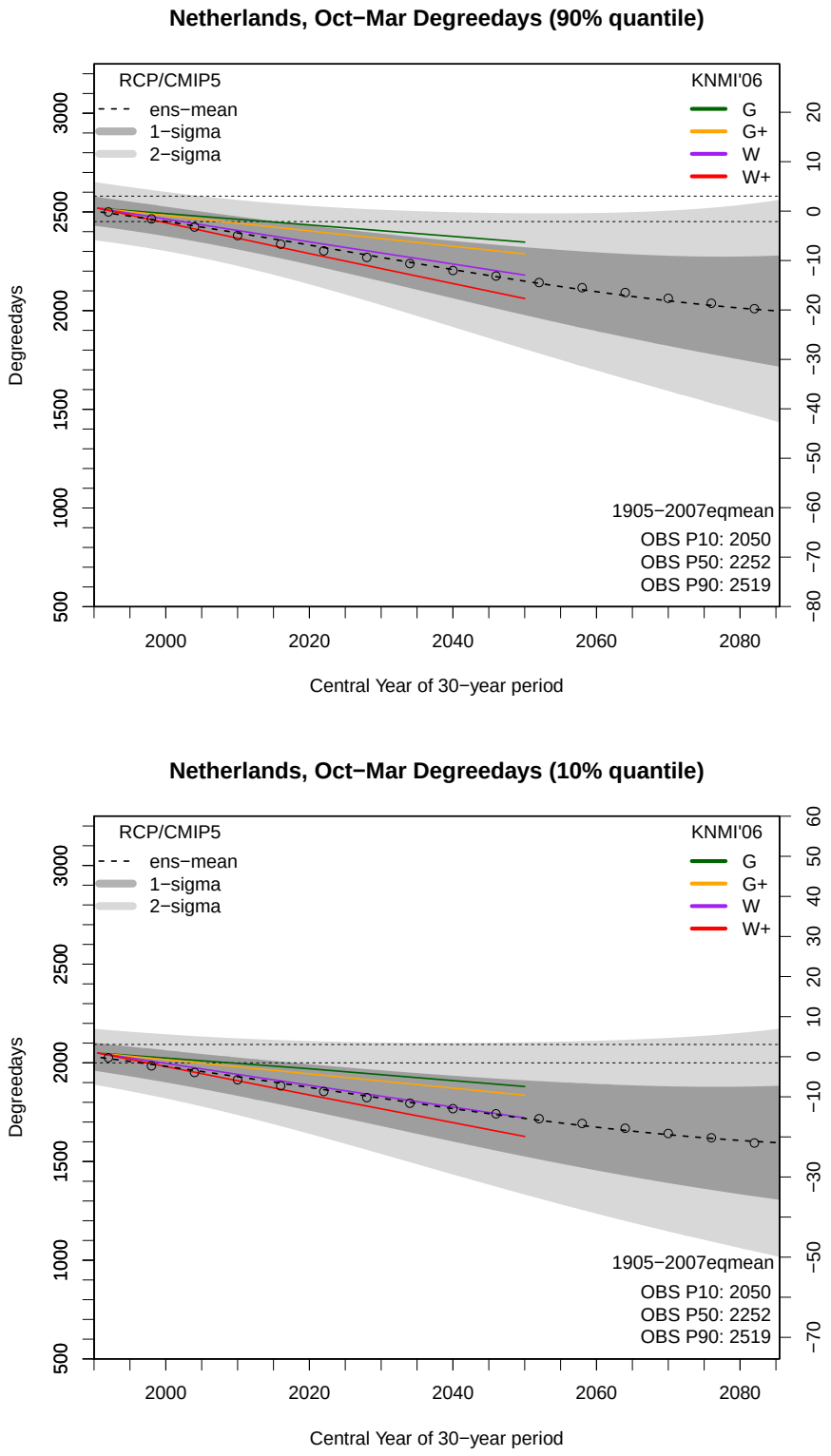

Figure 2.6: As in Figure 2.5 (p12) but for "cold" winters (P90, top) and "mild" winters (P10, bottom).

robustly within the dark-grey area, while G is at the edge. Finally (not shown), the mean responses for the different RCP-forcing scenarios stay very close together until 2040-2050, as in Figure 2.4 (p11).

Next we turn to the changes of the "cold" and "mild" winter[1] , which are shown in Figure 2.6. The change percentages (-20% in 21st century) are very similar to those of the "normal" winter. In absolute numbers however,

[1]Diagrams for the other quantiles are available on request.

the “cold” winters show a stronger decrease than the “mild” winters. This is in line with the results shown in de Vries et al (2012b). In the future, the warming occurs more rapidly at higher latitudes, which are the source regions of the cold air for the Netherlands. In contrast, the Atlantic warms less rapidly, as a result of which the “mild” winters (dominated by westerlies) will warm less than the “cold” winters. Both “cold” and “mild” winters display an ensemble spread (uncertainty) that increases with time. As with the “normal” winter, the W-scenario of KNMI’06 is very close to the multi-model mean, and only in the “cold” winter case the G-scenario falls outside the dark-grey band. Thus, also in the “cold” and “mild” winters, the KNMI’06 scenarios are not completely symmetric around the multi-model mean. These results lend support to the conclusion that the KNMI’06 scenarios remain relevant, in the sense that they span a considerable amount of the ensemble spread of the CMIP5 data.

2.6 Uncertainty. Sources of ensemble spread and uncertainty

Three important sources of spread are discussed: natural variability, model variability, and forcing scenario differences. Natural variability has the largest contribution up to 2050. Beyond 2050, model variability dominates until 2080. Variability resulting from differences in forcing scenario become relevant beyond 2050

As we have seen in the previous sections, the total ensemble spread increases strongly as time evolves. It is important and interesting to examine the origin of this ensemble-spread. Appendix C.2 (p45) outlines a method to separate between three important contributions to the spread in Fig.2.4. These three sources are

N Internal or natural variability, which describes the effect of the natural fluctuations that occur on a variety of time scales even if the climate is stationary. Generally the internal variability is largest at the shortest time-scales.

M Model variations. The climate models are all slightly different. Their response to changes in forcing, such as those arising from changes in greenhouse gas concentrations, is also different.

S Scenario variations. The same climate model responds differently to different forcings. The CMIP5 ensemble has been created using a variety of climate models that are forced with 4 different RCP (forcing) scenarios.

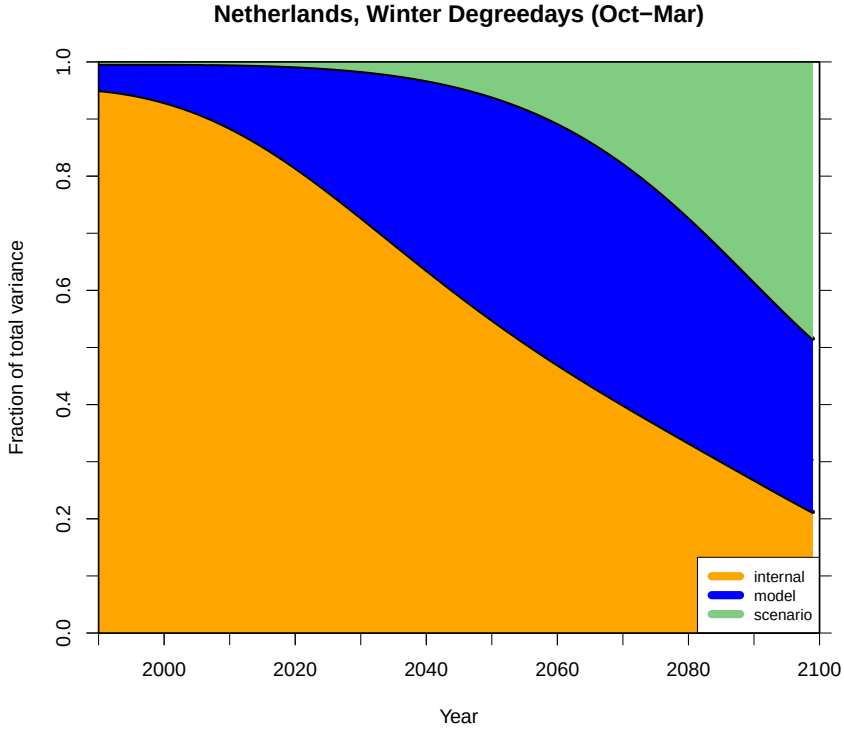

Figure 2.7: Origin of the spread of the ensemble of Figure 2.4 (p11). Distinguished is between variance caused by natural (or internal) variability, model differences and scenario differences, which have been computed using techniques explained in Appendix C.2 (p45).

The results of the decomposition (shown as relative fraction of the total variance) are shown in Figure 2.7. The orange area shows the relative contribution of the internal variability to the spread of the ensemble. This term is by

far the largest term at initial time, as should also be expected on the time-scale considered in Figure 2.4 (we consider yearly variability). The relative importance decreases gradually, but still accounts for about 20% of the variability at the end of the century. The blue area denotes the contribution from the model differences. While relatively modest at initial times, their contribution quickly grows, accounting for more than 40% of the total variance around 2040. Up to 2040 the contribution from the scenario differences is very small, as already concluded from Figure 2.4.

If we consider the uncertainty in the projected changes of the "normal", "cold" and "mild" winter, the story is different. Most importantly the natural variability in these quantities is much smaller, because they are estimated from 30-year running quantiles. Figure 2.8 shows this for the "cold" winter. At 30-year time scale about 40-50% is still determined by natural variability, while model differences have become more important.

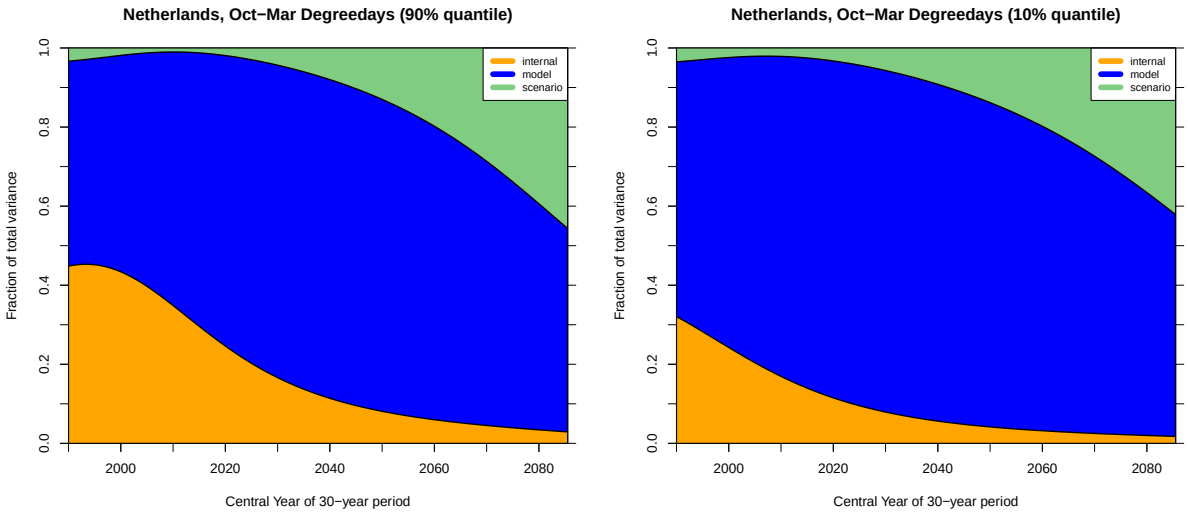

Figure 2.8: As in Figure 2.7 (p14) but for the "cold" winter (P90) and "mild" winter (P10) cases shown in Figure 2.6 (p13). The natural variability component is much smaller compared to the model differences.

2.7 Projected changes for the European region

All climate models predict that the rise of winter temperature will be the strongest in the high-latitude and continental areas. Compared to the current climate, most areas in Europe show 15-30% decreases up to the end of the 21st century, turning exceptionally mild winters of the present day, in to the average winter of the future

Figure 2.9 (p16) shows the differences between the ensemble mean climatology of $HDD(\bar{T})$ for the two periods 1950-2000 and 2051-2100 obtained with the Essence climate model. Significant decreases of $HDD(\bar{T})$ are seen over most parts of European continent (Figure 2.9 (p16)). The absolute decrease is largest at high latitudes. However, the relative decrease is largest over the Mediterranean region, which is mostly due to the fact that the threshold $T_{threshold}$ acts as a rigid cutoff. For large parts of the European continent the decrease is between 15 and 30 percent. It is worth mentioning that there are no gridpoints in the selected geographical region that show an increase in ensemble-mean value of $HDD(\bar{T})$. Zooming in on Western Europe, the predicted change roughly corresponds to a 2.5 °C increase of the daily mean winter temperature. To better appreciate the size of this change, one can say that winters which are exceptionally mild given current climate conditions (like the one showed in Fig. 2.3 (p10)) will become "average" winters near the end of the 21st century.

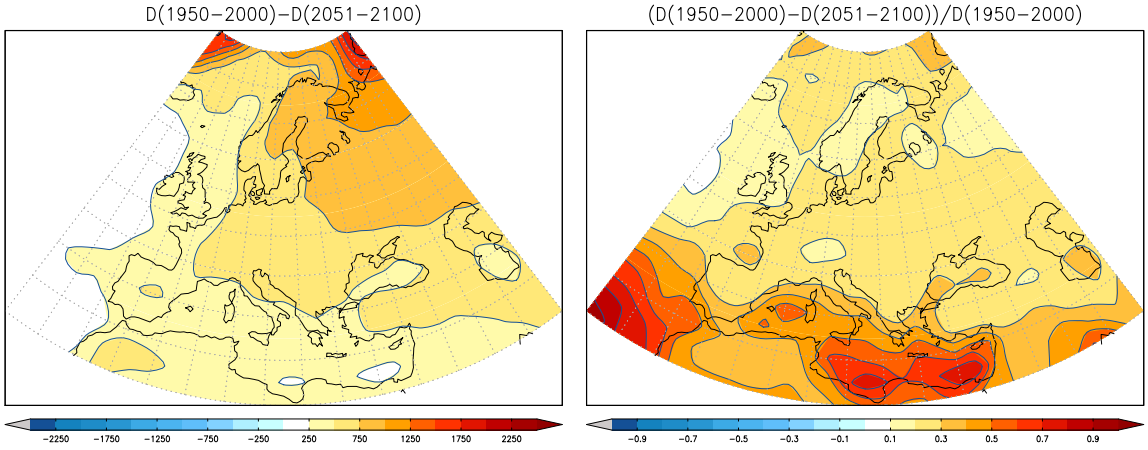

Figure 2.9: Absolute and relative differences between the ensemble-mean climatology of $HDD(\bar{T})$ for the periods 1950-2000 and 2051-2100, as obtained with $T_{threshold} = 18$ °C. Data: Essence climate model.

Chapter 3

Cold spells (CS)

3.1 About this part

Cold spells are defined as periods in which the daily mean temperatures stays below a certain threshold. This threshold can be defined in absolute terms, or relatively, with respect to a changing reference climate. Most of the future changes are explained by accounting for the changes of the mean and variance of the daily winter temperature distribution

3.2 Quality. Do climate models realistically simulate temperature variability?

There is good correspondence between the Essence climate model and ERA-40 reanalysis (pseudo-observations). There is considerable spread among climate models

Figure 3.1 (p18) shows the correspondence between the winter-mean temperature and standard deviation for ERA-40 reanalysis data (Uppala et al, 2005), as well as for output from the Essence project (Sterl et al, 2008). Essence is an ensemble climate simulation with one particular climate model that scored high in a model inter-comparison study (van Ulden and van Oldenborgh, 2006). There is good agreement between both the winter mean temperature (top row). Bias with respect to ERA-40 occurs mainly over the continent, where the climate model is a little too cold. The climate model also produces about the right amount of temperature variability. Especially this aspect is crucial if one aims to study the cold spells. For more details on the Essence climate model, see Appendix A (p42).

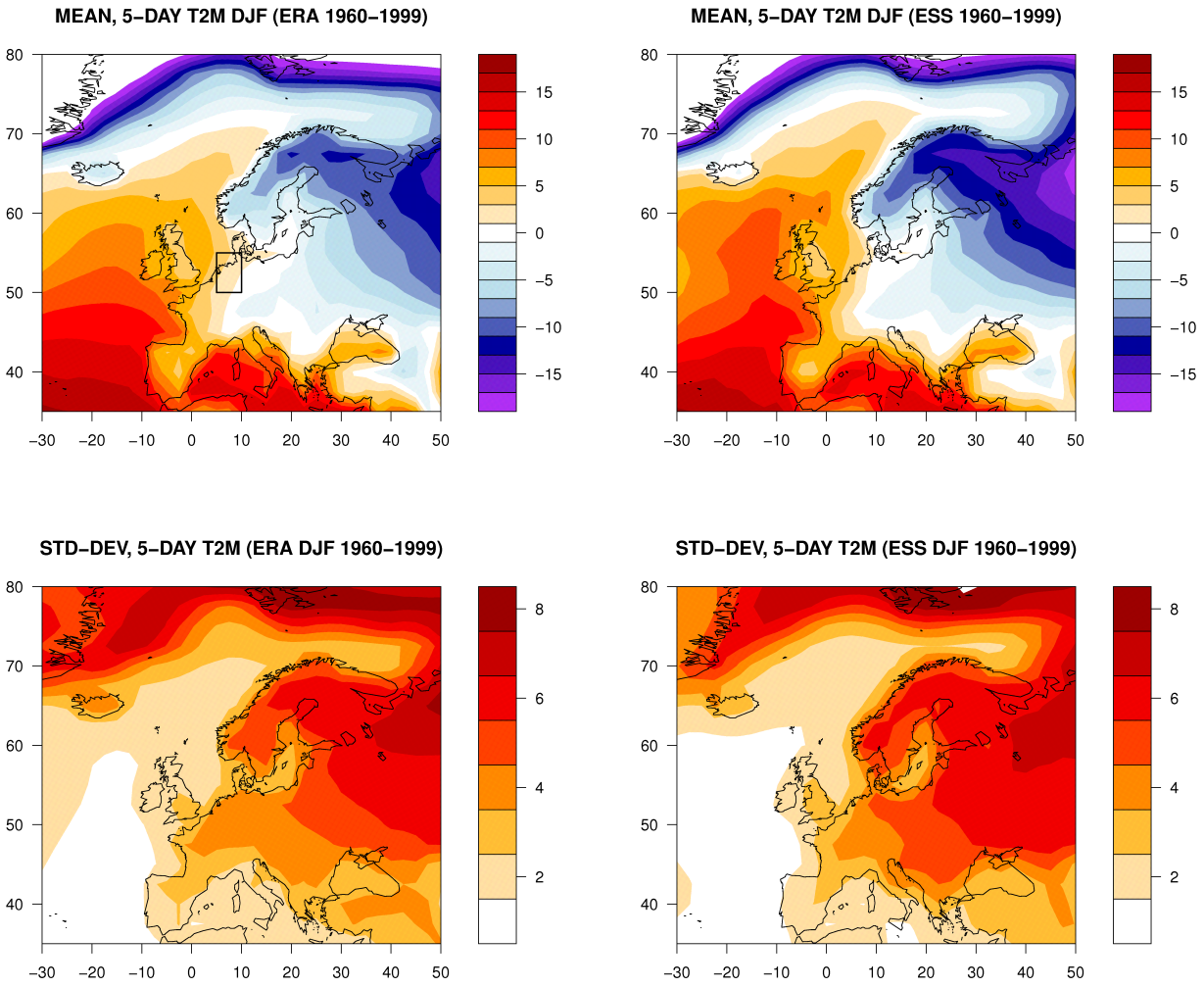

Figure 3.1: Winter climatology of 5-day running average 2m-temperature, obtained for (left) ERA-40 reanalysis and (right) 1960-1999 period of Essence (ensemble mean). Units: degree Celsius. Top: December-January-February (DJF) mean. Bottom: sample standard deviation. Taken from de Vries et al (2012b).

3.3 Future changes. The projected changes of winter temperature variability in the Netherlands

These are significant, with an upward trend in the mean, and a downward trend in standard deviation. These two effects strongly impact on the cold extremes. Climate models agree on the directions of change but vary in the amount

Figure 3.2 shows the time evolution of the winter-mean temperature and daily standard deviation for an area covering the Netherlands, according to climate model output (Essence model). There is a marked increase of mean winter temperature, with a trend of about 0.33 degree Celsius per decade. The signal of the winter daily standard deviation is noisier but has a negative trend. Both effects lead to a reduction of the cold extremes when measured in absolute numbers, such as frost days, etc. The reduction of variability is also seen in the left panel (the ensemble spread becomes less over time). The directions of change are robust among models, although the amount of change differs substantially.

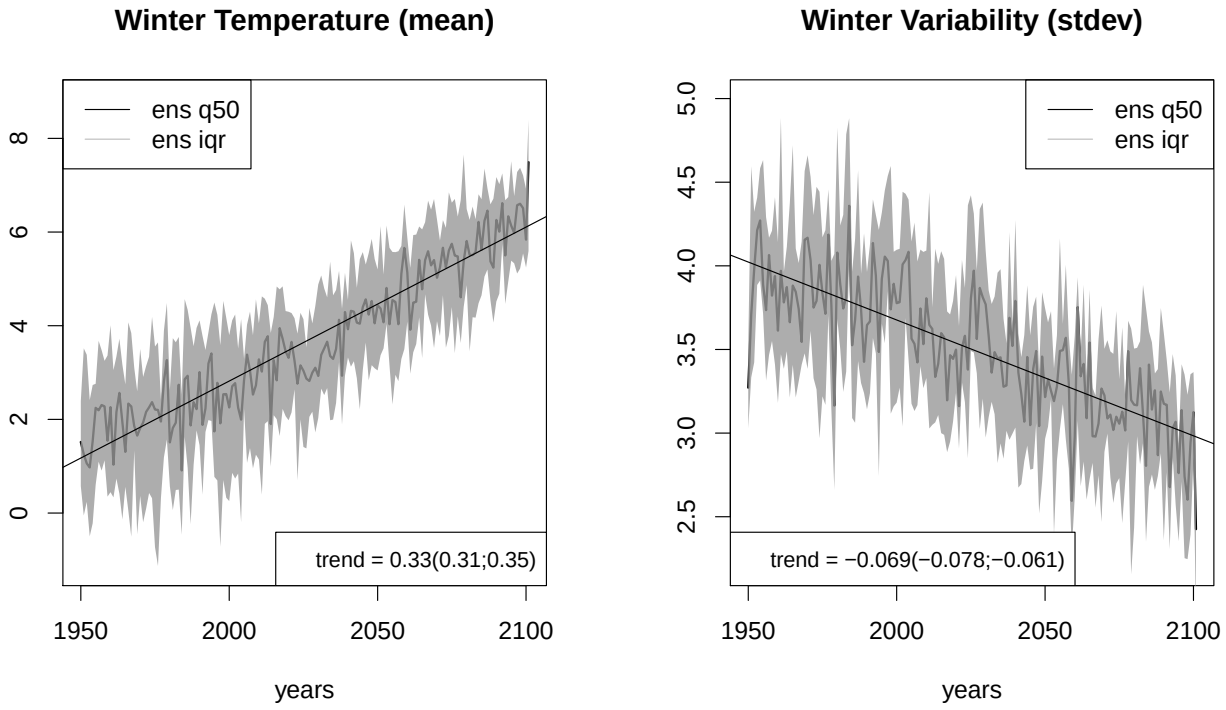

Figure 3.2: Changes over time of (left) winter temperature (DJF-mean) and (right) DJF standard deviation of daily mean temperature (both in degrees Celsius), obtained using the Essence model for the geographical box 5-10E, 50-55N. The grey band denotes the inter-quartile spread (iqr=q75-q25) of the ensemble members, while the line denotes the median.

Differs the future temperature distribution from that of present day?

Yes, but the most important changes are the change of mean and variance. After scaling (subtracting mean and dividing by the standard deviation), the distributions become very similar

Another way to compare two distributions is by means of a so-called quantile-quantile plot (Wilks, 2006). In such a plot the quantiles of one distribution are plotted against the quantiles of another distribution, for instance of the same variable but a different period. If the distributions are identical a straight line through the origin with slope 1 is found. Figure 3.3 (p20) shows a quantile-quantile plot for the winter mean temperature in an area near the Netherlands, obtained using climate model output (the Essence ensemble). On the horizontal axis the distribution of the present climate is shown. In the current climate all ensemble members (left panel, blue dotted lines) are scattered around the line through the origin with unit slope. For the future periods the most important difference is the vertical offset (straight lines have been drawn through the medians). However, the lines of the future periods also have a different slope, indicating that higher order moments are changed as well. The different slope is the result of the decreasing standard deviation, which leads to a lower maximum and a higher minimum. After correcting for these differences (right panel), the lines fall nearly on top of each other. This confirms that the most important changes of the temperature distribution are indeed a change of the mean and a change of the variability (standard deviation).

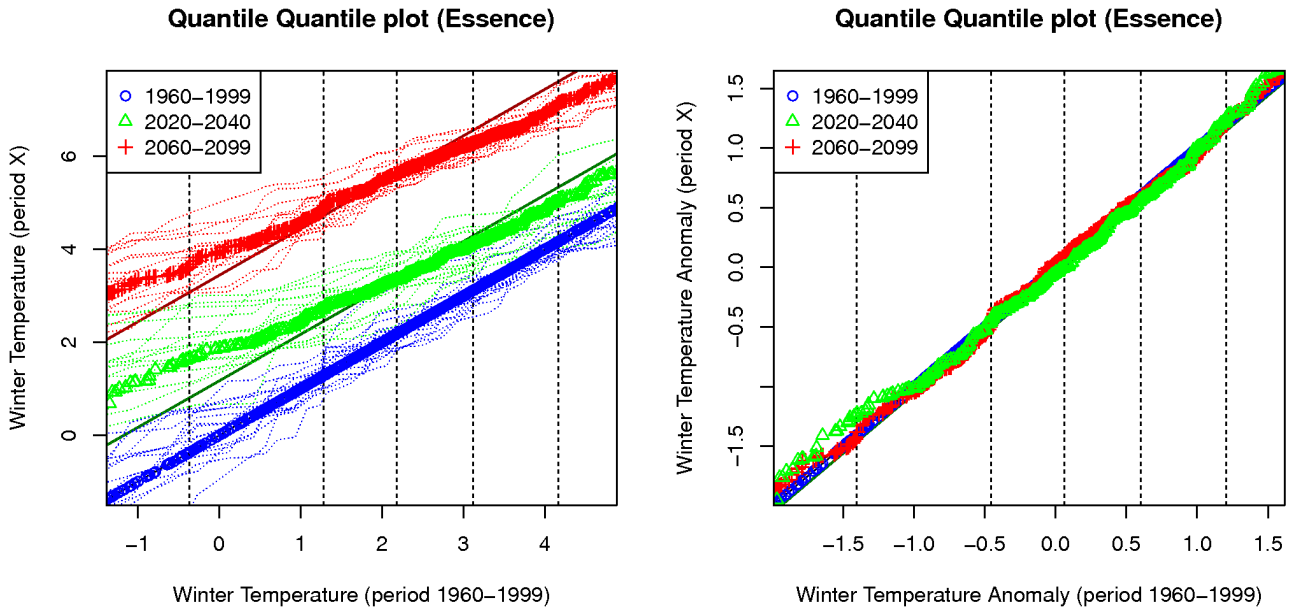

(a) absolute changes

(b) relative changes

Figure 3.3: (a) Quantile-quantile plot of winter mean temperature (in degrees Celsius), obtained from climate model output (Essence data). Horizontal axis shows quantiles for "present-day" winter climate (1960-1999), where all ensemble members have been used. Vertical axis, shows quantiles for other periods (dotted lines denote the individual ensemble members). Quantiles q10, q30, q50, q70 and q90 are indicated by lines. (b) The same plot, but after rescaling the data (subtract the mean and divide by standard deviation).

The impact of the projected future changes on the annual minimum temperature

The annual minimum temperature increases significantly in the future (0.5 degree per decade). As a result, the average return time for low temperatures increases. Similar changes can be expected for effective temperature

Panel (a) of the figure shows the evolution of winter minimum temperature for the box-average of 5-10E,50-55N region of Essence. The figure is an updated version of a figure shown in de Vries (2011a). The temperature trend increases with time and from 2030 onward the future mean minimum temperatures do no longer fall within an extrapolated uncertainty band based on current climate. The right panel shows the return times for annual minimum temperatures. Average return times for all temperatures increase in future. The increase is also larger for the really low temperatures. The large dataset allows for tight uncertainty margins, even at longer return times, in contrast to extrapolated series from observations (the black lines indicate the uncertainty in the estimated return times from ERA-40). It needs to be remarked that there is considerable inter-model uncertainty in these results. Some models give a stronger increase other models a weaker increase. There is no probability assigned to the realization shown in the figures.

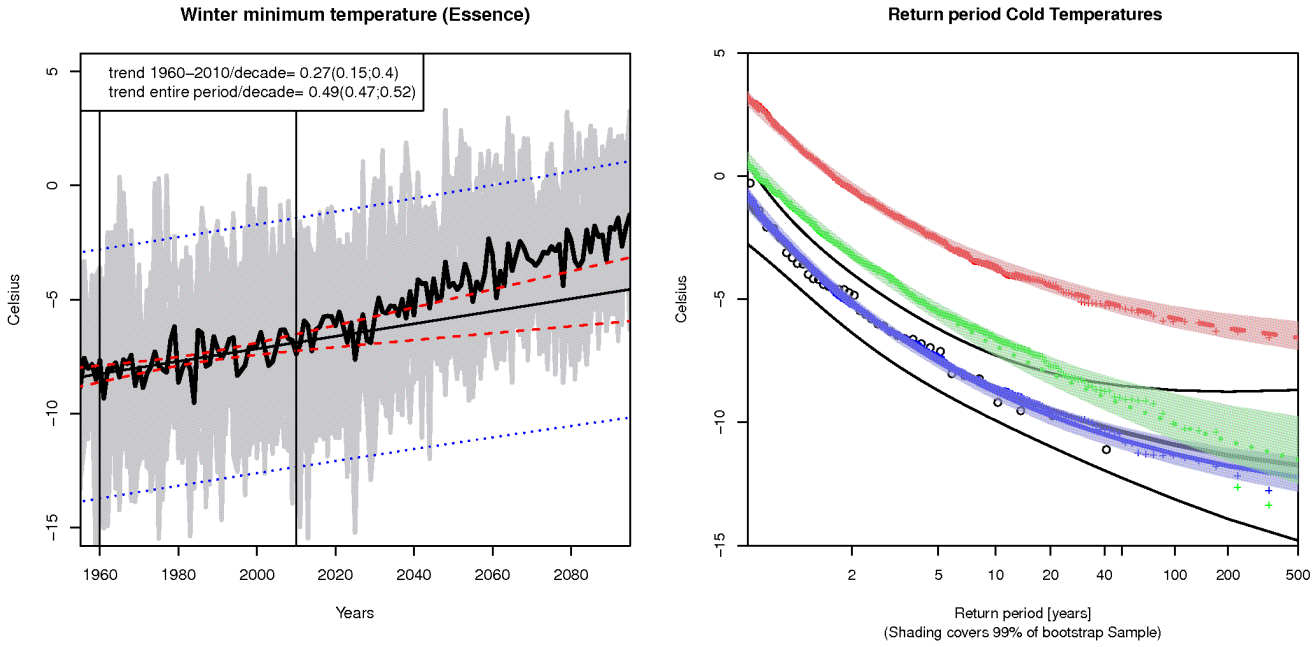

(a) (b)

Figure 3.4: (a) Evolution of annual minimum temperature for climate model output (Essence). The grey lines indicate individual ensemble members, black line the ensemble mean. Trends for two periods have been indicated. Also 95% confidence bands for the trend in mean winter minimum (computed for 1960-2010 and extrapolated from there) have been indicated (red dashed lines).(b) Return level plot for the annual minimum temperature obtained using Essence, for three different periods. Black: ERA-40 (reanalysis observations). Blue: Essence 1960-1999, Green=2010-2050, Red=2060-2099. Uncertainties are indicated by the bands and have been determined by a bootstrap method (assuming independent events).

Are there uncertainties within a single climate model (Essence)?

Yes, about 0.5 degree for mean winter temperature, and 0.2-0.4 degree for daily temperature variability

Figure 3.5 (p22) (left) shows a scatterplot between mean temperature and standard deviation. The Spearman rank correlation between the two components is $\rho = -0.77$ (computed over all points). Three periods are distinguished and plotted with different colors. Although there is significant overlap between the colors, it is clear that the later periods tend to produce winters with higher mean temperatures and lower standard deviation. The points are scattered around a line with negative slope. It is expected that for large enough rise of mean temperature, the slope must decrease (i.e., there will always be a nonzero variability around the mean). Marginal box-whisker plots summarize the changes (see caption description for explanation)

The right panel in Fig. 3.5 (p22) shows the ensemble spread for temperature and standard deviation for the period-averages of three different periods. Much more than in the left panel the three different periods are separated. Natural variability causes the ensemble members to have slightly different realizations of the climate, even though the climate model underlying all ensemble members is identical. The ensemble spread is around 0.5 degree in mean temperature for Essence.

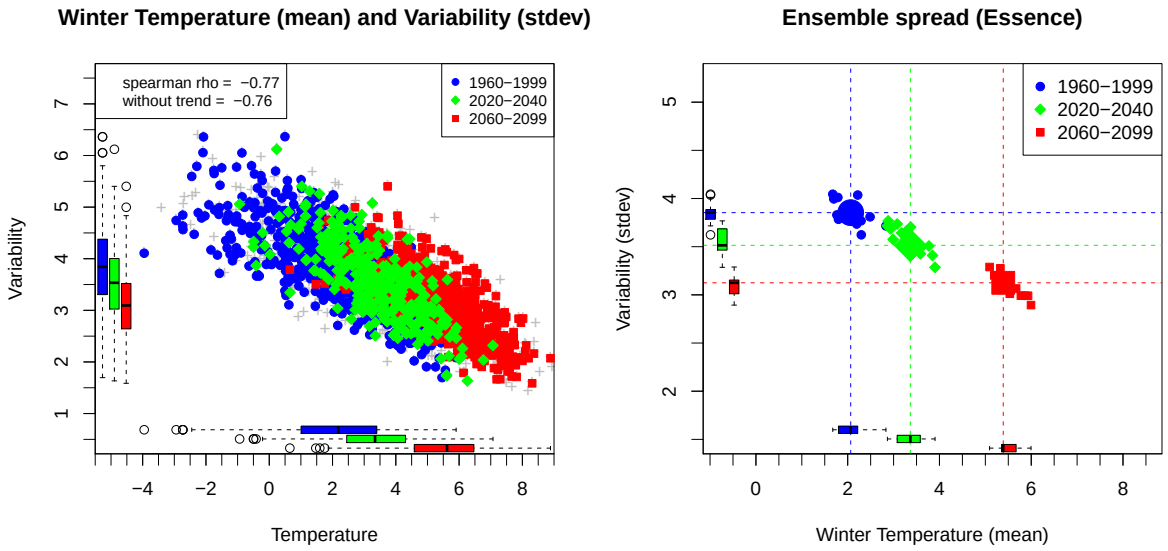

Figure 3.5: Ensemble spread of temperature and daily standard deviation (both in degrees Celsius), obtained using the Essence model. Each mark indicates the period-mean for an ensemble member. Different colors correspond to different periods. The big marks denote the ensemble median. Also shown are the marginal box-whisker plots for the three different periods. These indicate the median (q50, line), inter-quartile range (iqr=q75-q25, box) and the whiskers (maximal extension of whiskers is 1.5iqr above q75 and below q25. Data points outside whiskers are marked with black dots).

3.4 Intensity. Will future cold spells have a different temperature?

Yes. The minimum temperature reached in future (period 2010-2049) cold spells will on average be approximately 2 degrees less cold than in the 1960-1999 period (5 degrees less cold in 2060-2099). In contrast, if measured relative to a changing reference climate, no significant changes are observed. This is also seen for a large part of Europe

Cold spell days are defined as days in which the temperature drops below a certain level. This level is chosen to be the 10% level of the DJF winter distribution. Important to notice is that we allow the 10% level to change over time, as the climate evolves. Figure 3.6 (p23) below shows what happens in future to the cold spells when they are defined in this way. The average minimum temperature reached during cold spells will increase by 5 degrees near the end of 21st century. If the data is rescaled (subtract the mean and divide by standard deviation of DJF temperature), as is done in panel (b), the evolution is very similar. Figure 3.7 extends this to a larger part of Europe.

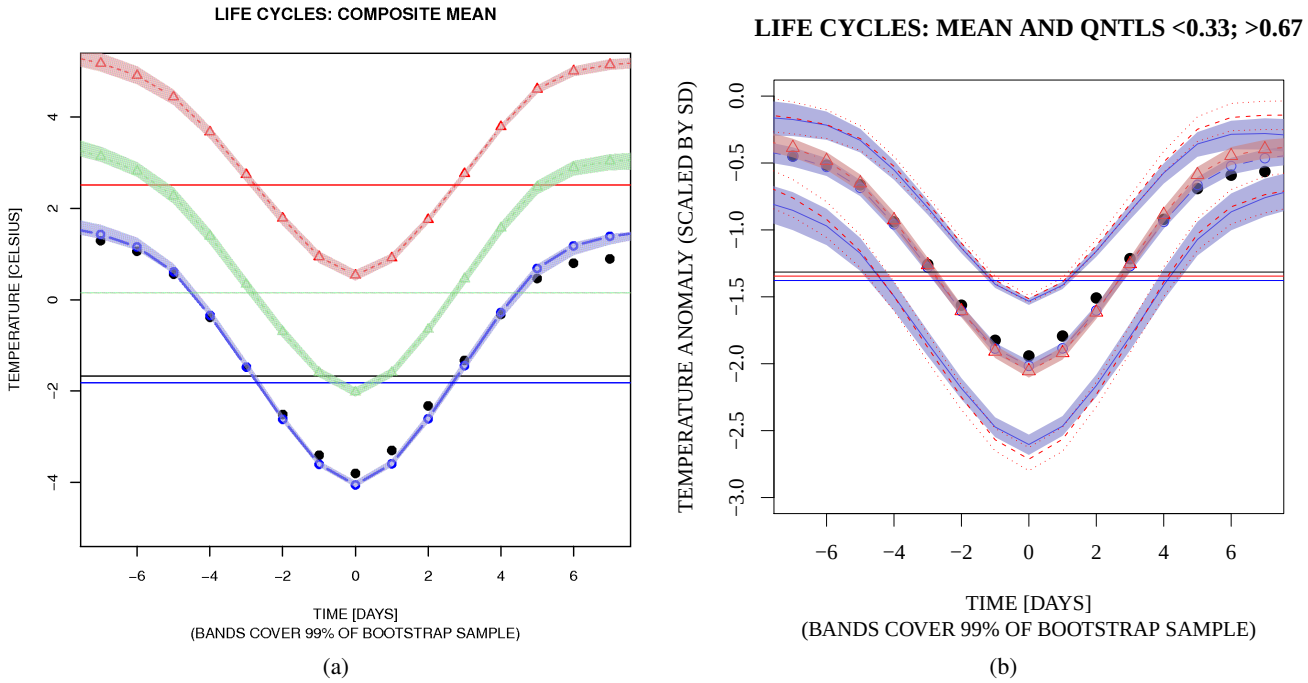

Figure 3.6: (a) Composite evolution of cold spells over the Netherlands region (5-10E,50-55N), using the Essence model. Blue: 1960-1999. Green: 2010-2049. Red: 2060-2099. Black: ERA-40 reanalysis. (b) The results for blue and red, after rescaling by the mean and standard deviation. For each color the middle line shows the evolution of the average cold spell, and the lower (upper) lines the evolution of cold spells that reach temperatures in the lower (upper) tercile. Modified after de Vries et al (2012b).

Cold spell temperature change for the larger European area

The entire European area experiences significant warming in winter. Most of the changes result from changes of the local mean temperature and variability

In figure 3.7 we examine the mean temperature during a cold spell (CS) for a larger part of Europe. For each grid box the 10% quantiles were determined separately for two periods using climate model output (Essence ensemble). The top row contrasts the mean CS temperatures of the two periods. The bottom left panel shows their absolute difference. CS get warmer everywhere in Europe, with the amount of warming being the strongest in the coldest regions. The bottom right panel shows the difference in CS temperature after scaling the data by the mean and

standard deviation. For most areas the changes of mean and standard deviation are sufficient to explain the change of the CS temperature.

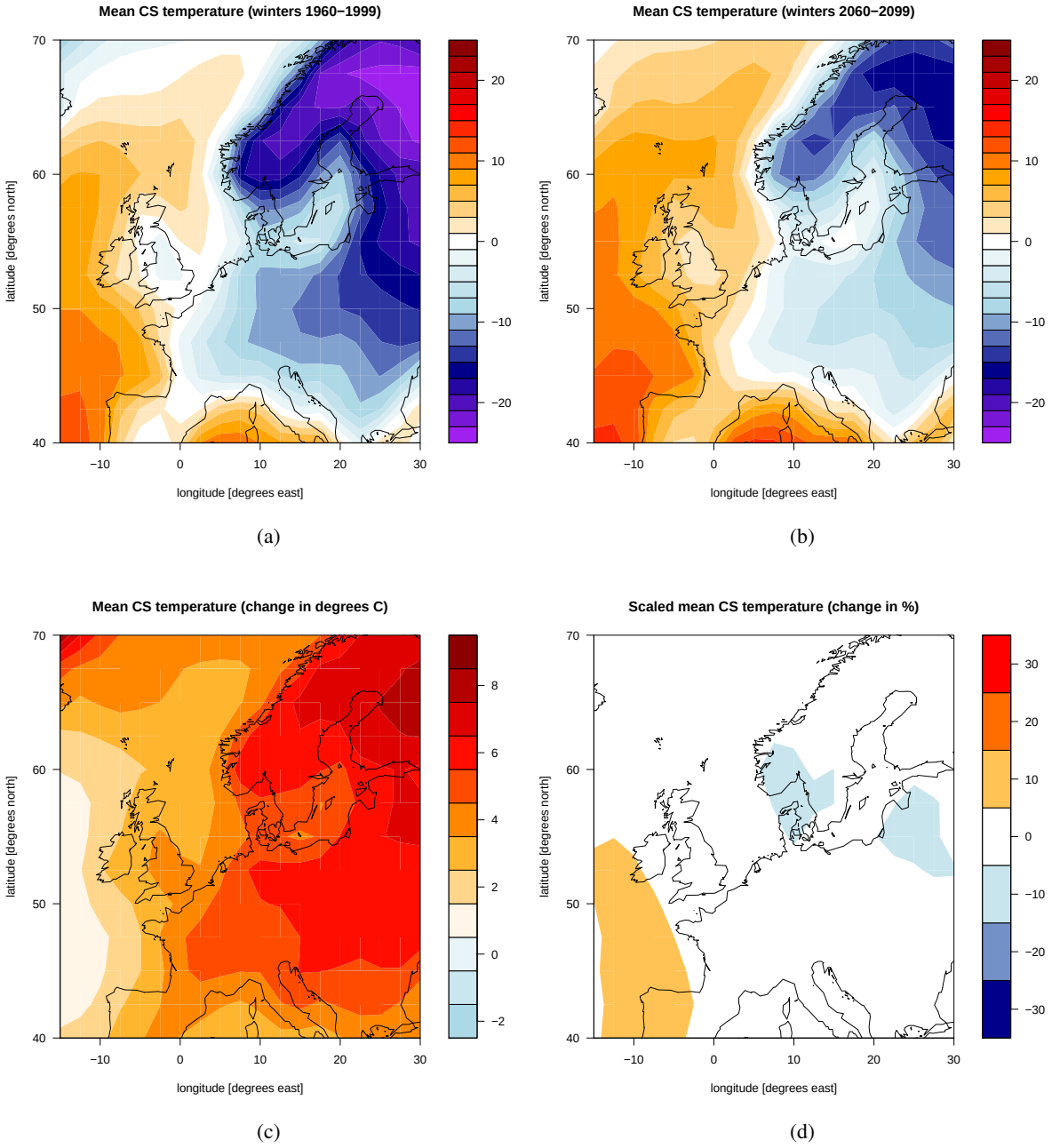

Figure 3.7: (a) Composite evolution of cold spells over the Netherlands region (5-10E,50-55N), using the Essence model. Blue: 1960-1999. Green: 2010-2049. Red: 2060-2099. Black: ERA-40 reanalysis. (b) The results for blue and red, after rescaling by the mean and standard deviation. For each color the middle line shows the evolution of the average cold spell, and the lower (upper) lines the evolution of cold spells that reach temperatures in the lower (upper) tercile. Taken from de Vries et al (2012b).

How large is the spread among models (IPCC / CMIP3)?

There is considerable uncertainty between different climate models. However, once differences in mean temperature and standard deviation are accounted for, the cold spells evolve reasonably similarly

The left panel in Figure 3.8 shows the cold spell evolution composite for a subset of the CMIP3 climate models (Meehl et al, 2007). The panel is very similar to that discussed in Fig. 3.6 (p23), where the cold spell evolution has been discussed for the Essence model. Similar to the Essence model, after rescaling the results for the different periods become very similar, thereby showing that a large part of the inter-model uncertainty in cold spells is caused by the differences in mean and standard deviation. The right panel shows the model spread.

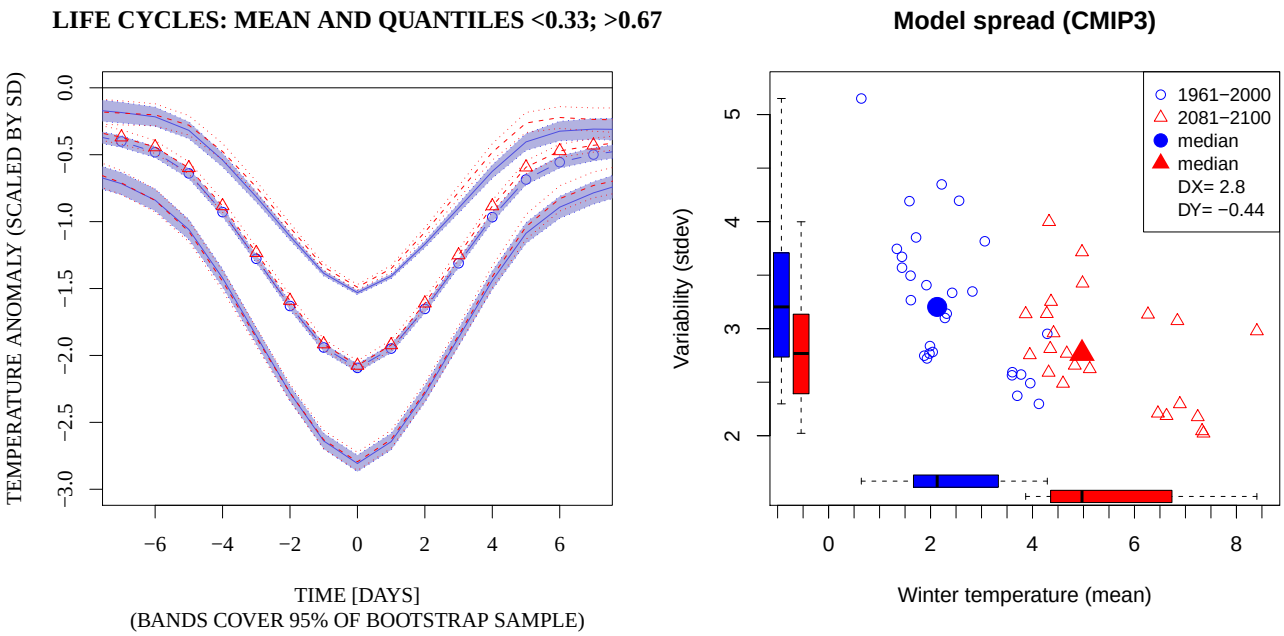

Figure 3.8: Composite evolution for cold spells over the Netherlands region (5-10E,50-55N), obtained for a subset of the models that entered CMIP3 with the same emission scenario as Essence (sresA1B). Taken from de Vries (2011b). Now the future period is 2081-2100. The data has been rescaled by by mean and standard deviation of each model. The right panel shows the distribution of means and standard deviations.

3.5 Duration. Will future cold spells have a different duration?

Yes. If measured with a present-day threshold, future (2020-2040) cold spells will last 20% shorter than in the 1960-1999 period. In contrast, if measured relative to a changing reference climate, the cold spells will have the same duration (4-5 days)

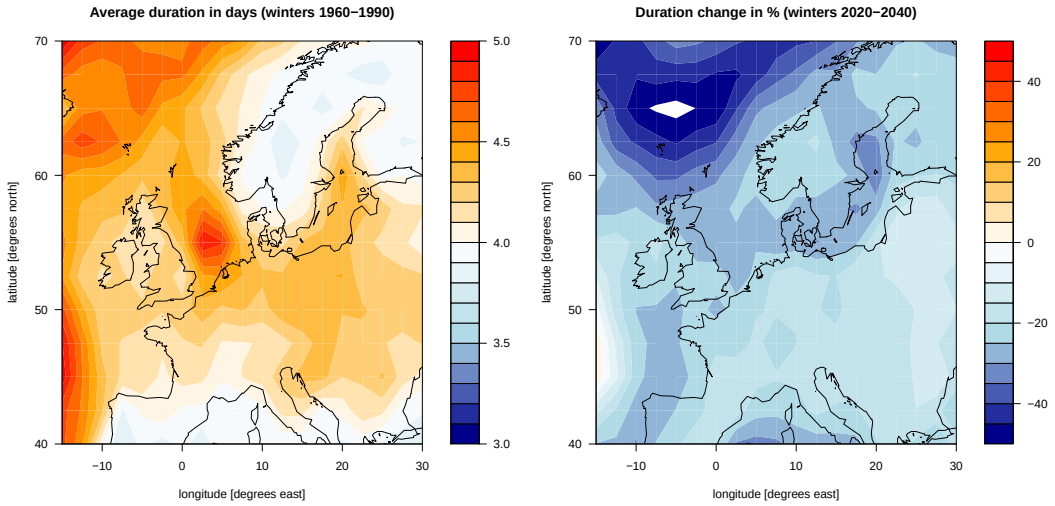

(a) Present day

(b) Future with present-day threshold

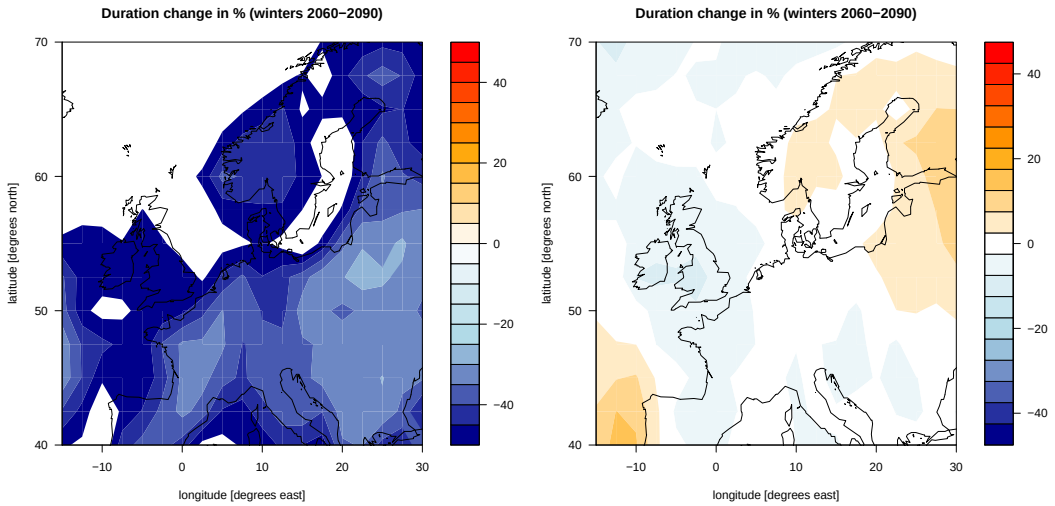

(c) End 21st century with present-day threshold

(d) Future with future threshold

Figure 3.9: (a) Average duration in days of a cold spell for 1960-1990 period in Essence (ensemble mean). (b) Difference in % between 2020-2040 period and 1960-1990 period (threshold from 1960-1999 period). (c) As in (b) but for 2060-2099 period. White areas indicate reductions by more than 50%. (d) Difference in % between 2060-2099 period and 1960-1990 period when thresholds are taken for each period separately. Based on de Vries (2011b).

Figure 3.9 (top left panel) shows the average duration of a cold spell (a consecutive series of days in which the 10% coldest levels are reached) in the 1960-1990 period obtained with climate model output (Essence). Large parts of western and central Europe experience average cold spell durations between 4 and 5 days. Note that the typical temperatures of these cold spells differ substantially (Fig. 3.7 (p24)). Panel (b) and (c) show that for 2020-2040 and end of 21st century the average duration of cold spells decreases significantly everywhere. However, panel (d) shows that the far-future (2060-2099) displays only minor changes if we take a threshold based on the future climate.

3.6 Return times. Cold spell of 10 days in the near future (2020-2040)

Return time increases substantially (factor 3 to 4) if one retains the same cold-spell threshold. Not much change if we include the change of threshold

The left panel in Figure 3.10 (p27) shows the average return period for cold spell of a given duration. The return period is equivalent to one over the average probability for getting at any winter a cold spell that lasts for at least a given number of days. A cold spell of 10 consecutive days (defined on the 10% threshold of 1960-1999 period) had an average return time of 10 years in that period (Both Essence and ERA-40, 5-10E,50-55N). For the 2010-2050 period, the return period increases by a factor between 3 and 4, or equivalently, it becomes 3-4 times less likely that a cold spell of 10 days will occur at any winter. If one, however, accounts for the changes of the 10% of temperature (i.e., if a relative threshold is used), no significant changes are observed. This is shown in the right panel, for two even further separated periods. Also shown are the individual ensemble members (grey dots), which well cover the observed record.

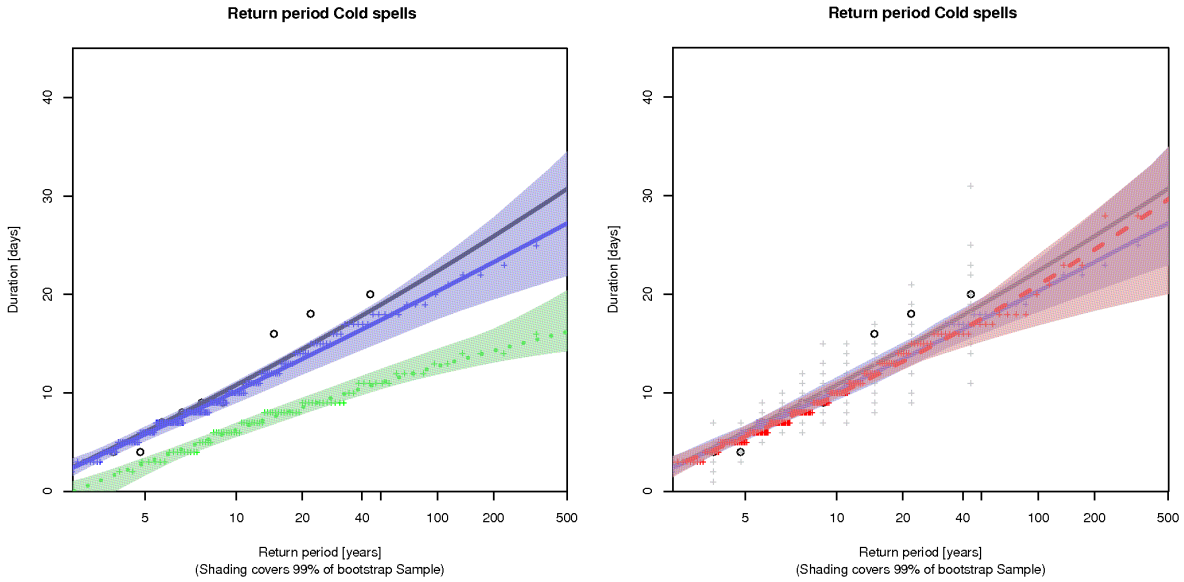

(a) Threshold based on 1960-1999 period

(b) Each period uses its own threshold

Figure 3.10: (a) Return period plot for cold spells (Absolute measure). Black: ERA-40. Blue 1960-1999 Green 2010-2050 period.(b) Return period for cold spells (Relative measure). Black: ERA-40. Blue 1960-1999. Red: 2060-2099. Grey crosses indicate the individual ensemble members for 1960-1999. Modified after de Vries et al (2012b). Blockmaxima period: 4 years.

3.7 Mechanism. What causes the reduction of the daily temperature variability?

Both a stronger mean westerly circulation and a reduced east-west temperature gradient lead to a reduction of temperature standard deviation

Figure 3.11 shows several scatter plots to illustrate the sentence above. For each ensemble member of Essence we computed the changes of three variables (temperature standard deviation, large-scale westerly circulation and large-scale east-west temperature gradient) over 150 years (using linear regression with time). These time-regressed Δ values are shown as fraction with respect to their 1960-1990 average values. Subsequently, regressions were made for the scatter plots. The physical picture in mind is consistent with the regression relations. That is, an on average stronger westerly circulation will lead to a reduction of the temperature standard deviation. In a similar way, the temperature standard deviation decreases if the large-scale east-west temperature gradient (which is already negative – it is colder to the east of us) decreases. The extent to which the two explaining variables (Tx and Gwest) are coupled has not yet been investigated in full rigor.

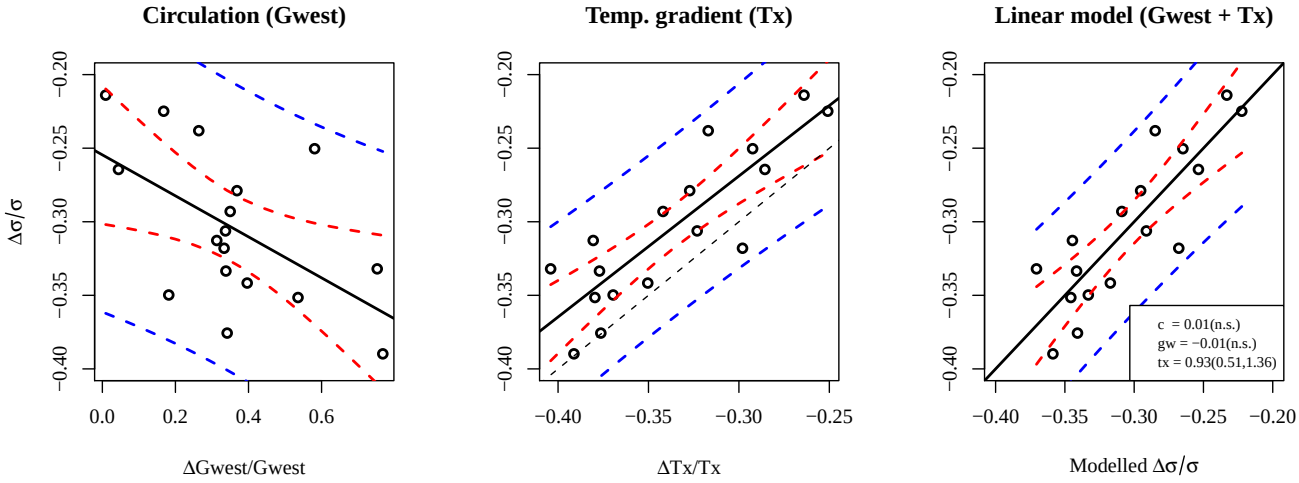

Figure 3.11: Scatterplots of projected change coefficients for each of the ensemble members. (left) Fractional change of standard deviation σ as a function of fractional change of westerly circulation ($Gwest$). (middle) Fractional change of σ as a function of fractional change of temperature gradient (Tx). Dashed line denotes $y = x$. (right) Multiple linear regression model using Gwest and Tx. Uncertainty estimation are also indicated by the red lines (uncertainty in the fitted regression lines) and blue lines (uncertainty band for standard deviation if the linear regression model is used for prediction). This figure is taken from de Vries et al (2012b).

Chapter 4

Atmospheric blocking

4.1 About this part

Cold weather in the Netherlands requires special circulation conditions. This part deals with this connection between cold days and the anomalous circulation

4.2 The circulation on very cold days

The European winter pressure climatology involves a large-scale low pressure system with its center near Greenland/Iceland and high pressures near the Azores. This dipole results in south-westerly winds that bring relatively mild and wet weather to our region. In contrast, the average pressure map for the 1% coldest days has high pressure over Scandinavia and Greenland, confirming that the circulation is "blocked" during very cold days

In this chapter we look more closely at the circulation associated with the coldest days. Circulation plays an important role in determining the temperature. In the introduction, where we compared the average pressure distributions of very cold and very mild winters, we have already seen a few examples of this strong connection. The wind direction and approximate strength is easily extracted from the pressure maps. Because they are in approximate geostrophic balance, the winds blow along rather than across lines of constant pressure (Holton, 1979). The wind direction is clockwise around a high-pressure system, and anti-clockwise around a low pressure system. The strength can be inferred from the density of pressure contours (higher density implies stronger winds).

Most of the very cold days (1% level) occur in January (Table 4.1 (p29)). Therefore it is instructive to discuss the cold-day circulation with respect to the January climatology. The climatology of mean sea-level pressure (mslp) and 2 meter temperature is shown in the top panel of Figure 4.1 (p30). The most distinct feature of the mslp-field (contours) is the low-pressure cell which reaches its minimum between Iceland and Greenland (termed the Icelandic low). The South-Westerly flow associated with this low-pressure brings relatively mild and moist air to Western Europe. Further in land the mean January temperatures quickly drop below zero °C. Also visible is the Azores High, a region of high pressure in the Atlantic off the coast of Morocco.

The bottom panel shows the composite pattern for mslp (contours) and 2m-temperature (colors) that accompany the coldest 1% days (measured with effective temperture) at De Bilt. Both the mslp and t2m pattern are markedly different from the January climatology. Clear features of the pressure field are (1) the high-pressure cell above Scandinavia exceeding 1025 hPa, and (2) the complete change of structure of the Icelandic Low. Its pressure minimum has moved South Westwardly. More importantly, rather than being almost zonally oriented, the pressure contours now move Southward and return over the Mediterranean.

Coldest (T_{eff})	**Oct**	**Nov**	**Dec**	**Jan**	**Feb**	**Mar**	**Apr**
1 % coldest	0%	0.6%	20.6%	51.5%	26.1%	1.2%	0%
5% coldest	0%	4.8%	22.7%	32.4%	30.0%	9.8%	0.2%

Table 4.1: Monthly distribution of 1% and 5% coldest days ($T_{eff} < -7.4$ °C and $T_{eff} < -2.7$ °C respectively) at De Bilt, according to the ERA-40 data. Taken from de Vries (2011a)

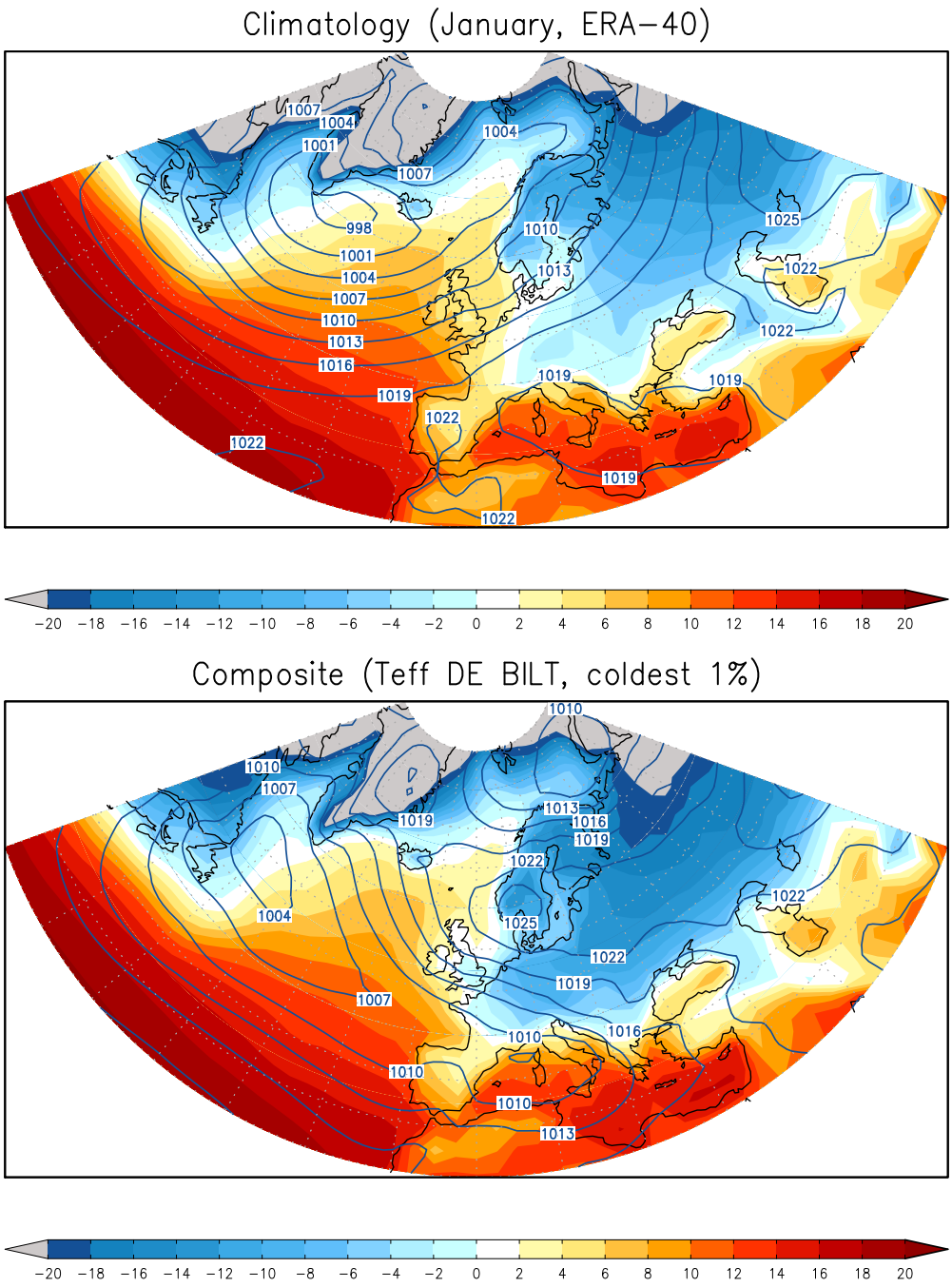

Figure 4.1: (top) January climatology of mean sea-level pressure (contours, interval 3 mbar) and 2-meter temperature in °C (colors). (bottom) composites of mean sea level pressure (contours, interval 3 mbar) and 2m temperature in °C.

The differences between climatology and the extremes can be analyzed in more detail by looking at their difference. Figure 4.2 (p31) shows the composites for the anomaly fields. The anomalies have been taken with respect to the multiyear monthly mean fields. The most striking feature of the mslp anomaly field is the presence of the large-amplitude dipole, with a positive maximum between Scandinavia and Iceland, and a minimum over Spain. With this mslp pattern, the temperature anomalies are hardly surprising: negative over Western and central Europe and positive over Greenland. Also visible is the positive anomaly over Turkey, caused by the South-Westerly flow bringing in air that originated over Africa.

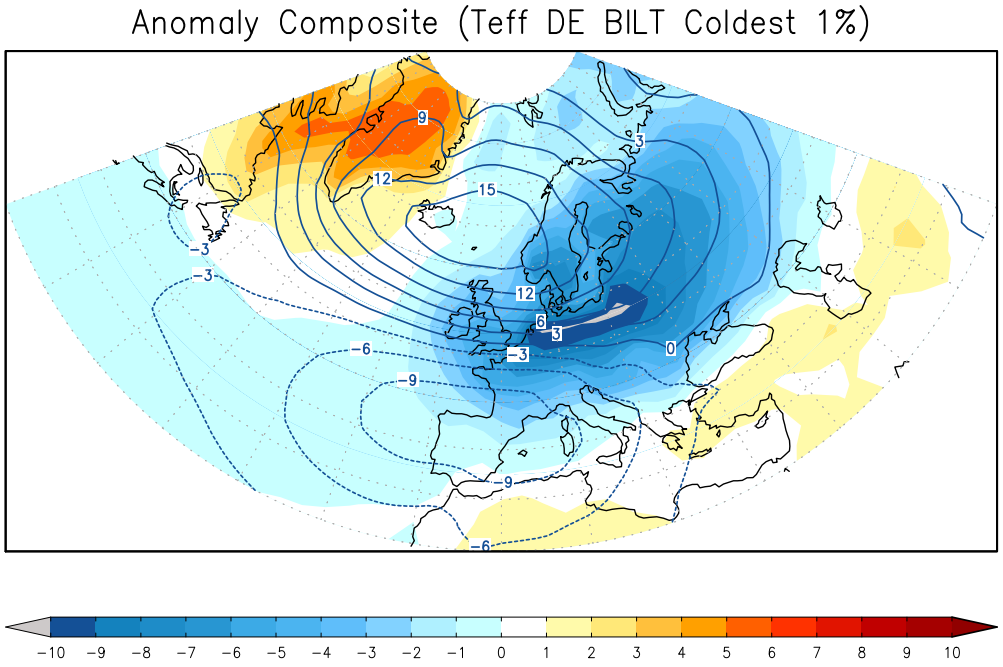

Figure 4.2: Composites of mean sea level pressure (contours, interval 3 mbar) and 2m temperature in °C for the anomalies from monthly-mean climatology.

Duration. How long lasts a typical cold spell that reaches 1% levels?

The blocking high-pressure pattern exists for at least two weeks at a similar geographical location (center between Iceland and Scandinavia). During this period cold air originating in Siberia is transported. On the north western flank of the high pressure pattern, Greenland experiences anomalous heating

In this section we examine the time-evolution of the composite fields. By this we mean that for each record that satisfies the composite criterion (coldest 1% T_{eff}), we extract the 10 days prior to this event, as well as the 10 days after the event. As a further restriction we do not allow the events to overlap. In the algorithm we first select the coldest day on record, and subtract the 10 days prior and after from the record. Then we seek the next coldest day (that still satisfies the 1% coldest T_{eff} condition) and repeat the process. Using the procedure leaves us with a total of 48 21-day events, approximately once every winter.

Figure 4.3 (p32) shows the evolution for a few selected times. More than a week prior to the event anomalously high pressure above Iceland is clearly visible together with a cold-air reservoir over the continent. In the following days, Easterly windspeeds increase and the high pressure cell gains amplitude. Simultaneously the negative pressure anomaly over the Mediterranean increases in amplitude, further enhancing the Easterly winds. As the cold air anomaly from Northern Siberia moves in a south-westerly direction, its amplitude increases (remember that air of the same cold temperature will correspond to a larger anomaly in the Netherlands than e.g. in Poland). At the day of the extreme event (the right panel on the second row), negative temperature anomalies of more than 10°C are observed. In our area the isobars are close together, implying that there is significant wind. After the event, the decay is a relatively rapid process. The high pressure anomaly moves eastward and decays in a couple of days. Note that because of the constraint of the events being isolated, the panel at $t = T$ differs slightly from that shown in Figure 4.2 (p31). The diffrence that has most effect is the location of the pressure maximum, and the associated temperature anomalies.

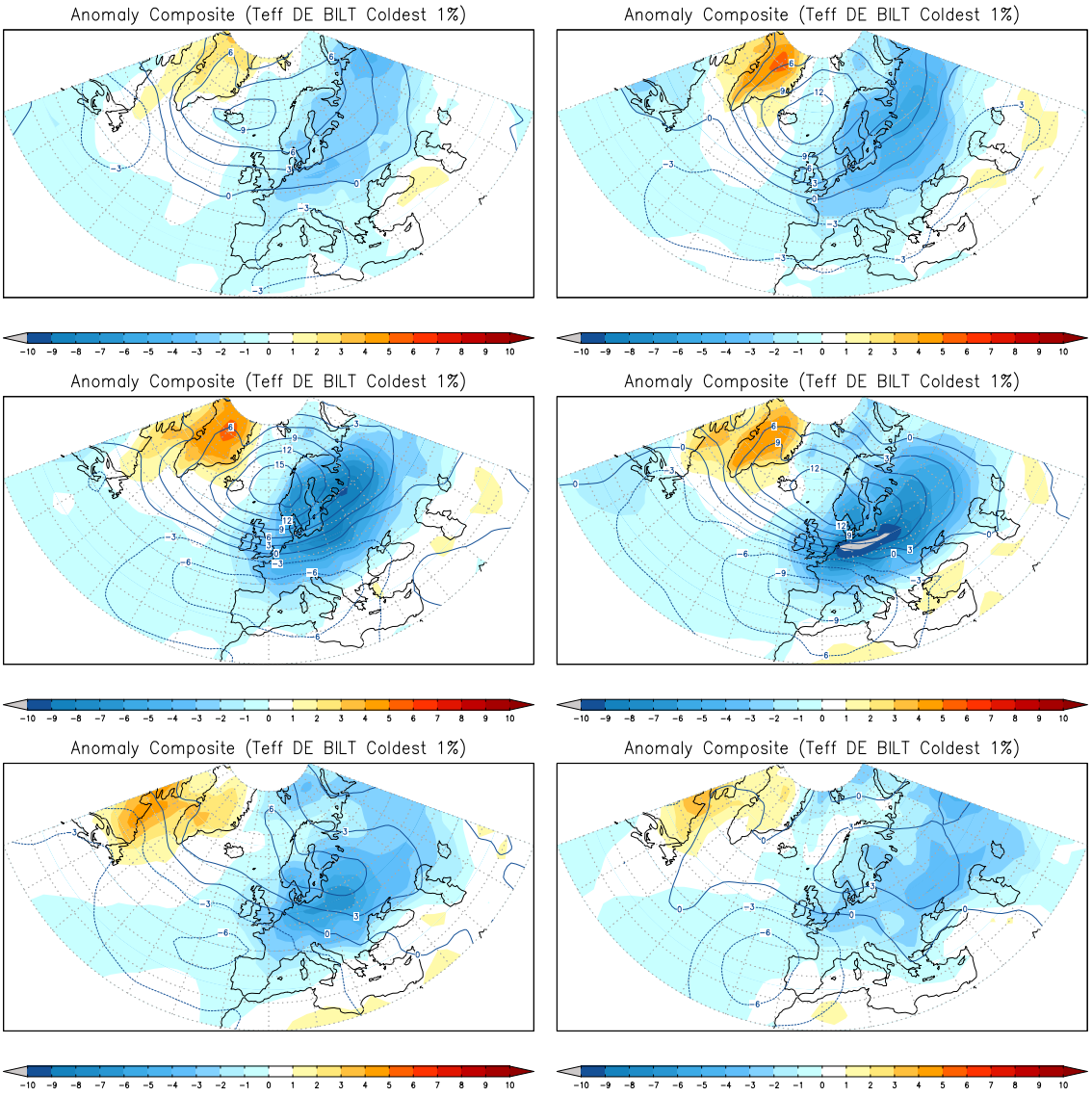

Figure 4.3: Time evolution (T-9 top-left,T-5,T-2,T,T+2,T+5 bottom-right) of the composites of mean sea level pressure (contours, interval 3 mbar) and 2m temperature in °C for the anomalies from monthly-mean climatology.

4.3 Frequency. How often occurs atmospheric blocking on a very cold day (1%)?

Atmospheric blocking in the Euro-Atlantic region occurs on 60-80% of the very cold days (1%) in the Netherlands. Spatially extensive blocking occurs during 20-40% of the very cold days. While this is up to 3 times more than expected from random selection, it also shows that blocking is not the only mechanism by which cold days can be found

Figure 4.4 (p33) shows for the European Atlantic region the probability for having atmospheric blocking during a very cold day (1%, locally defined). Atmospheric blocking is diagnosed using a conventional metric (Tibaldi and Molteni, 1990), applied at 60N. Following this metric [see also section C.1 (p45)] a longitude can be blocked or not blocked only. The left panel shows the probability for having a continuous section of at least 5 degrees longitude blocked in the domain 40W-40E. Clearly, this is not a very stringent condition, as it is satisfied around 40% of the time in the winter. Therefore, the probability for finding this type of blocking on a random day is about 40% (we will call this the "be-lucky" probability). Over the Netherlands, the probability is between 20-40% higher than the "be-lucky" probability. However, for a region south of the Netherlands, the probability increases further, to over 90%.

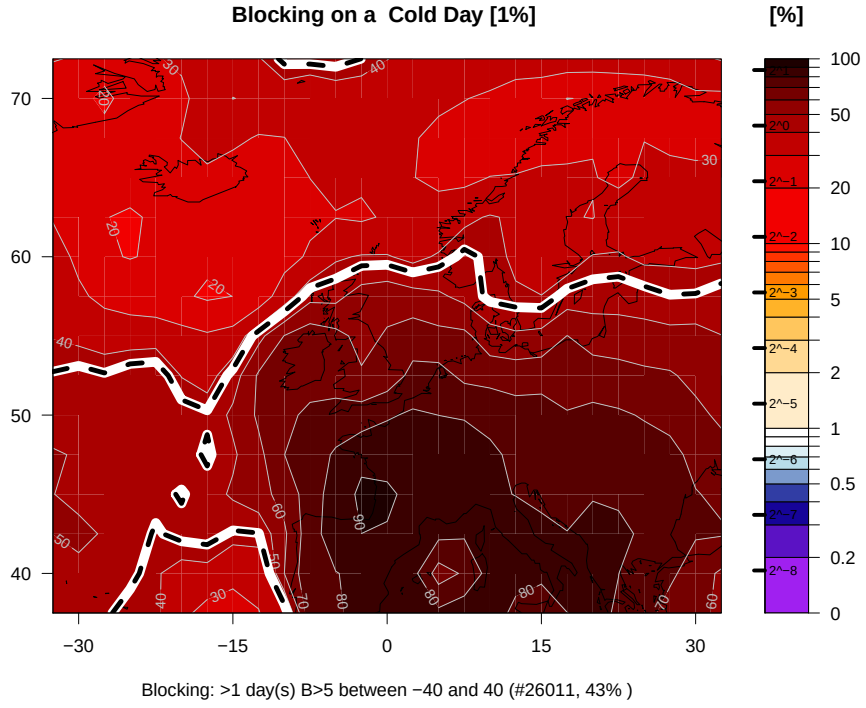

Figure 4.4: Probability for finding the atmosphere in an atmospherically blocked situation on a very cold day (1%). The thick black-white dashed line marks the "be-lucky" contour. Source: Essence 1960-1999 DJF.

Figure 4.5 (p34) (top) shows what is effect if one requires spatially extensive blocking (more than 30 degrees longitude blocked). Now, the "be-lucky" probability is much lower, around 12%. For the Netherlands, the probability for having a very cold day is up to 3 times higher than the "be-lucky" probability. Further south, this factor further increases, while it reduces strongly to the north. The bottom panel shows the effect of requiring a persistent block to be present at the coldest days. For the Netherlands, this happens only in 5-10% of the coldest days. Clearly, atmospheric blocking is not guaranteed to result in very cold days.

4.4 Probability. Increases blocking the probability for getting a cold spell (10%)?

If large-scale persistent blocking occurs, the probability for having at least 5 cold days in the Netherlands is a factor 75-150 larger than the random probability. However, the overall probability remains relatively low (30-40%), indicating that even persistent blocking not always produces a series of cold days

Figure 4.6 (p35) displays the probability for having at least 5 cold days (10%) in the 11-day period centered around a day with spatially extensive and persistent blocking. The black-white dashed contour indicates the "be-lucky", or

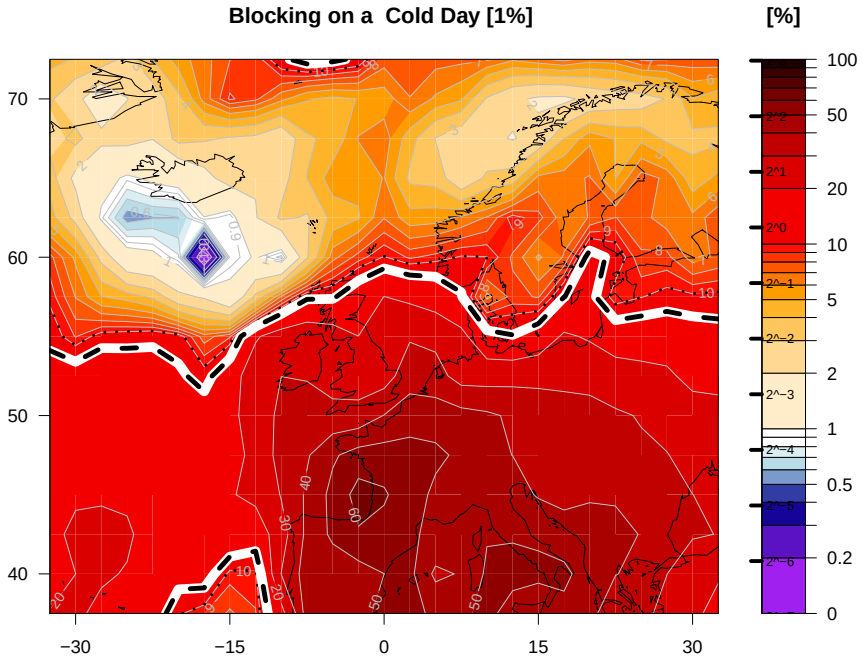

Blocking: >1 day(s) B>30 between −40 and 40 (#7353, 12%)

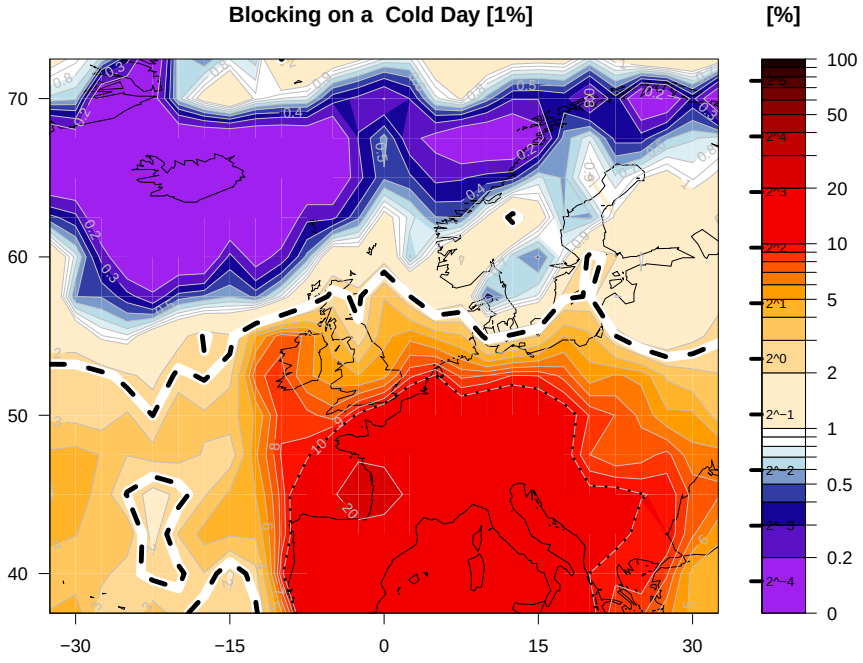

Blocking: >5 day(s) B>30 between −40 and 40 (#1424, 2.4%)

Figure 4.5: As in Fig. 4.4 (p33) but for spatially extensive blocking (top) and (bottom) spatially extensive and persistent blocking. Source: Essence 1960-1999 DJF.

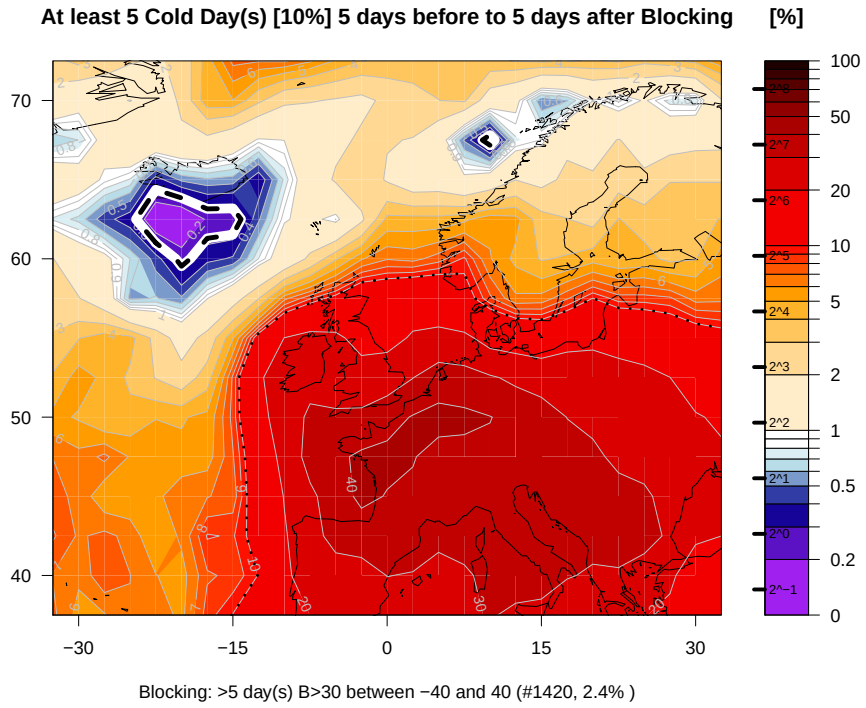

Figure 4.6: Probability for finding at least 5 cold days (10%) during the 11-day period centered around a day which met the following criteria: blocking at 60N, at least 30-degrees of longitude, for at least 5 days (2.4% of winter days). The 10% contour is dotted in black. The "be-lucky" contour computed from (4.1 (p35)) is drawn with the black and white line. The powers of two in the legend bar denote powers of two of the be-lucky probability. Data: Essence 1960-1999.

random probability for finding at least 5 cold days in an 11-day sub-series of winter days. This probability is easily calculated. It can be shown that the probability for finding at least n days (each with a probability of occurrence y) in an m-day window is

$$P(n, m, y) = \sum_{j=n}^{m} \left(\begin{array}{c} m \\ n \end{array} \right) y^j (1-y)^{m-j} \tag{4.1}$$

Using this equation with $m = 11$ and $n \in (5)$, we get $P(5, 11, .1) = 0.27\%$. This means, that on average only in 0.27% of the 11-day sub series, one will find at least 5 cold days, a very low probability indeed. For the Netherlands region, the "observed" probability obtained from the climate model output is much higher, between 30-40%. This corresponds to a factor 75-150 higher than the random probability. Further south, the probability increases to more nearly 50%, while it reduces strongly over northern Scandinavia. Indeed, atmospheric blocking generally causes mild weather over northern Scandinavia, due to the westerlies which occur to the north of the blocking high-pressure system.

Note that although the increase of probability is substantial compared to the random probability, the net probability for getting at least 5 cold days during strong persistent blocking remains relatively small, on the order of 15-30%. This means that spatially extensive blocking, as identified by the most commonly used index, can not be used very well to predict the occurrence of very cold days. In figure 4.7 (p36) various criteria (temperature percentile) and (minimal number of cold days) are varied. These variations show that the pattern is rather robust "across" the bottom-left to top-right diagonals: a similar pattern is obtained if the temperature threshold and the minimal number of cold days are reduced/increased simultaneously. Generally, the probabilities reduce (strongly) if more cold days and or a lower temperature threshold are imposed. The "be-lucky" probability also varies strongly with both, as expected.

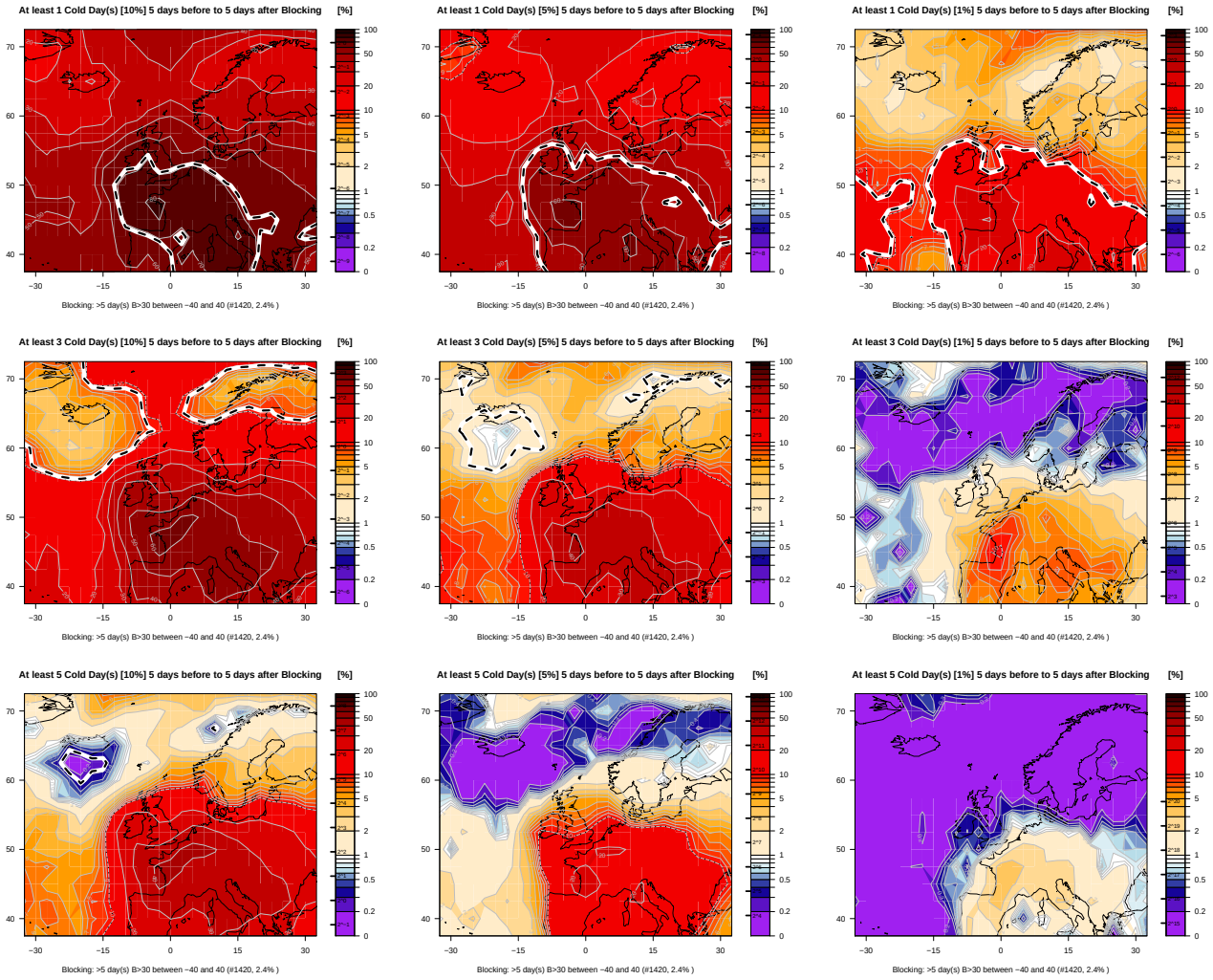

Figure 4.7: The sensitivity of the probability pattern to increasing number of cold days in the 11-day period around persistent blocking (top to bottom), and to a decreasing the temperature threshold (left to right). Data: Essence 1960-1999.

4.5 Future changes. Will the circulation on cold days be different in the future?

Following climate model output (Essence) the circulation patterns that make up the coldest days in the Netherlands will be very similar. However, the temperature of these coldest days increases markedly

In this section we discuss the mean sea-level pressure (mslp) climatology and dominant clusters obtained for the very cold days at De Bilt (now measured with $\bar{T}$). The mslp climatology of the coldest days in the Essence climate model is shown in Fig. 4.8 (p37). The right panel shows the difference, which is rather small, and can mostly be explained from a change of the mean winter pressure (not shown).

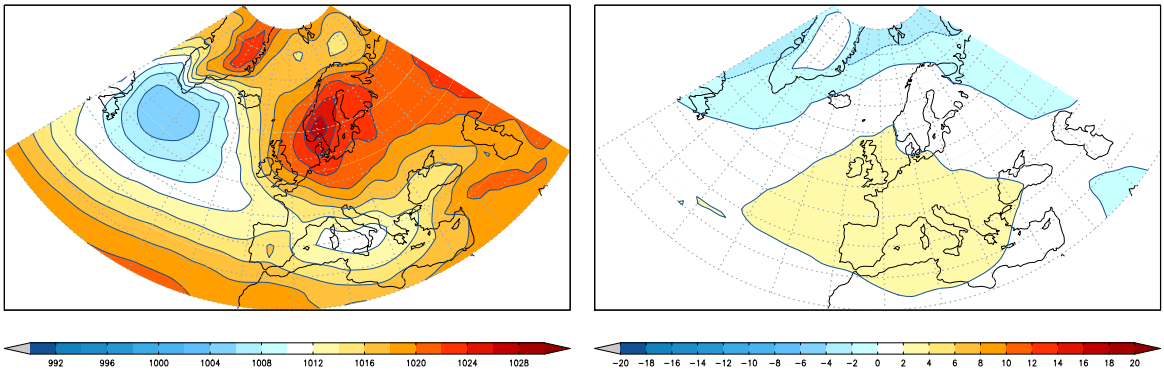

Figure 4.8: Mean sea level pressure climatology (in mbar) for the 1% coldest days (measured by $\bar{T}$) at de Bilt. (left) the 1951-2000 period of the Essence climate model (right) The difference FUT-NOW. Note that each dataset has been computed with its own 1% threshold.

4.6 Cold spells during persistent blocking in the future

There appears to be a small but systematic eastward shift of the preferred location for atmospheric blocking, as well as a reduction of the frequency. These changes lead to small increases of the probability that persistent blocking results in a cold spell of at least 5 days. However, if the future cold spells are computed with respect to current climate conditions a radically different picture emerges: these cold spells no longer occur in the future climate

Figure 4.9 is similar to Figure 4.6 (p35), but has been computed from the future period of the Essence climate model (2060-2099). In the future climate, atmospheric blocking frequencies are slightly reduced. In addition, there appears to be a small but systematic eastward shift of the preferred location of atmospheric blocking. This is a consequence of the increased strength of the mean zonal circulation, and is seen also in other climate models than Essence. The consequence is that the probabilities for having a future cold spell (defined with respect to the future climate!) during atmospheric blocking increase slightly (5-10%) for a large part of western and central Europe. The significance of these results have not been investigated. If the cold-spell thresholds are kept at their 1960-2000 levels a radically different picture emerges, as for none of the grid boxes shown in the figure any such cold spell is found in the future period (bottom panel). This demonstrates the huge decrease of the length of cold spells if measured with respect to current climate conditions.

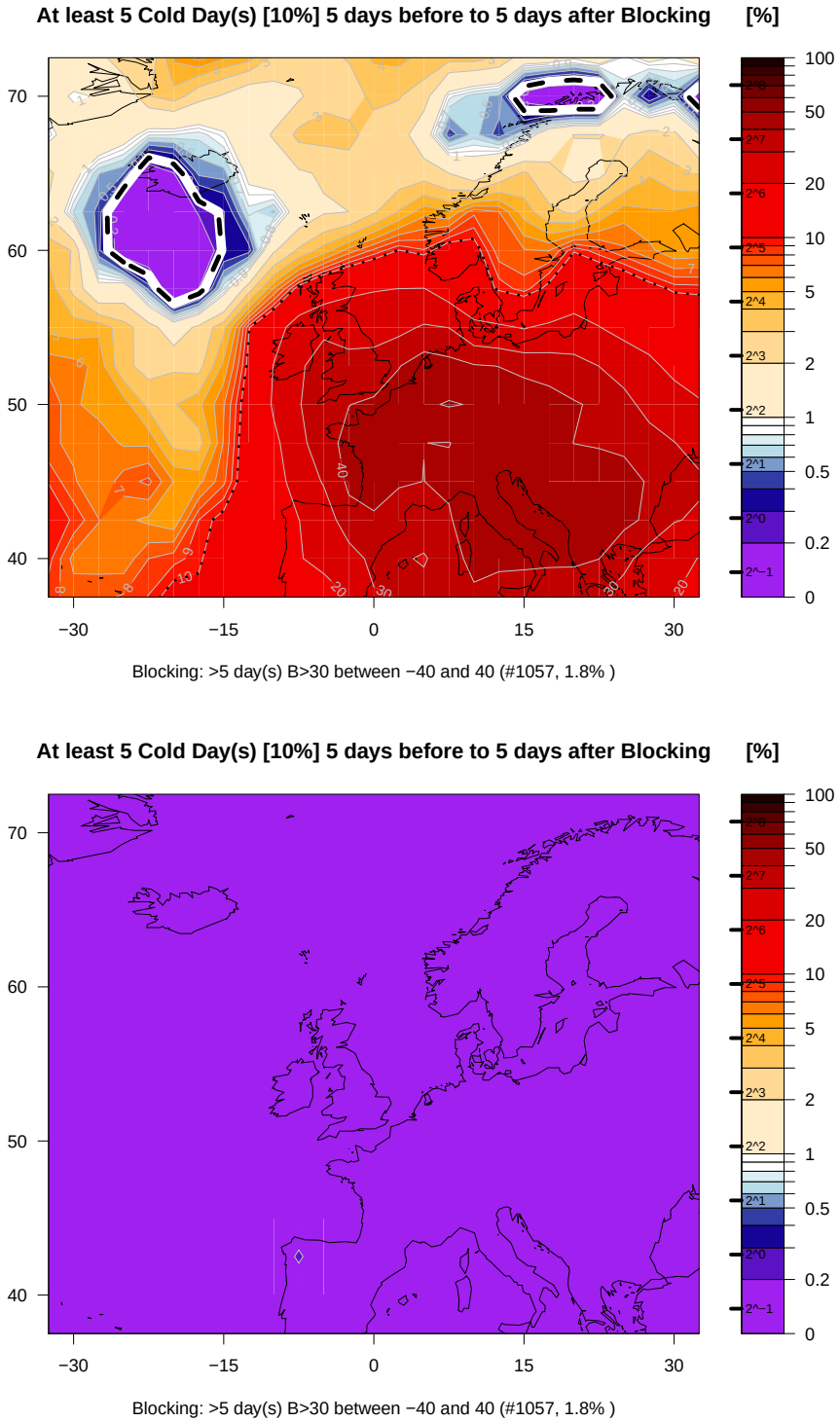

Figure 4.9: (top) As in Fig.4.6 (p35) but for the cold spells defined with respect to the future climate (2060-2099). (bottom) As in top panel, but when cold spells are defined with respect to present-day climate. Data: Essence 2060-2099.

Final remarks

Afterword

At the end of the previous KNMI report on low effective temperatures and heating degreedays, Wever (2008) stated that climate models would be needed to investigate the future changes of the extreme tails of the temperature distributions. The fundamental reason for this need was that, because of the short length of the observational time series, the transformation approach of Wever (2008) used linear extrapolation of the changes of the soft-tails to determine the changes in extreme tail-quantiles and their probabilities.

In the present study we have used ensembles of climate models. Nevertheless, most of the results described in the current report indicate, perhaps surprisingly, that the future changes of winter temperatures (heating degreedays, cold spells) and even atmospheric blocking (de Vries et al, 2012c) can indeed be reasonably accurately understood by just changing the mean and variance (or standard deviation) of the relevant underlying distributions.

The changes of the winter heating degreedays distribution are captured by just changing the mean and interannual variability. Many statistical properties of the cold spells of the future become similar to those of the current climate after rescaling (de Vries et al, 2012b). This basically means that the research has provided more evidence of the applicability of the methods used in KNMI'06 and Wever (2008). In addition, sound physical reasoning can now be given to explain why the scaling-approach may work so well. For example, the standard deviation of the temperature distribution decreases in the future because the east-west temperature differences reduce in the winter. This reduction of the temperature gradient is robustly simulated in many climate models with future concentrations of greenhouse gases, although the amount of reduction varies between models.

If one goes to the extreme quantiles (coldest 10% of all cold spells, approximately one day per winter), the simple scaling by just winter mean and daily standard deviation may become insufficient. However, we have not attempted to study these extreme quantiles in detail for the following reason.

There are considerable differences between the cold spells simulated with different climate models. To first order the model-differences in cold-spell statistics are caused by differences in the mean climate and variability of the models, and only in second order by the differences in dynamics of the extremes. This implies that there is a large spread between and thus uncertainty of the model predictions of for instance cold spells that reach low temperatures on an absolute scale (e.g., -5°C). Immediately coming up are questions like: Does one correct for bias with respect to observations? Does one discard models that are "bad" in simulating current climate if they have a "wrong" mean climate? Questions that deserve answers which are difficult to give. For one thing, the Netherlands is located on the border between extensive land and sea masses (Europe and Atlantic). Areas that are notoriously difficult for climate models to represent statistically well.

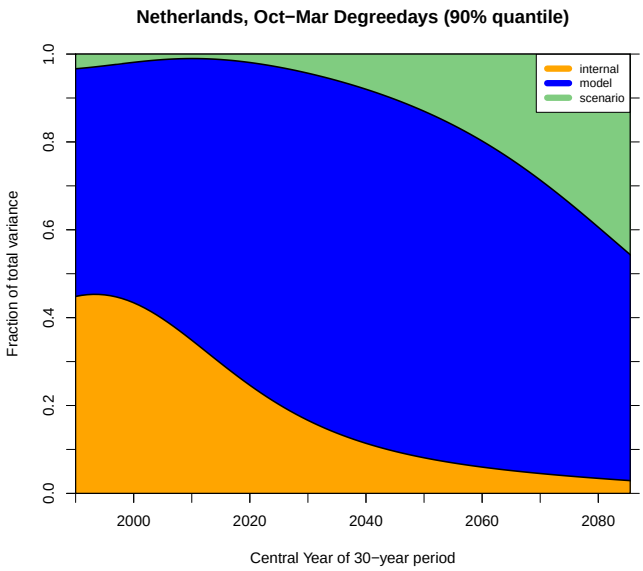

We conclude with one recommendation. The graph above represents the relative contributions to the total uncertainty of "cold" winters (natural variability in orange, model differences in blue and scenario differences in green). This graph is further explained on page 15. The blue area indicates the relative contribution of the model differences to the total ensemble spread (and hence the total uncertainty of the future predictions). This term is already large at short lead times, but further increases as time evolves. If this spread is to large extent determined by the spread in the simulated future mean climate and variability – the key outcome of this study – this calls for further research into the origin of the inter-model differences of the mean climate and variability. What are the physical underlying arguments causing these differences, and is there scope for improvement? If answers can be found to questions like these, this would be potentially of significant benefit to sectors like the gas and energy industry.

Appendices

Appendices

A Data

A.1 Reanalysis data – ERA-40

When talking about observations, we refer to data from the ERA-40 reanalysis project (Uppala et al, 2005). This data set, which describes the state of the atmosphere between September 1957 and August 2002, has been produced with a recent version of the ECMWF model using a process called data assimilation. With data assimilation all available observations (e.g., in-situ measurements, radiosondes, aircraft, ships, satellites) are combined to produce the best available estimate of the true global atmospheric state (called analysis) at 6-hourly intervals. The 'observations density' is generally very high over densely populated areas such as Western and Central Europe. Therefore we may expect a reliable reanalysis product over these regions. However, observations are relatively scarce over large parts of the oceans and over Antarctica which may result in possibly large (but unknown) deviations from the true state of the atmosphere.

A.2 Global climate models – Essence

For the projections in to the future, we use climate-model output from the Essence project (Sterl et al, 2008). Essence is an ensemble climate simulation with one particular climate model that scored high in a model intercomparison study (van Ulden and van Oldenborgh, 2006). The climate model was run 17 times, with slightly different initial conditions, starting in 1950 and ending in 2100, and adopting a specific greenhouse emission scenario (A1b, business as usual) from 2000 onward. As a result of the chaotic nature of weather fluctuations the different ensemble members can be considered as different (but equally likely) climate realizations. The large size of the ensemble makes Essence ideal for studying extremes, since for that aim one needs to capture natural variability as well as possible.

There are (small) biases between the climatologies of ERA-40 and Essence of for instance heating degreedays for the control period (Fig. S1 (p43)). In terms of surface temperature, Northern Scandinavia is a bit too cold compared to ERA-40. The variability is very similar for the two dataset. For this reason we have not further calibrated the Essence data set to European climate, except in certain cases. These exceptions will be mentioned explicitly.

A.3 CMIP3/CMIP5 – IPCC

The CMIP3 (Climate Model Intercomparison Project) database[1] consists of all climate model simulations that have been used in the development of the 4th IPCC assessment report (Meehl et al, 2007). Of this dataset we have used only those climate model simulations that had the same emission scenario as Essence (SRESA1b).

The CMIP5 archive (`http://cmip-pcmdi-llnl.giv/cmip5/`) consists of the data that will be used in the 5th IPCC report (IPCC-AR5). The CMIP5 ensemble has been created using a variety of climate models that are forced with 4 different Representative Forcing Pathways (forcing scenarios). These RCPs provide a range of possible future for the atmospheric composition. The RCPs complement and are meant to replace earlier scenario-based projections of atmospheric composition, such as those from the Special Report on Emissions Scenarios (SRES). Further details can be found in Meinshausen et al (2011) (open access).

[1] We acknowledge the modeling groups, the Program for Climate Model Diagnosis and Intercomparison (PCMDI) and the WCRP's Working Group on Coupled Modelling (WGCM) for their roles in making available the WCRP CMIP3 multi-model dataset. Support of this dataset is provided by the Office of Science, U.S. Department of Energy.

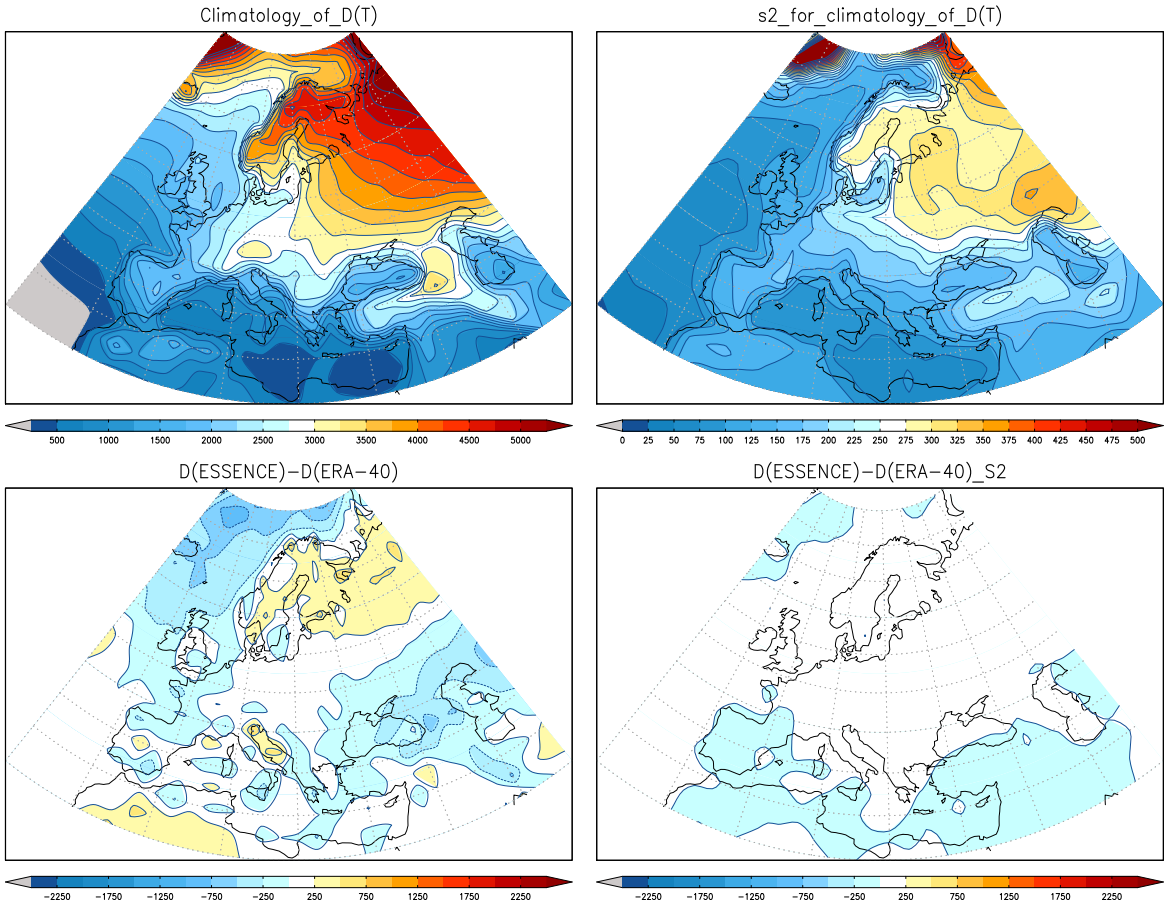

Figure S1: (top) Mean and standard deviation of winter HDD in ERA40. (Bottom) Difference between winter HDD of ERA-40 and Essence (control climate). (left) mean, (right) standard deviation

B Variables

B.1 Effective temperature

Various factors determine gas demand. Most obviously, gas demand is influenced by temperature. Furthermore, 'wind chill' not only influences human beings, it also affects buildings. The effect of wind speed can be measured and is generally in the direction of larger gas demand. Other factors, such as cloudiness and humidity also play a role but their effect is not taken into account in this study. Following Wever (2008), effective temperature is defined as

$$T_{eff} = \bar{T} - \frac{2}{3}|\bar{U}|, \tag{A.2}$$

where $\bar{T}$ is the daily mean temperature [°C] and $|\bar{U}|$ is the daily mean wind speed [m s^{-1}]. The factor $2/3$ has been determined empirically.

B.2 Heating degreedays

One of the many possible ways to assess the 'strength' of an entire winter half year (or any other time interval), is by computing the so-called heating degreedays D, which is defined as

$$HDD(\bar{T}) = \sum_{all\ days} \max(T_{threshold} - \bar{T}, 0), \tag{A.3}$$

where HDD has units °C day. In (A.3) above, the assumption is that gas is being used (for heating) whenever the daily mean temperature falls below $T_{threshold} \equiv$18 °C. For this threshold, the time series of yearly HDD values correlates well with total winter gas demand. However, as already noted by Wever (2008), for all winter days at De Bilt in the period from 1904 up to 2007 there were only 4 days where the threshold of 18°C was exceeded, implying that (at least for De Bilt) there is a strong relation between gas demand and the mean winter temperature. For this reason, an alternative way to compute the winter HDD is based on simply using monthly-mean or seasonal-mean temperatures. In this approximation, winter HDD is directly proportional to mean winter temperature. In some parts of this study, the latter approach has been taken, and heating degreedays are computed from monthly-mean temperatures (October-March) using 30 days per month

$$HDD' = 30 \sum_{months} (18 - \langle\bar{T}\rangle_{month}), \tag{A.4}$$

where $\langle\bar{T}\rangle$ denotes the monthly mean. For the winter half-year the differences between HDD' and HDD are generally very small for the Netherlands region, on the order of 1% or less.

C Methodology

C.1 Diagnosing atmospheric blocking

Atmospheric blocking can be diagnosed using a variety of measures. In this study, we have adopted the most commonly used method, which is due to Tibaldi and Molteni (1990). The blocking index is based on analysis of the geopotential height field at the 500 mbar pressure level. From this field (Z500 as it is usually called), one can directly obtain the large-scale circulation, and the blocking index basically diagnoses mid-tropospheric easterly flow. First, the meridional gradient of Z500 is computed as

$$GZ(\phi, t) = \frac{Z^+ - Z^-}{\phi^+ - \phi^-} \tag{A.5}$$

where ϕ denotes latitude and $\phi^\pm = \phi \pm \Delta$ with $\Delta = 10$ degrees latitude. Blocking is diagnosed at latitude ϕ and time t if the following two conditions are satisfied for any value of $\delta \in (-5, 0, 5)$:

$$GZ(\phi^- + \delta, t) \geq 0, \quad GZ(\phi^+ + \delta, t) \leq -10. \tag{A.6}$$

In this study we have computed the blocking index for $\phi = 60°$N.

C.2 Ensemble spread in climate-model output

In the main text we have related the spread in the climate model results to three different sources:

N Internal or natural variability, which describes the effect of the natural fluctuations that occur on a variety of time scales even if the climate is stationary. Generally the internal variability is largest at the shortest time-scales.

M Model variations. The climate models are all slightly different. Their response to changes in forcing, such as those arising from changes in greenhouse gas concentrations, is also different.

S Scenario variations. The same climate model responds differently to different forcings. The CMIP5 ensemble has been created using a variety of climate models that are forced with 4 different RCP (forcing) scenarios (Meinshausen et al, 2011).

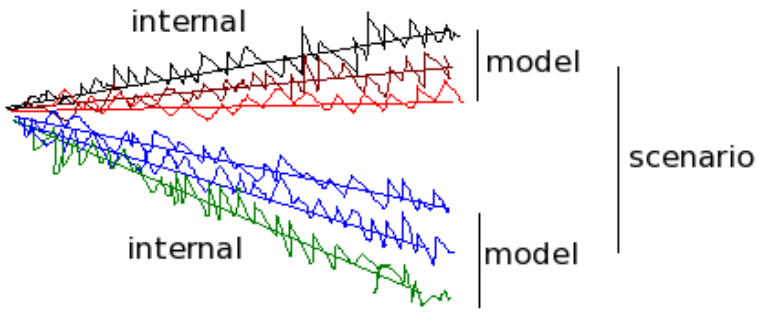

Figure S2: Cartoon of the three sources of spread (uncertainty) in the climate model ensemble results. The wiggliness of the lines represents internal variability. The differences between the lines fitted through the data, summed for each scenario represent the model uncertainty. The differences between the mean response for each scenario represents the effect of scenario differences.

Figure S2 shows a cartoon of the three sources of uncertainty. In a recent paper Hawkins and Sutton (2009) devise a simple method to separate the three source of spread (uncertainty)[2]. The same method is applied here. Let $X_{m,s}(t)$

[2]Interested readers are advised to go `http://climate.ncas.ac.uk/research/uncertainty`, for more details.

denote the raw model output at time t of ensemble member m, which is created with scenario s. In the first step, a smooth line $x_{m,s}(t)$ is fitted through this data:

$$X_{m,s}(t) = x_{m,s}(t) + \epsilon_{m,s}(t) \tag{A.7}$$

In this study we used a polynomial of degree 3, but more sophisticated methods can be used. The natural variability of this component is $\epsilon_{m,s}(t)$. The total natural variability N^2 is defined as just the average of the time-variance of ϵ of all models:

$$N^2 = \frac{1}{N_m} \sum_m var_t \left[\epsilon_{m,s}(t)\right] \tag{A.8}$$

where N_m is the total number of ensemble members. In this method, therefore, the natural variability is considered to be approximately independent of time. Also here more sophisticated methods could be used (for instance using running variability measures), but this has not been considered. The next step is to identify the model variability. Given the smooth fits $x_{m,s}(t)$, the total model variability $M^2(t)$ is defined as the model variability at each time, averaged over the different scenarios:

$$M^2(t) = \frac{1}{N_s} \sum_s var_m \left[x_{m,s}(t)\right] \tag{A.9}$$

Here the assumption is that model spread is similar for the different scenarios. Finally, the scenario differences are computed as:

$$S^2(t) = var_s \left[\bar{x}_s(t)\right], \tag{A.10}$$

where $\bar{x}_s(t)$ denotes average response for each scenario. If all sources of variability are independent, the total variability can be written as:

$$T^2(t) = N^2 + M^2(t) + S^2(t) \tag{A.11}$$

In practice this relation is approximately satisfied. The one and two σ levels shown in Figure 2.5 (p12) have been computed using this approximation.

C.3 Transformation of time-series in KNMI'06

The statistical transformations used in the KNMI'06 scenarios and Wever (2008) are based on the following steps. (More information can be found at the KNMI website: http://www.knmi.nl/klimaatscenarios) First, three quantiles and the mean of the distribution are estimated from the observations and from simulation with climate models: T10, T50, TMEAN and T90. They are determined from climate model output for two target times: 2050 and 2100. In the next step, temperatures smaller than T50 in 1990 are transformed as

$$T_{2100}(t) = TMEAN_{2100} + a\left[T_{1990}(t) - TMEAN_{1990}\right] \tag{A.12}$$

where,

$$a = \frac{T50_{2100} - T10_{2100}}{T50_{1990} - T10_{1990}} \tag{A.13}$$

A similar transformation is used for temperatures larger than T50. For different time horizons, linear interpolation is used between the closest target years:

$$T50_{2030} = \left(\frac{2030 - 1990}{2050 - 1990}\right) T50_{2050}. \tag{A.14}$$

The connection with the scaling approach used for the cold spells (subtract mean and divide by standard deviation) is clear, since for a normal distribution $T50 - T10 = 1.2815\sigma$. Thus, for a normal distribution

$$a = \frac{T50_{2100} - T10_{2100}}{T50_{1990} - T10_{1990}} = \frac{\sigma_{2100}}{\sigma_{1990}}. \tag{A.15}$$

Thus for normal distributions the time-series transformation used in KNMI'06 and those used in the cold-spell research are equal.

D Does chaotic mean random?

The Earth atmosphere is in chaotic state, not in a random state. A random state would render single deterministic forecasts useless beyond the shortest time scale. In reality, deterministic forecasts loose relevance usually within 10 days, due to strong nonlinear interactions. Useful probability statements can still be made beyond 10 days, if a model can be run multiple times, with different initial conditions

Living in a country where the weather is extremely variable, people in the Netherlands (almost) invariably like discussing the weather. When the winter season (October to March) approaches, typical questions are discussed. When will the first snow fall? Will we get a period with temperatures low enough to make ice-skating on the lakes and canals possible? Will we get another 'Elfstedentocht' ("It should be, shouldn't? We've had none for so long")? Such questions are not easy, if not impossible to answer exactly. What are the reasons behind this? What prevents us from predicting with high chance of success the occurrence of a cold winter, or more generally, the weather on time scales longer than roughly ten days? The short answer is that observations suggest that the atmosphere is highly chaotic. The consequence of chaoticity is the often quoted 'butterfly-effect', first termed so by Lorenz (1963). The butterfly-effect (see also Figure S3) describes the possible effect of a flying butterfly (small spatial scale) somewhere in the Brasilian rainforest, on the development of a major storm (large scale) a few days later over Western Europe. In this description, the butterfly is used as a metaphor for extreme sensitivity to initial conditions. Apparently, our earth-ocean-atmosphere system is in such a state that even the slightest initial disturbance (such as an observational error) will quickly accumulate and influence the larger (observed) scales. The limited observational network inevitably confronts us with a predictability horizon. Beyond this horizon deterministic forecasts made with a single model quickly loose their validity.

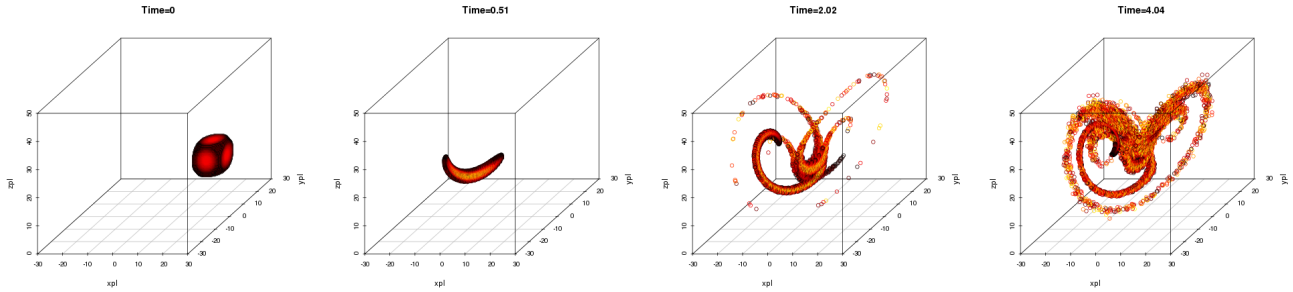

Figure S3: Lorenz '63 model. 3 simple, but nonlinear differential equations display for certain parameters sensitive dependence to initial conditions. The initially cubic cloud of 8000 points is quickly distorted, after which the characteristic double-winged pattern develops. Color coding is such that yellow (black) are points that are initially close to (far from) the center of the cube. The entire animation can be viewed at: `http://www.knmi.nl/~vries/Research/research_lorenz.html`

It is important to note that chaotic should not be read as 'completely random'. For suppose we knew all equations describing the evolution of all variables (like for example temperature, pressure and wind, ocean state etc) exactly, then, in theory at least, one could predict the future state of the system by solving these equations with an accurate numerical algorithm (even if the system were chaotic). With a random process this would not be possible. However, the solvability of the future state requires an exact description of the current state of the system and exact knowledge of the equations governing their evolution. Unfortunately, we have neither. First (and possibly foremost) we do not know the current state of the earth-atmosphere system exactly (e.g., the clapping wings of the butterfly in the distant Brasilian rain-forest). There are uncertainties in the observations. These uncertainties result in initial-condition errors. Second, we do not know all equations. In fact, many aspects of the earth-atmosphere evolution are 'parameterized', which means that we describe the behavior using approximate equations that involve one or more empirically determined parameters. The errors introduced by the imperfections of the model will be termed model-error.

Researchers nowadays use statistical techniques to assess or even to improve the reliability of forecasts. All major weather prediction centers use ensemble techniques where a whole ensemble of forecasts is created (often at lower resolution to reduce computational costs), that start from slightly perturbed initial conditions. In many cases it is found that the ensemble-mean better describes the future state than the future state described by the single model

run. Moreover, by using the ensemble, one also gets approximate knowledge of the probability density function, which describes the chance of occurrence.

Unfortunately it is rather less trivial to overcome the problems associated with model error and much research is being undertaken to tackle this problem (e.g., multi-model ensembles, ensembles with perturbed physics). KNMI is carrying out pioneering research in this direction in an EU-funded project called SUMO (SUper MOdeling). In "super-modeling" different models are dynamically coupled. As a consequence they interact and exchange information while running a simulation. By using the observations to train the inter-model "connections" the hope is that the super-model outperforms the individual models. The first results of super-modeling, applied to idealized yet fully nonlinear chaotic models such as the Lorenz'63 model are promising (van den Berge et al, 2011)[3].

[3]Interested readers are advised to go to `http://www.knmi.nl/samenw/sumo/`.

E De koudegolven van de toekomst

Klimaatstudies laten veelal zien dat in een globaal opwarmend klimaat de winters in Nederland ook aanzienlijk warmer zullen worden. Niet alleen gemiddeld zullen de winters warmer worden, strenge winters zullen ook minder voorkomen. Over de precieze hoeveelheid opwarming verschillen de modellen onderling nog behoorlijk. In dit artikel bestuderen we klimaat-model simulaties op veranderingen van 'relatieve' kou

[4]Kou is een relatief begrip. Wat voor de één reeds als herfst aanvoelt, ervaart een ander nog als zomer. In Rusland klaagt men niet als het in de winter -15^{o}C wordt; hier in Nederland komt de maatschappij praktisch tot stilstand. De menselijke ervaring en beleving van kou hangt af van het klimaat waarin men leeft. Daarom zullen we ook in de toekomst koude periodes blijven beleven. Helaas voor de schaatsers onder ons: voor ijsvorming heeft men alleen wat aan 'absolute' kou. Bij +1^{o}C, hoe waterkoud het ook aanvoelt, krijgen we geen ijs.

Traditioneel worden in Nederland in de winter het aantal ijsdagen en vorstdagen bijgehouden. Deze meten respectievelijk het aantal dagen dat de temperatuur de gehele dag of gemiddeld onder het vriespunt ligt. Het zogenaamde Hellmann getal is ook belangrijk. Dit is het getal dat je krijgt door de som van de gemiddelde etmaal temperaturen onder nul bij elkaar op te tellen en het minteken weg te halen. Het Hellmann getal, dat in milde winters kleiner is dan 50, maar in zeer strenge winters kan oplopen tot 300, geeft een maat voor de totale hoeveelheid kou, of 'strengheid' van een winter [5]. Er zijn inmiddels vele observationele studies verschenen die laten zien dat er in deze getallen reeds enige tijd een dalende trend zit, en dat niet alleen voor Nederland. Als voorbeeld dient Figuur S4, die is ontleend aan de website `eca.knmi.nl`.

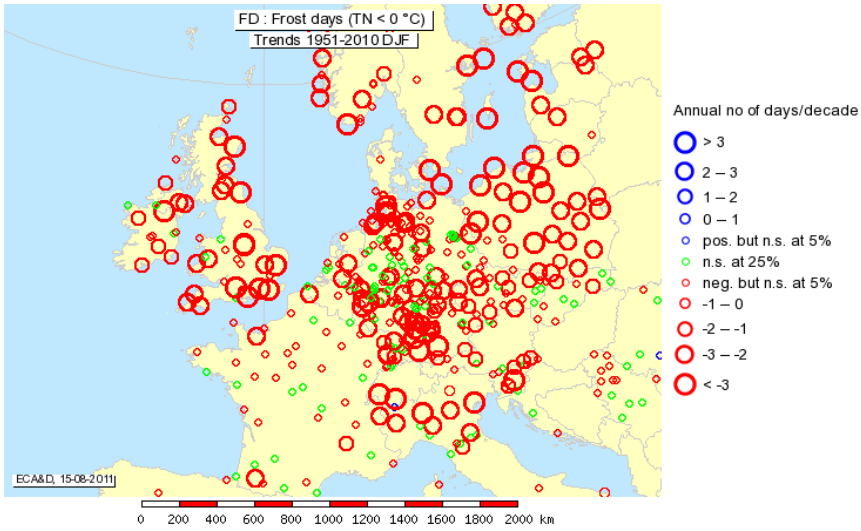

Figuur S4: Lineare trend in het aantal vorstdagen per decade (negatief betekent afname), berekend over de periode 1951-2010. Bron: `http://eca.knmi.nl`.

Ook model-simulaties, waarin mogelijke toekomst-scenario's worden gerealiseerd met behulp van geavanceerde klimaat-modellen, laten vrijwel unaniem verdere afnamen zien van deze getallen. Een voorbeeld. In een vrij recente simulatie met het klimaat model van het Max Planck Instituut in Hamburg (het zogenaamde Essence ensemble (Sterl et al, 2008)) wordt een toekomstig klimaat gesimuleerd dat niet al te sterk opwarmt. Toch schetst dit model reeds een somber beeld voor de toekomst van de ijspret liefhebber: De koudste winters in de periode 2060-2100 zullen in Nederland niet kouder zijn dan de warmste winters uit de periode 1960-2000. Dit is geïllustreerd in Figuur S5, waarin de zogenaamde graaddagen zijn berekend. Analoog aan het koudegetal van Hellmann, worden graaddagen gedefinieerd als de som van 18-T over alle winterdagen. De 18 graden limiet komt vanuit de energie sector: dit is bij benadering de temperatuur waarop de kachels aan gaan. Echter, model onzekerheid is nog substantieel. Sommige modellen geven een kleinere opwarming, andere een grotere. Dit maakt het moeilijk om precieze uitspraken te doen over de veranderingen die gaan plaatsvinden.

[4]This appendix has appeared in *Meteorologica* as (de Vries, 2011b), and in modified form on the KNMI website `http://www.knmi.nl/cms/content/104358/koudegolven_van_de_toekomst`.

[5]Meer informatie over het Hellmann getal is te vinden op `http://www.knmi.nl/cms/content/27255/koudegetal`.

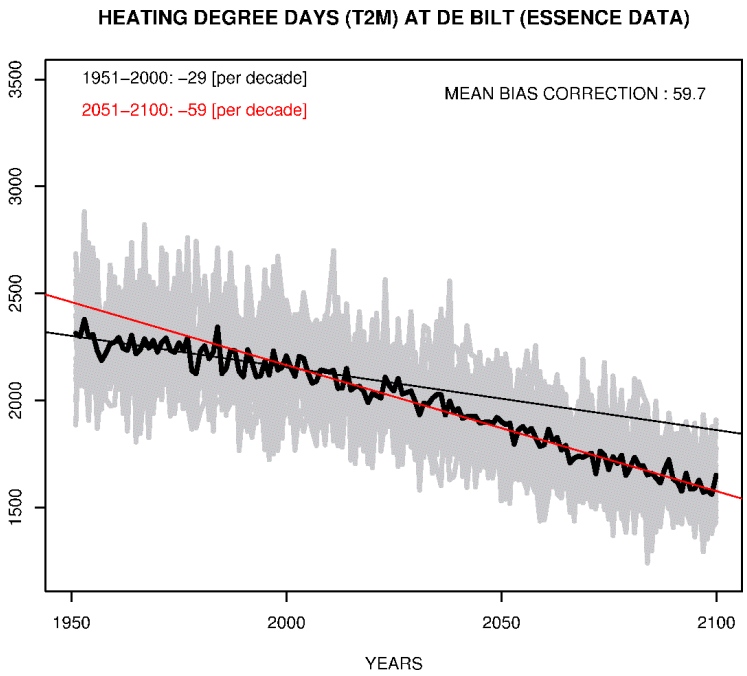

Figuur S5: Graaddagen (winter som van $18 - T$, hier genomen over de maanden Oktober tot en met Maart) in Essence, berekend voor Nederland. Lineare trends door de eerste en laatste 50 jaar van de door Essence beschreven period zijn door middel van respectievelijk een zwarte en een rode lijn weergegeven. Een correctie heeft plaatsgevonden om het model klimaat beter bij de waarnemingen te laten passen.

Relatieve kou

Maar dan terug naar het begin. Kou is een relatief begrip. De perceptie van kou hangt samen met het klimaat waarin wij leven. Hoe beschrijven klimaatmodellen 'relatieve' koude golven? Met 'relatief' bedoel ik hier, relatief ten opzichte van het referentie temperatuur klimaat uit het betreffende klimaatmodel. Zo'n referentie klimaat kunnen we beschrijven met behulp van de waarschijnlijkheidsverdeling voor de temperatuur. De belangrijkste parameters van deze verdeling zijn de bekende begrippen gemiddelde μ en standaard afwijking σ. Een zogenaamde 'normale' verdeling ligt vast door deze twee parameters. Echter, de waargenomen (en gemodelleerde) waarschijnlijkheidsverdeling voor temperatuur is niet precies 'normaal'. In de winter blijkt dat deze verdeling een relatief lange linker-staart heeft: extreem lage temperaturen komen relatief vaker voor dan extreem warme dagen. De oorzaak hiervoor kan gevonden worden in atmosferische circulatie anomalieën (zoals blokkades) die een asymmetrische temperatuur response hebben.

Het kan beargumenteerd worden dat de eerste twee centrale momenten van de verdeling, zoals μ en σ ook wel genoemd worden, goeddeels onze perceptie van kou bepalen. We hebben allemaal een soort gevoel voor de gemiddelde temperatuur en de meest voorkomende variaties daaromheen. Het is daarom zinnig om een anomalie temperatuur te definiëren

$$T'(x,t) := \frac{T(x,t) - \mu(x,t)}{\sigma(x,t)}, \tag{A.16}$$

waarbij x de geografische positie en t de tijd. Omdat we ons in een veranderend klimaat bevinden zullen μ en σ mee veranderen. We schrijven dus $\mu(t)$ en $\sigma(t)$, waarbij gekozen is om $\mu(t)$ en $\sigma(t)$ te bepalen als 21-jaars lopende wintergemiddelde waarden. Het zijn ook deze twee momenten die in de klimaatmodellen de grootste veranderingen naar de toekomst laten zien. Het gemiddelde neemt toe, de standaard afwijking neemt af. De laatste afname is consistent met een substantiële afname van de gemiddelde oost-west temperatuur gradiënt (de zee warmt minder snel op dan het land), alsmede een lichte toename van de gemiddelde west circulatie in de winter (de Vries et al, 2012b) (zie tevens kader).

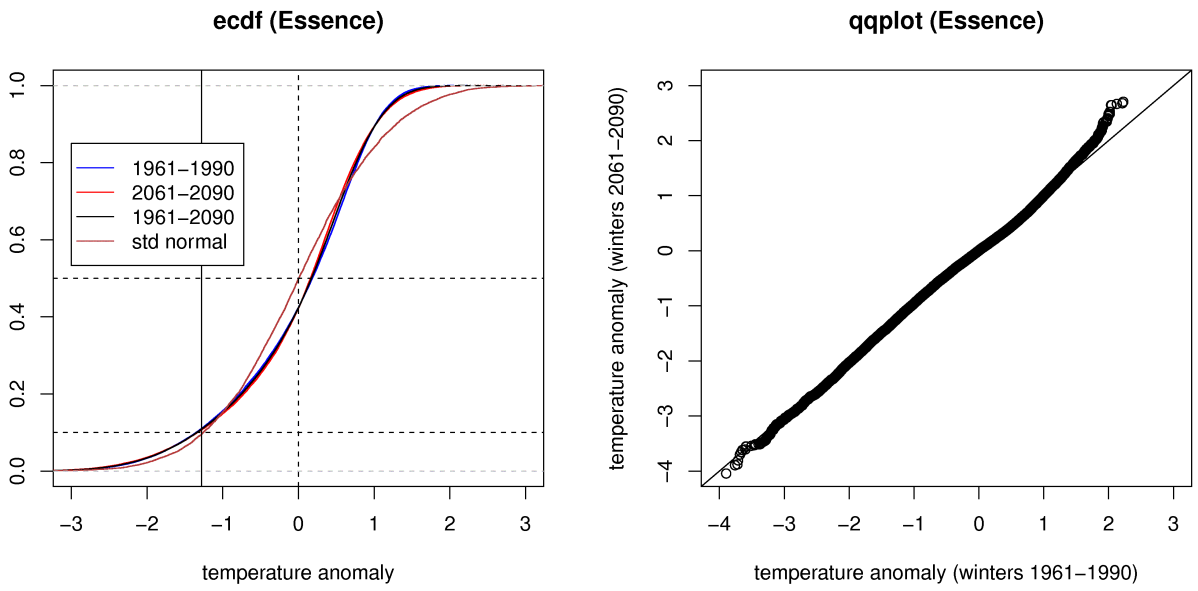

Figuur S6: (links) Empirische cumulatieve distributie functie voor Essence temperatuur anomalieën. Tevens wordt de normale cumulatieve distributie gegeven, die door $(0, 0.5)$ gaat. De verticale lijn markeert de positie $x = -1.2815$, het 10% niveau van de standaard normale verdeling. (rechts) Zogenaamde "quantile-quantile plot" waarbij de temperatuur anomalieën van de ene periode van Essence tegen die van de andere periode zijn uitgezet.

Standaard afwijking van de temperatuur

De instantane temperatuur wordt bepaald door locale processen (straling e.d.) en transportprocessen. In de temperatuurbalans vergelijking (typische vorm $\partial T/\partial t = \sum_i p_i$ met p_i alle processen) is een belangrijke rol weggelegd voor temperatuuradvectie. Temperatuuradvectie is de temperatuurtendens die het gevolg is van lucht die ons bereikt (via de wind) maar die een andere temperatuur heeft. Als het in het oosten kouder is dan bij ons, dan zal het geleidelijk kouder worden als de wind uit het oosten waait. De modellen laten zien dat de horizontale temperatuurverschillen in de toekomst geleidelijk zullen afnemen (het land warmt sneller op dan de zee). Deze afname leidt direct tot een afname van de standaard afwijking van temperatuur. Voor een aantrekkende gemiddelde westcirculatie geldt een dergelijke redenering: met het toenemen van de westenwind zal de wind ook vaker van zee komen. De temperatuur verschillen boven zee zijn stukken kleiner dan die boven land, en dus zal ook bij toenemende westenwind de temperatuur standaard afwijking afnemen.

De meeste klimaatmodellen laten voor de toekomst een (lichte) toename zien van de gemiddelde sterkte van de west circulatie. De afgelopen winters hebben echter overtuigend laten zien dat de (natuurlijke) variabiliteit van het klimaat systeem thans (nog) zo groot is dat lange perioden met oostenwind zeker nog tot de mogelijkheden behoort. Toch heeft de recente opwarming van Europa in zekere zin al zijn 'tol' geeist: de 2009-2010 winter was dan qua circuatie karakteristieken en persistentie wel te vergelijken met die van 1962-1963, maar kwam daar qua 'absolute' kou toch bij lange na niet bij in de buurt (Cattiaux et al, 2010).

Laten we nu terugkeren naar de temperatuur anomalieën en de koudegolven. We definiëren het begrip 'koude dag' ('koudegolf' voor een opeenvolging van koude dagen) als een dag waarop de gemiddelde temperatuur niet hoger komt dan die behorend tot de koudste 10%, indien de temperatuur verdeling een normale verdeling zou zijn met gemiddelde $\mu(t)$ en standaard afwijking $\sigma(t)$. Deze aanpak geeft de mogelijkheid om extremen in heden en toekomst te vergelijken zonder de invloed van de (veranderende) extremen zelf. Er wordt hierbij aangenomen dat de extremen weinig invloed hebben op gemiddelde en standaard afwijking. In een vergelijking betekent dit dat

$$T_{koud} := T' \leq -1.2815\cdots \tag{A.17}$$

De factor $1.2815\cdots$ in vergelijking (A.17) is nodig om precies op de 10% koudste uit te komen in geval van een normale verdeling.

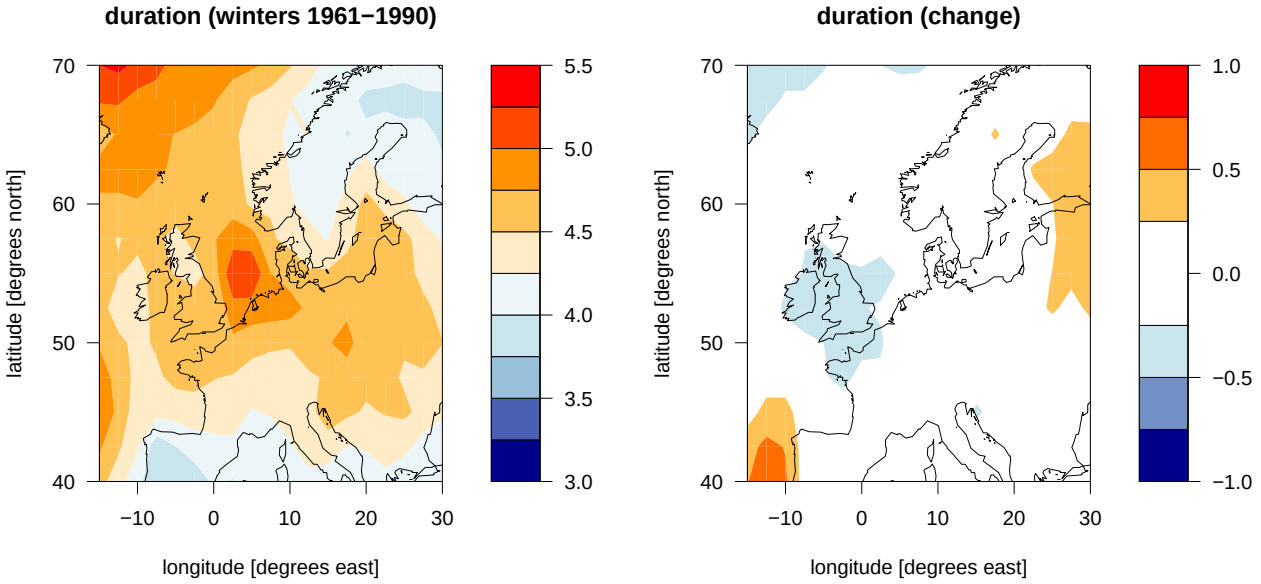

Figuur S7: Gemiddelde lengte van de koude periodes in Essence voor (links) winters 1961-1990 en (rechts) het verschil tussen de periode 2061-2090 en 1961-1990. Negatieve waardes betekenen een afname van de gemiddelde lengte. Als maat voor de bepaling van koude dagen diende vergelijking (A.17).

Resultaten

De vraag die we hier bestuderen is of de verdeling van de temperatuur anomalieën en koude dagen, gedefinieerd volgens vergelijking A.17, in de toekomst zullen veranderen. Voor het antwoord gebruiken we opnieuw de data van het Essence ensemble.

Allereerst vergelijken we de empirische cumulatieve distributie functie (ecdf) voor verschillende perioden uit Essence (Figuur S6 links). De ecdf geeft voor iedere x op de x-as de (empirisch bepaalde) kans dat de temperatuur lager is dan x (we delen simpelweg het aantal dagen waarop de temperatuur lager of gelijk aan x is door het totaal aantal dagen). Wat direct opvalt is dat het weinig verschil maakt welke periode we nemen, de lijnen vallen vrijwel over elkaar heen. Ook duidelijk is dat de ecdfs anders zijn dan die van een normale verdeling. Zo is is er de relatief overbevolkte koude kant ($x \leq -1$). Wat nog sterker opvalt is het systematisch ontbreken van extreem warme dagen waarbij $x > 0.75$, door de sterke invloed van zee.

Door de geordende temperatuur anomalieën van de ene periode tegen die van de andere uit te zetten, verkrijgen we een zogenaamde “quantile-quantile plot”(qqplot). Voor identieke verdelingen vallen de punten bij benadering op de lijn $y = x$. Figuur S6 (rechts) laat zien dat voor Essence de temperaturen over een groot gebied vrijwel hetzelfde verdeeld is.

Als laatste berekenen we de gemiddelde duur van de koudegolven, waarbij we verglijking (A.17) als definitie voor koude dagen hanteerden. De gemiddelde duur wordt bepaald door het totaal aantal koude dagen te delen door het totaal aantal koudegolven. Figuur S7 toont het resultaat voor de 1960-1999 periode van Essence als mede de geprojecteerde veranderingen in de toekomst. De gemiddelde lengte van een koudegolf varieert tussen 3 en 5 dagen. De geprojecteerde toekomstige veranderingen zijn erg klein. Voor grote delen van West en centraal Europa zijn de veranderingen kleiner dan 1/4 dag en mogelijk niet statistisch significant.

Conclusies

Wat vertellen de voorgaande resultaten ons? Ten eerste dat, althans volgens het Essence model hierboven beschreven, de statistiek van de koudegolven vrijwel niet wijzigt buiten een verandering van de klimaat parameters (gemiddelde en standaard afwijking). De dynamica die aanleiding geeft tot temperaturen in de linker staart van de temperatuur verdeling lijkt vrijwel ongevoelig voor veranderingen van het klimaat. Na herschaling blijken de geteste statistische relaties geldig voor zowel huidig als toekomstig klimaat. Verdere analyse laat zien dat ook

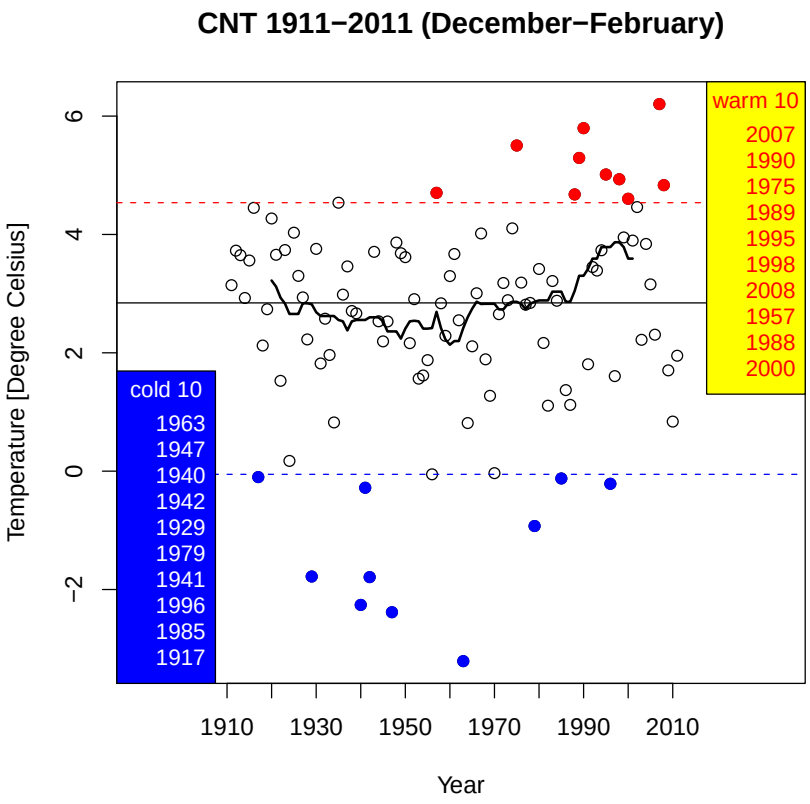

Figuur S8: Gemiddelde winter waarde voor CNT (Central Netherlands temperature, gemiddelde van een aantal meetstations waaronder De Bilt, Winterswijk en Eindhoven. Voor meer details, zie van Ulden et al (2009)). De horizontale lijnen geven het 10%, 50% (mediaan) en 90% niveau aan, berekend over de totale periode. Ook is de 20-jaars lopende mediaan weergegeven. De tabellen geven de top-10 koudste en warmste winters tussen 1911 en 2011. Data: bhlclim.knmi.nl.

de terugkeertijden voor koudegolven van bepaalde lengte niet of nauwelijks veranderen, noch de distributie van event-lengtes. Ook andere klimaatmodellen lijken een dergelijke invariantie te in grote lijnen te reproduceren (in de Vries et al (2012b) bestuderen we onder andere ook een subset van de modellen die hebben bijgedragen aan het 4e IPCC rapport). Als dergelijke schalingen ook geldig blijken voor de observationele records, betekent dit wellicht dat we meer over toekomstige kou kunnen leren door herschaling van huidige relaties. Als we de modellen vertrouwen, kunnen we ook een preciezere statistiek van koudegolven krijgen, door niet langer twee ver uit elkaar gelegen periodes op verschillen te bekijken, maar in plaats daarvan de gehele (anomalie) reeks te bestuderen.

De voorgaande conclusies nemen natuurlijk niet weg dat sneeuw- en ijspret in de toekomst minder zullen gaan worden, in ieder geval volgens de klimaatmodellen. Zoals al eerder gezegd hebben sneeuw en ijs niets te maken met relatieve kou, maar zijn zij gebonden aan vorst en temperaturen onder nul, een absolute maat voor kou. De waarnemingen lijken de trend die zichtbaar is in de modellen te ondersteunen (Figuur S8). Als voorbeeld dient de recente winter van 2009-2010. Deze werd gekenmerkt door een zeer lange periode waarin de atmosferische circulatie zich in een geblokkeerde toestand bevond. Een groot deel van Nederland kende een langdurig sneeuwdek en 'vrijwel iedereen' ervaarde de winter als een van de strengste van de eeuw. Desondanks komt de winter toch niet voor in de top tien van koudste winters van de afgelopen 100 jaar (Figuur S8, winter 2009-2010 staat op plaats 16). Het was de strengste sinds 1996, het jaar van de laatst verreden Friese Elfstedentocht, een winter dus met een herhalingstijd van ongeveer 15 jaar. Niet exceptioneel dus in absolute zin. Wel in relatieve zin, want voor veel kinderen betekende dit de eerste ervaring met langdurige sneeuw sinds hun jeugd. Een klassiek voorbeeld dus waarbij de perceptie (=relatieve gevoel voor kou) niet goed overeen kwam met de 'absolute' werkelijkheid.

F Weer (g)een Elfstedentocht

De recente koudegolf heeft ons niet koud gelaten. Tot teleurstelling van velen zat een 16e Elfstedentocht er niet in. Het ijs bleek op veel plaatsen net niet, of zelfs verre van dik genoeg. Wat heeft ons ditmaal de das omgedaan? Was het de temperatuur? Waren het de sneeuw, zon of wind? De milde december en januari misschien? Of toch klimaatverandering?

[6]Dat een aantal opeenvolgende ijsdagen nodig is om een minimaal 15 cm dikke ijslaag op de Elfstedenroute in Friesland te geven behoeft geen betoog. Zonder vorst geen ijs. Maar hoeveel kou was historisch gezien noodzakelijk? En hoe dik was daarbij het ijs?

Omdat er tot voor kort geen lange homogene reeks van de temperatuur in het noorden van het land was, heeft men traditioneel de temperatuur in De Bilt als uitgangspunt genomen. Voor de meeste locaties in Friesland blijkt er meestal een vrij lineaire relatie met de temperatuur in De Bilt te zijn. Om een maat te hebben voor de dikte van het ijs is gebruik gemaakt van het KNMI ijsmodel (de Bruin and Wessels, 1988). Dit model bepaalt de aangroei en afsmelting van ijs voor water van opgegeven diepte, op basis van lokaal beschikbare meteorologische gegevens (meestal wordt meetstation Eelde gebruikt voor Noord Nederland).

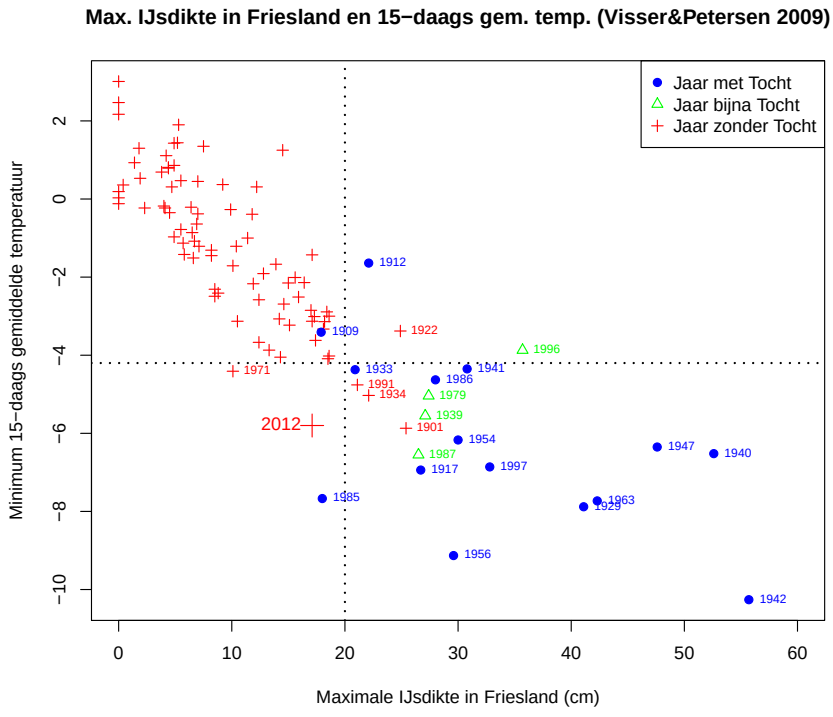

Figuur S9: Verband tussen 15-daags gemiddelde temperatuur in De Bilt en de ijsdikte in Friesland berekend via het KNMI ijsdikte model. Rode symbolen markeren "Zonder Tocht", groene "Bijna Tocht" (geschikte condities maar ongeschikte planning), en blauwe "Met Tocht". Bron data: (Visser and Petersen, 2009)

Gebruik makend van deze twee gegevens – de gemiddelde temperatuur in De Bilt en de berekende dikte van het ijs volgens het KNMI ijsmodel – hebben Visser and Petersen (2009) laten zien dat de Elfstedentocht meestal gehouden kon worden als het gedurende 15 dagen achtereen gemiddeld kouder was dan -4.2 °Cof als de gemiddelde ijsdikte volgens het KNMI ijsmodel meer dan 20cm was (Figuur S9). Twee keer vond de Tocht wel doorgang hoewel het ijsmodel een kleinere dikte aangaf. In 1909 werd de tocht door 23 (!) toerrijders verreden na slechts enkele dagen vorst en bij sterk dooiweer. In 1985 werd de Tocht in eerste instantie afgelast, maar kon na een tweede vorstperiode later die winter toch nog verreden worden (opnieuw dooiweer). In de afgelopen eeuw kwam het daarentegen ook vier keer (of zeven keer, indien men de "Bijna Tochten" mee rekent) voor dat de Tocht niet door ging ondanks dat het temperatuur-criterium gehaald werd. In slechts één van die vier gevallen (1971) gaf het model daarbij ook daadwerkelijk te weinig ijs.

[6]This appendix has appeared in *Meteorologica* (de Vries and van Westrhenen, 2012), and in modified form on the KNMI website `http://www.knmi.nl/cms/content/104925/weer_geen_elfstedenwinter`.

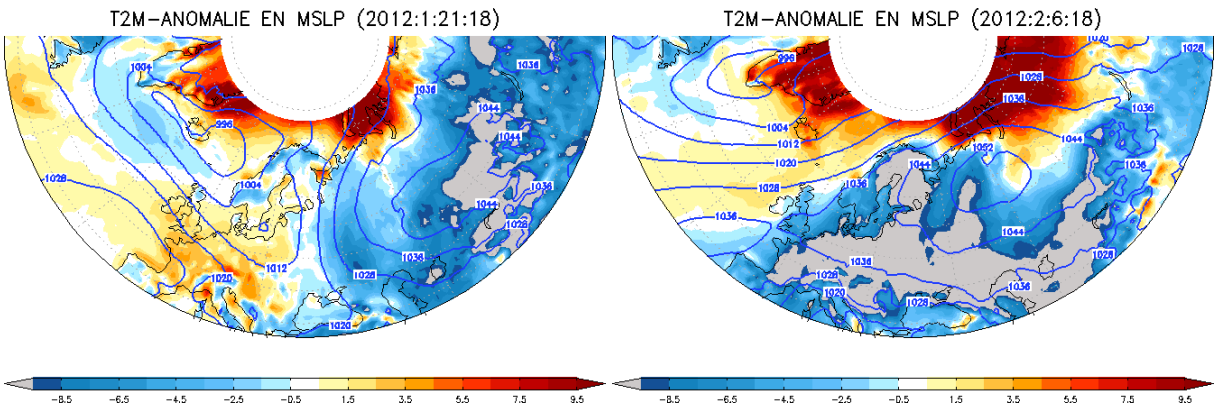

Figuur S10: 7-daags gemiddeld drukpatroon (lijnen) en temperatuur-anomalie ten opzicht van 1981-2010 winter-gemiddelde (kleuren), voorafgaand (links) en tijdens (rechts) de koudegolf van 2012. De aangegeven datum is het midden van de 7-daagse periode. Bron data: ECMWF.

Koudegolf 2012

De huidige vorm van de Tocht, een wedstrijd-race (paar honderd profs), en een toertocht (16.000 deelnemers) vereist een zeer stringent veiligheidsbeleid. Doorgang kan plaatsvinden als over de gehele route de waargenomen ijsdikte minimaal 15 cm is. Het is aannemelijk dat dit beleid voor de eerst georganiseerde, kleinschalige Elfstedentochten minder streng was. Met huidige massaliteit zou de Tocht van 1909 waarschijnlijk niet plaatsgevonden hebben. Er zijn voor de organisatie echter ook voordelen aan het leven in de 21e eeuw. De koudegolf werd ruim op tijd opgepikt door de weermodellen. Dit had tot gevolg dat gemalen en scheepvaart over de kanalen in Friesland stil gezet konden worden nog voordat de vorst het land had bereikt, om zo de eerste ijsdagen niet mis te lopen. Water-verontreiniging, nog een probleem in de jaren 70 en 80 van de vorige eeuw, speelde ook minder. Nederland was in rep en roer. Er werd alles op alles gezet om de Tocht te kunnen uitschrijven.

Het werd ook erg koud. Het Russisch hoog, dat zich gevormd had ver ten oosten van het Oeral gebergte verplaatste zich langzaam westwaarts en nam in sterkte toe. In zijn kielzog zette dit hoog een enorme hoeveelheid koude lucht op transport, met oorsprong ver vanuit Siberië. In de periode tussen 3 en 9 februari 2012 lag de temperatuur in grote delen van Europa meer dan 10 graden onder het klimatologisch gemiddelde (Figuur S10). Op hoge breedten was het juist meer dan 10 graden te warm. Dit is karakteristiek voor een dergelijk circulatie-patroon. De struktuur van het hoog (reusachtig, en zeer spatieel uitgestrekt), heeft grote overeenkomst met de patronen die in het verleden de koudste februari's hebben opgeleverd. In dat soort situaties bereikt de kou niet alleen vrijwel geheel Europa, maar vaak zelfs ook Noord Afrika.

In de koudegolf van 2012 was met een 15-daags gemiddelde van -5.8 ^{o}C van 29 januari tot 12 februari in De Bilt ruimschoots voldaan aan het temperatuur-criterium uit Visser and Petersen (2009). Het KNMI ijsmodel bleef echter steken op 17.1 cm, en kwam niet tot de 22-27 cm die we historisch gezien konden verwachten bij deze temperaturen (Figuur S9). Het ijs-criterium werd dus niet gehaald. Een Elfstedentocht bleek ook onmogelijk. Hierin zijn het ijsmodel en de realiteit dus consistent. Maar waarom wilde het ijs niet dikker worden in Friesland?

IJsgroei

Theoretisch verandert water in ijs bij 0 °C. En dus lijkt het eenvoudig een schatting te maken van de ijsdikte op basis van dag-gemiddelde temperatuur T_g: IJsaangroei bij $T_g < 0$°Cen afsmelt bij $T_g > 0$°C. In de Bruin and Wessels (1990) en de Bruin (2010) staan heldere beschrijvingen van de redenen waarom ijsgroei in de praktijk op sloten en meren toch niet altijd even makkelijk plaats vindt.

Ten eerste moet het water voldoende worden afgekoeld voordat sprake kan zijn van ijsvorming. Deze afkoeling vindt plaats door warmte-uitwisseling met de bovenliggende lucht. Omdat water bij 4 graden zijn maximale dichtheid bereikt, zal tot het punt dat de hele waterkolom 4 graden is, het water goed gemengd zijn (het zware water dat boven gevormd wordt zakt namelijk naar beneden). Pas als de temperatuur van de hele waterkolom 4 graden bedraagt zal de top-laag verder kunnen afkoelen. Dit verklaart onder meer waarom diepe meren later bevriezen dan ondiepe slootjes. De warmte-uitwisseling met de lucht zal sneller gaan als de temperatuur van de lucht lager is,

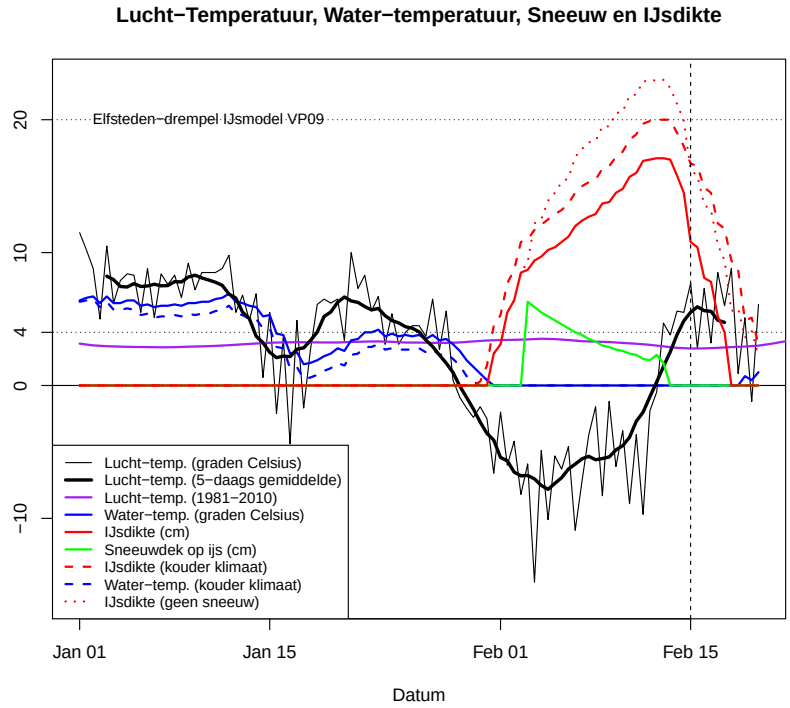

Figuur S11: De koudegolf van 2012 zoals gesimuleerd met het KNMI ijsmodel. De zwarte kartelige lijn is de geobserveerde 12-uurlijkse lucht-temperatuur, de dikke zwarte lijn het 5-daags gemiddelde terwijl de paarse lijn de 1981-2010 klimatologie weergeeft. Water-temperatuur is weergegeven in blauw, en ijsdikte in rood. De gestreepte rode lijn geeft de ijs-dikte aan in de simulatie van een kouder klimaat (en blauw gestreept de erbij behorende water-temperatuur). De gestippelde rode lijn toon de ijs-dikte voor een simulatie zonder sneeuw. Zie tevens de legenda. Data: KNMI.

of als het waait. Wind is dus goed om een groot meer sneller af te koelen. Maar als het water eenmaal 4 graden is en de toplaag verder afkoelt door verdere warmteafgifte, vertraagt wind verdere ijsvorming. De door wind veroorzaakte wervelingen in het water zorgen voor menging van de koude toplaag met het diepere water. Dergelijke door wind veroorzaakte wervelingen in het water zorgen ook voor de bekende windwakken. Als er eenmaal een aaneengesloten ijsdek ligt kan de wind de ijsgroei weer versterken.

Ten tweede, als eenmaal een ijslaag gevormd is, zal het ijs zijn verdere groei (naar beneden, dieper het water in) steeds meer gaan belemmeren. De warmteafgifte kan nog steeds alleen via de lucht plaatsvinden, en dus moet de stollingswarmte die vrijkomt bij de ijsvorming zich eerst door het ijs heen bewegen, alvorens aan de lucht te kunnen worden afgegeven. Het ijs groeit dus steeds langzamer aan. Een ruwe maat voor de ijsdikte is dat deze (bij gelijkblijvende weersomstandigheden) met de wortel van de tijd toeneemt. Een sneeuwdek, zeker als de sneeuw recent gevallen is, werkt hierbij als een sterk isolerende deken. Hoewel temperaturen vlak boven de sneeuw zeer snel kunnen afnemen (en dit de gemiddelde temperatuur op thermometer hoogte sterk kan beïnvloeden), zal het vormende ijs nog meer moeite hebben om zijn warmte af te staan. Als de sneeuw langer ligt en inklinkt, neemt deze isolerende eigenschap weer enigszins af.

Als laatste noemen we hier de rol van straling. Zonnestraling speelt een belangrijke rol, zeker in februari als de dagen weer langer worden. De instraling van de zon overdag zorgt voor opwarming van (met name) het zwarte ijs. Een dun sneeuwdek kan dan (door zijn hoge reflectie eigenschappen) weer compenserend werken. Overdag hebben we bij vriezend weer dus meer aan wat bewolking. ‘s Nachts juist weer niet, want wolken voorkomen de afkoeling door uitstraling. Overhangende bomen zullen door IR-straling ook de ijsgroei kunnen belemmeren (o.a., probleem bij de Luts, in Friesland). Kortom een subtiele balans van factoren.

Sneeuw, zon, en een warme start

Al deze factoren speelden in het verloop van de koudegolf van 2012 een rol. De koudegolf van 2012 werd voorafgegaan door een zeer milde start van de winter. Een maat voor de kou in een winter is het Hellmann getal. Het Hellmann getal verkrijgt men door etmaal-gemiddelde temperaturen onder nul bij elkaar op te tellen met weglating van het minteken. Tot de vorst-inval stond het Hellmann getal op 0,1. Voor een gemiddelde winter staat dit getal eind januari rond de 30-40 (Figuur S12). Het is dus aannemelijk dat de ijsvorming in het begin werd geremd omdat het water simpelweg nog te warm was. “Mijn vijver had drie dagen nodig om dicht te vriezen”, aldus Harry Geurts van het KNMI. Figuur S11 bevestigt dat de temperatuur van de meren hoger was dan normaal. Temperaturen (zwarte lijnen) voorafgaand aan de ijsperiode waren flink hoger dan het langjarig gemiddelde (paarse lijn). Het ijs begon

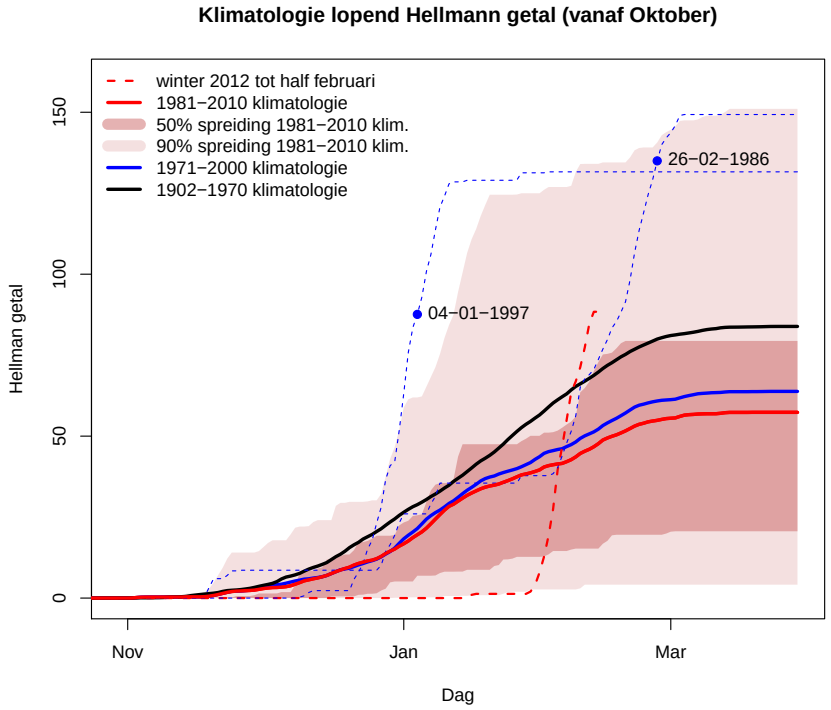

Figuur S12: Klimatologie van lopend Hellmann getal voor De Bilt, met daarin opgenomen tevens de stand van de huidige winter 2012, en de Elfstedenwinters 1986 en 1997 (de stip geeft de datum van de Tocht). In de winter van 1997 lag er geen sneeuw. Hellmann getal gemeten vanaf 1 oktober. Bron data: KNMI.

pas te groeien na twee ijsdagen. Daarnaast speelde de zon een belangrijke rol. De eerste 10 dagen van februari 2012 behoren tot de zonnigste van de afgelopen 100 jaar. Volgens Henk de Bruin, die aan de wieg stond van het KNMI ijsgroeimodel krijg je dan ijssmelt van onderaf. “Het zonlicht gaat door het ijs en warmt het water op”. De zon droeg zeer waarschijnlijk dus ook bij aan de belemmering van de ijsgroei.

En toen kwam er sneeuw. Net toen de eerste centimeters ijs gevormd waren, kwam er een zwak front over en viel er ongeveer 6 centimeter sneeuw. Deze sneeuw-depressie (met kerndruk 1033 hPa, vrij exceptioneel) ontstond doordat zeer koude lucht via een uitloper van het Siberisch hoog over een relatief warme Oostzee stroomde (Oostzee meer dan 2.5 graden warmer dan 1981-2010 gemiddelde in Januari 2012), en daarna verder intensiveerde over de eveneens voor de tijd van het jaar veel te warme Noordzee. De sneeuw viel op een erg ongunstig moment, namelijk juist in de periode dat het ijs de potentie had om het snelst te groeien. In Figuur S11 zien we direct respons: de groeisnelheid van het ijs neemt sterk af, ondanks de zeer lage temperaturen. De temperatuur was zo laag dat de sneeuw zeer poederig bleef. Poederige sneeuw isoleert beter dan plaksneeuw door de grote hoeveelheid lucht die erin zit opgesloten. Als de sneeuw later in de ijs-periode was gevallen, had wellicht sneller of zelfs direct actie ondernomen kunnen worden om deze van het ijs te vegen. De sneeuw matigde wel de invloed van opwarming door de zon. De invloed van de sneeuw op de temperatuur boven het sneeuwdek was substantieel. Extreem lage temperaturen kwamen voor vlak boven het oppervlak. De 5-daags gemiddelde temperatuur bereikte dan ook reeds rond 5 februari een minimum, terwijl de ijsdikte toen nog gering was.

Zonder sneeuw, of in een koeler klimaat wel een Tocht?

Het KNMI ijsmodel biedt de mogelijkheid de invloed van deze factoren te onderzoeken door de ijsdikte te berekenen in een (experimentele) omgeving waarin sommige er van uitgeschakeld zijn. We hebben twee situaties getest. Als eerste een situatie waarin alle meteorologische condities dezelfde waren, maar de sneeuw werd weggelaten. Als we dit doen komen we uit op 23cm ijsdikte (Figuur S11 (p56)). Gegeven figuur S9 (p54) zou het dan vrijwel zeker mogelijk geweest zijn een Elfstedentocht te laten plaatsvinden. We moeten hierbij opmerken dat dit “no-snow” scenario de ijsgroei vermoedelijk overschat, omdat sneeuw, zoals reeds opgemerkt, een behoorlijke impact heeft op de temperatuur. De temperaturen zouden zonder de sneeuw zeker in de nacht enkele graden hoger zijn geweest, waardoor de ijsgroei minder snel zou hebben plaats gevonden.

Een historisch sneeuwvrij precedent met vergelijkbare temperaturen is beschikbaar. Op 4 januari 1997 werd de 15e Elfstedentocht verreden onder koude, maar sneeuwvrije condities. Vergelijken we de opbouw van het Hellmann getal in 2012 met dat in 1997 (Figuur S12 (p57)) dan zien we dat de koudegolf van 2012 (qua temperatuur verloop)

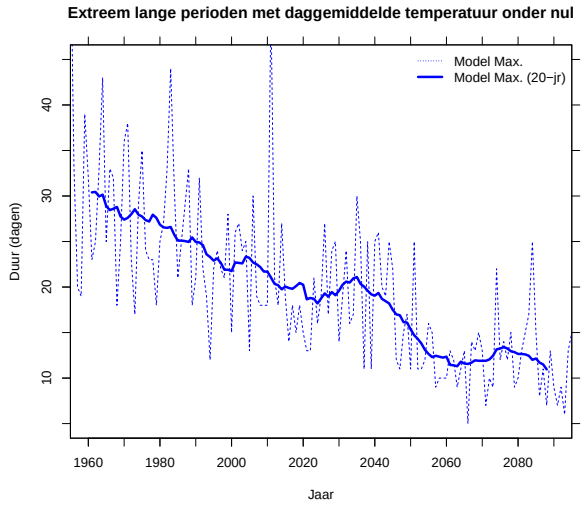

Figuur S13: De lengte van de langste aaneengesloten perioden met dag-gemiddelde temperaturen onder nul, gesimuleerd met het Essence klimaat model. Voor ieder jaar is de lengte genomen van de langste periode opgetreden in alle 17 ensemble leden. Bron data: KNMI.

erg vergelijkbaar moet zijn geweest met die van 1997. Vijftien jaar geleden hield de kou echter langer aan en bleef het ook na de Elfstedentocht nog vriezen. Bij eenzelfde Hellmann getal (80-90) maar zonder sneeuw lukte het die winter dus wel...In een tweede simulatie hebben we met het KNMI ijsmodel een simulatie gemaakt voor een historisch klimaat waar de gemiddelde temperatuur 1,5 graad lager lag dan de huidige, maar waarbij we wel de sneeuw, de zon en de andere meteorologische condities hetzelfde hebben gelaten. Nederland is sinds 1950 zo'n 1,5 graad opgewarmd (Kattenberg et al, 2008) en er zijn geen aanwijzingen dat de trend in de winter anders was dan in de rest van het jaar. Dit is een conservatieve schatting omdat koudegolven sterker opwarmen dan het gemiddelde onder invloed van de sterkere opwarming van Siberië (de Vries, 2011a; de Vries et al, 2012b). In dat geval wordt een maximale ijsdikte van 20cm bereikt (Fig. S11). Ook dat is een twijfelgeval: net wel of niet een Tocht.

Conclusie en blik op de toekomst

Ondanks zeer lage 15-daags gemiddelde temperaturen, en maximale inzet van rayonhoofden, technische hoogstandjes (zoals ijs-transplantaties) en honderden enthousiaste vrijwilligers, heeft de koudegolf van 2012 niet voldoende ijsdikte opgeleverd om een 16e Elfstedentocht mogelijk te maken. De 17.1 cm die het KNMI ijsmodel simuleerde (voor water van 2-meter diepte) was ook historisch gezien vrijwel nooit genoeg voor een Elfstedentocht. Sneeuwval vrij kort na het dichtvriezen van de meren heeft een belangrijke rol gespeeld in het afremmen van de ijsgroei, zo laat het KNMI ijsmodel zien. Tevens heeft de warme periode voorafgaand aan de koudegolf ertoe bijgedragen dat het twee ijsdagen duurde voordat het eerste ijs zich vormde. Simulaties met het KNMI ijsmodel laten tevens zien dat in een historisch, kouder klimaat (gemiddelde afkoeling van 1.5 graden), mogelijk een dikte van 20cm gehaald was. Dit bevestigt eerdere berekeningen van het KNMI dat de kans op een Elfstedentocht door de opwarming van de aarde (en dus ook Nederland) kleiner is geworden (Brandsma, 2001). Of een Elfstedentocht onder die koudere condities verreden had kunnen worden, is onduidelijk. Een simulatie zonder sneeuw geeft zelfs een maximale ijsdikte van 23cm, maar deze ijsdikte is vermoedelijk te optimistisch omdat zonder sneeuw de temperaturen ook hoger geweest zouden zijn. Toch lijkt het er op dat de sneeuw ons de das heeft omgedaan, aangezien in 1997 onder sneeuwvrije condities bij eenzelfde Hellmann getal wel een Tocht verreden kon worden.

Tot slot, ook in een opwarmend klimaat zullen koudegolven vooralsnog blijven voorkomen. De effecten van mondiale opwarming op de koudegolven hier zullen echter substantieel zijn. De opwarming zal namelijk niet overal hetzelfde zijn. Het vaste land en de hogere breedtegraden warmen sneller op dan lagere breedtegraden en gebieden nabij zee. In Nederland zijn wij afhankelijk van de koude lucht vanuit Siberië. Omdat de opwarming daar sneller gaat heeft dit een dubbel effect bij ons: de koudegolven worden korter en minder koud dan verwacht kan worden op basis van een simpele verschuiving van de gemiddelde temperatuur alleen (de Vries et al, 2012b). Een voorbeeld is gegeven in figuur S13. Deze toont per winter de lengte van de langste aaneengesloten periode met daggemiddelde temperaturen onder nul (in Nederland), gesimuleerd met het Essence klimaatmodel (Sterl et al, 2008). Ondanks dat de duur drastisch afneemt, blijven lange perioden met temperaturen onder nul tot het eind van deze eeuw gewoon mogelijk.

G Less snow on future cold days

Large parts of western and central Europe face a 20-50% future reduction in snowfall on Hellmann days (days with daily-mean temperatures below freezing). This strong reduction occurs in addition to the expected 75% decrease of the number of Hellmann days. The result is insensitive to the exact freezing-level threshold, but is in sharp contrast with the winter daily precipitation, which increases under most global warming scenarios. Observational records also reveal that probabilities for precipitation on Hellmann days have been larger in the past. The future reduction is a consequence of the freezing-level threshold becoming a more extreme quantile of the temperature distribution in the future. Only certain circulation types can reach these quantiles, and it is shown that these have intrinsically low precipitation probability

[7]Global climate simulations almost invariably show warming trends in the future (e.g. Klein Tank et al, 2005). In Europe, winters are expected not only to become milder, they will also become wetter, with extreme precipitation intensities becoming increasingly likely (Frei et al, 2006; Pall et al, 2006; Lenderink and van Meijgaard, 2008; Kew et al, 2011; van Haren et al, 2012). One of the basic physical arguments to explain the increase of precipitation, is related to the fact that warmer air can contain more moisture (O'Gorman and Schneider, 2009). Therefore, one may be inclined to think that, in a warming climate the amount of precipitation on cold days will likely also be increasing, despite the decrease of the number of such (cold) days. However, that this does not need to be the case, may become clear through the following argument.

Temperature advection is a dominant source of temperature variability (e.g. de Vries et al, 2012b). This means that in the current climate only certain circulation types can produce days with daily-mean temperature below freezing in western Europe. Such days are referred to as Hellmann days. However, as a consequence of the spatially non-uniform pattern of global warming (Joshi et al, 2008), only a subset of these current-climate cold-circulation types will still be able to result in such days in the future. These circulation types, however, have low probability for generating precipitation, either due to the proximity of a blocking high pressure system, or due to dry easterly winds (Trigo et al, 2004). In addition, the frequencies and structure of these circulation patterns may also change as a result of climate change.

In de Vries et al (2012a) we show how it can be physically consistent (and can even be expected) that precipitation on Hellmann days will decrease in the future, while the temperature during such days typically increases on average. Here we only show the basic result, the reduction of snowfall on Hellmann days, as simulated with the climate models.

Data and methodology

Climate-model output is used from the Essence project (Sterl et al, 2008). The Essence dataset is a 17-member ensemble of 150-year integrations obtained with one climate model (ECHAM5/MPI-OM) for the period 1950-2100, assuming the SRES A1b emissions scenario beyond the year 2000. The members were generated by perturbing the initial state of the atmosphere. In addition, a subset of the CMIP3 archive (Meehl et al, 2007) is used in a multi-model comparison.

Although the basic results are shown for western and central Europe, much of the subsequent detailed analysis is carried out for a smaller region. This region is referred to as the target area (TA) and is bounded by 5-10E and 50-55N. Observational data is used from the ECA-database (Haylock et al, 2008). From the ECA-data set we have used the time series of De Bilt (Netherlands), which is close to the TA. The TA consists of multiple grid boxes. Therefore, one has to decide whether to perform the field-averaging before or after the other statistical operations. Because we will use composite and cluster analysis techniques, for which the timing of events is important, it has been decided to perform the field-averaging first. In the discussion of the results we will comment on the differences that might arise from taking the other route (field averaging after statistical operations).

A Hellmann day is defined as a day in which the daily-mean temperature (Tg) falls below freezing level. More details on methodology are given in the relevant sections.

[7]This is a small section of the paper de Vries et al (2012a) that has been submitted to *Climate Dynamics*.

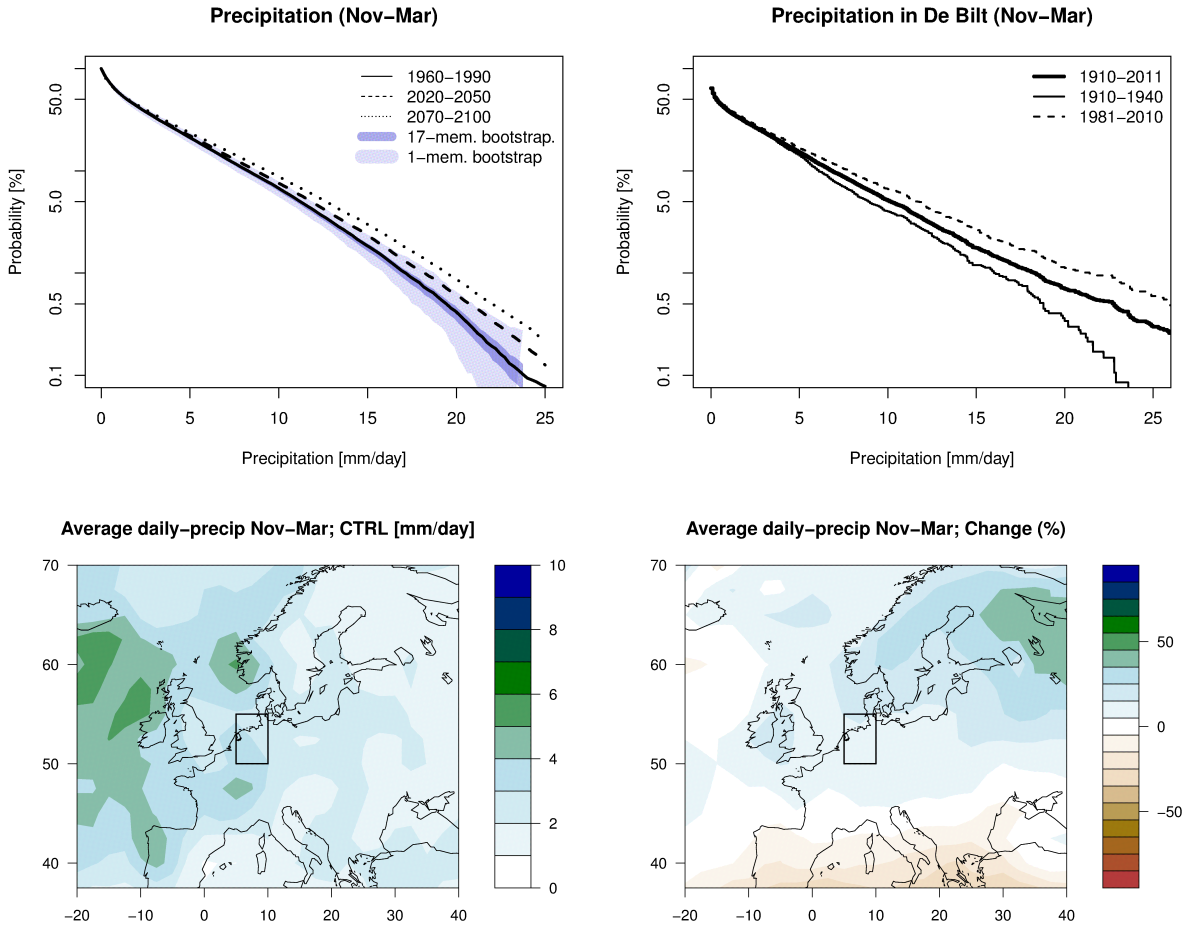

Figure S14: (top left) Winter (Nov-Mar) daily precipitation probabilities over the target area in the climate model. Shaded areas indicate 95% confidence intervals, estimated by a 10-day block bootstrapping of the 1960-1990 period. (top right) for ECA-data from De Bilt (Netherlands). (bottom row) Daily-mean precipitation on winter days (Nov-Mar) in the climate model and future change (bottom right). Control period: 1960-1990. Future period: 2070-2100. Target area is indicated by a box. Taken from de Vries et al (2012a).

Climatology

Figure S14 (top left panel) shows the cumulative density function (cdf) for TA-averaged daily precipitation for three periods. The cdf can be interpreted as the probability to get at least x mm of precipitation on a winter day. The result is well known and shows that the future probability increases for all precipitation amounts. Moreover, the increase is stronger at larger precipitation rates, with extremes becoming 2-3 times more likely than today near the end of 21st century. Confidence estimates (shading) are obtained using a 10-day block-bootstrap method with different ensemble sizes (light shading indicates a equivalent size of 1 member, dark shading an equivalent size of 17 members). The confidence intervals widen at larger precipitation rates, yet virtually rule out the possibility of a no-change scenario.

Similar results are obtained if one first obtains the cdf for each grid box, and performs the field average afterward. However, because of the localized nature of intense precipitation, the field-averaged cdf will decrease less rapidly than the cdf of the TA-averaged precipitation.

The top right panel displays the precipitation probabilities for the observations of De Bilt (Netherlands). The winter precipitation has gradually increased, with extremes in the 1981-2010 period becoming more likely than in the beginning of the 20st century. Note that the shapes of the cdf of observations and climate model output are slightly different, with high precipitation rates being less likely in the latter. This bias is caused by the field-averaging used in the climate model output, as well by model limitations.

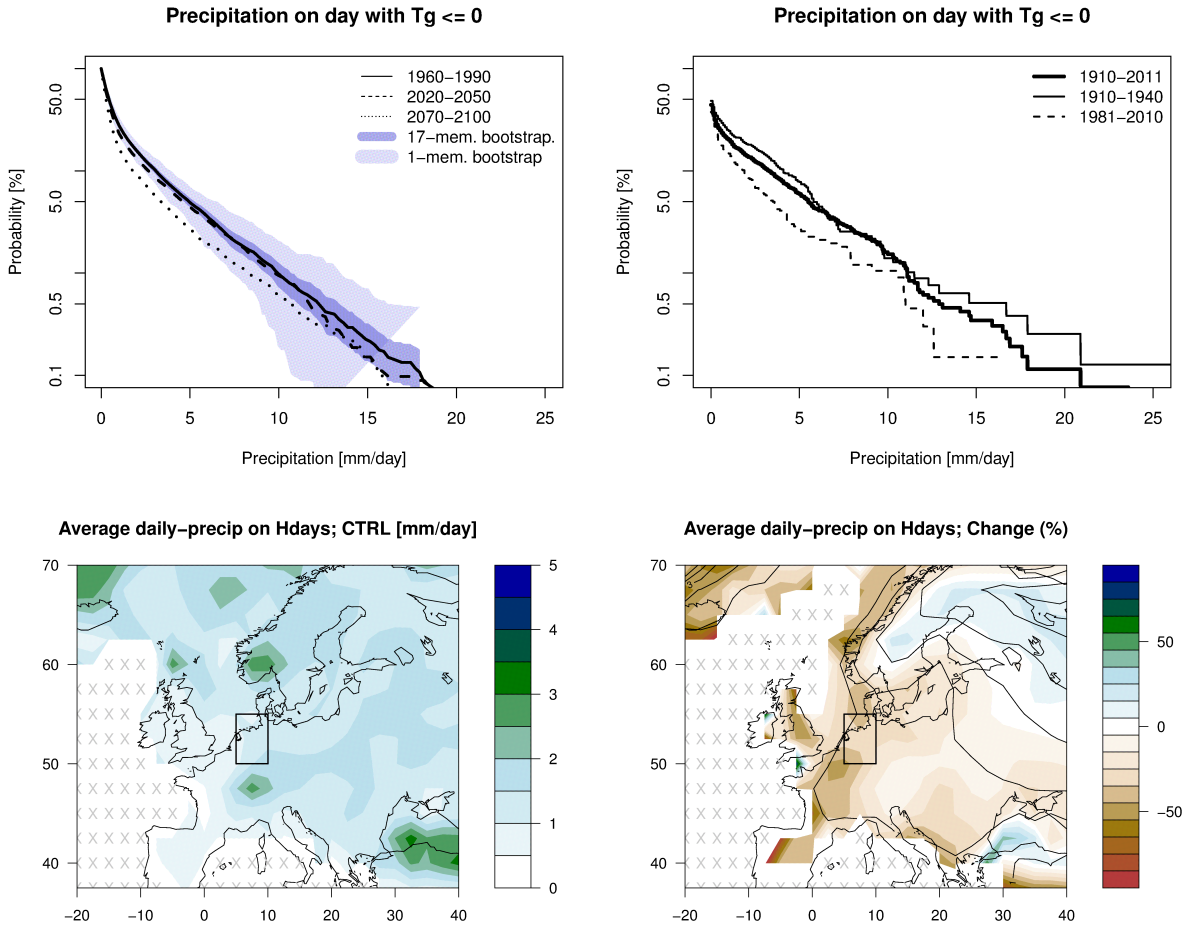

Figure S15: As in Figure S14, but for Hellmann days in the target area for the climate model (left) and in De Bilt for observations (right). (Bottom row) Average daily-mean precipitation on Hellmann days in winter (Nov-Mar) in the climate model and future change (bottom right). Note that shading levels are different compared to Fig. S14. The solid contours denote the increase of Hellmann-day temperature (contour interval 1 degree Celsius). Crosses denote grid boxes in which no Hellmann days occurred (in present-day or in the future period). Taken from de Vries et al (2012a).

These results – an increase of daily precipitation in future winters, and a stronger increase at the higher precipitation intensities – are consistent with many other studies (e.g. Kew et al, 2011). As a further illustration of the robustness for other areas in Essence, Fig. S14 (bottom row) displays the average daily precipitation on winter days and the future change. Most areas experience increases of daily-precipitation amounts.

Hellmann days

In contrast to the changes of the daily precipitation climatology, the probabilities for precipitation on Hellmann days decrease in the future (Fig. S15 (p61)). This is seen both in climate-model output (top left and bottom row) and in observations from De Bilt (top right). Thus, it is less likely to snow on Hellmann-days in the future, while for the Netherlands snow was more likely on such days in the past. In addition, of course, the number of such days also decreases significantly (Figure S16). Note that the coldest regions of Europe (Northeast Scandinavia and Siberia) experience an increase of Hellmann-day precipitation. However, in these areas the average winter temperature is well below freezing; accordingly, the Hellmann-day threshold leads to the selection of nearly all days, as a result of which the global-warming footprint becomes visible again (Fig.S14 (p60)). The region near the Black Sea appears to be exceptional but has not been studied in detail.

The results are robust: thresholds varying from -5°C to +5°C all give the same direction of change (i.e., decrease in future). Most of the models from the CMIP3 archive also display a decrease (Fig. S17), although the precise re-

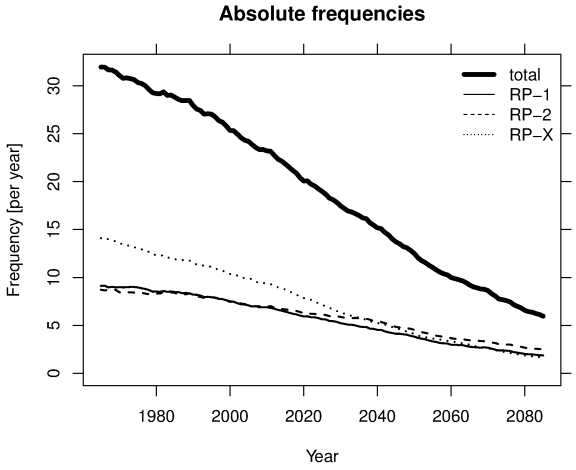

Figure S16: Frequency of Hellmann days in TA and number of days spent in each response pattern. Units: number of days per winter. Taken from de Vries et al (2012a).

duction varies and is generally strongest for the models that exhibit the largest increase of mean winter temperature. In the following sections, only Essence data is used to examine the details of the precipitation decreases.

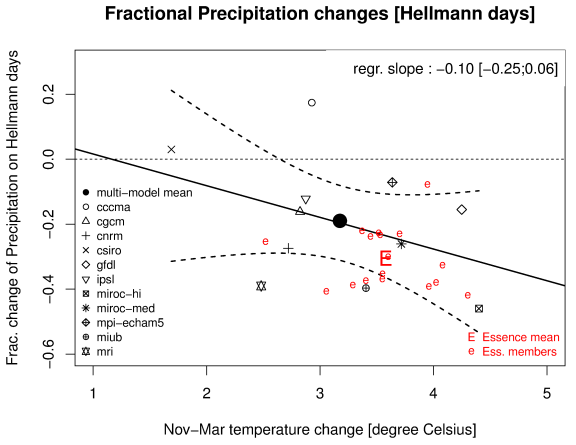

Figure S17: Scatter plot of Nov-Mar mean temperature change and fractional change of mean daily TA-precipitation on Hellmann days, obtained from several CMIP3 models. Future period: 2081-2100. Control: 1960-1990. From each model, one member has been used. The linear regression (solid line) as well a 95% confidence interval (dashed) are indicated. Note: In this figure we used the field-average after the computation. Taken from de Vries et al (2012a).

Further details on the reasons why the snowfall reduces in the future, can be found in the paper de Vries et al (2012a).

Acknowledgments

Writing a report that summarizes three years of research makes me feel a bit like writing a second PhD thesis. Of course, this report is not a thesis at all (it has never aimed to be such a thing) and neither is it concluded by a viva. Nevertheless some acknowledgments need to be made. Why not here?

Several people have contributed directly or indirectly to this project. Thanks, Rein and Wilco (KNMI), for valuable discussions and for keeping me on track. While many of my scientific wanderings in these years have not made it to this report finally, it seems we are getting out some papers as well. Unfortunately the project ends.

Thanks also to the people from GasTerra and NAM for listening to my presentations and reflecting on them. Without your support the project would not have taken place at all.

I am grateful for being part of KS-MK, the global climate division at KNMI. Nice staff, nice group, nice people. I do hope the future is bright for KNMI, despite the terrible start of the summer this year and the ban on wearing shorts.

Finally, thanks to Aline for continuous support and love, and to my two little heroes at home. Without the three of you life would have been a lot less amazing.

The research reported on in this study has been made possible by GasTerra and NAM.

Bibliography

van den Berge LA, Selten FM, Wiegerinck W, Duane GS (2011) A multi-model ensemble method that combines imperfect models through learning. Earth System Dynamics 2(1):161–177, DOI 10.5194/esd-2-161-2011

Brandsma T (2001) Hoeveel Elfstedentochten in de 21e eeuw? Zenit 28:194–197

Cattiaux J, Vautard R, Cassou C, Yiou P, Masson-Delmotte V, Codron F (2010) Winter 2010 in Europe: A cold extreme in a warming climate. Geophys Res Lett 37:L20,704, DOI 10.1029/2010GL044613

de Bruin H (2010) De natuurkunde van nederlandse ijspret. Nederlands Tijdschrift voor Natuurkunde pp 76–78

de Bruin H, Wessels H (1988) A model for the formation and melting of ice on surface waters. J Appl Meteorol 27:64–173

de Bruin H, Wessels H (1990) IJs in de Lage Landen. Zenit 17:437–444

Frei C, Schöll R, Fukutome S, Schmidli J, Vidale P (2006) Future change of precipitation extremes in Europe: intercomparison of scenarios from regional climate models. J Geophys Res 111:D06,105, DOI 10.1029/2005JD005965

van Haren R, van Oldenborgh GJ, Lenderink G, Collins M, Hazeleger W (2012) SST and circulation trend biases cause an underestimation of European precipitation trends. Clim Dyn DOI 10.1007/s00382-012-1401-5

Hawkins E, Sutton R (2009) The potential to narrow uncertainty in regional climate predictions. BAMS 90:10951107

Haylock M, Hofstra N, Klein Tank A, Klok E, Jones P, New M (2008) A european daily high-resolution gridded dataset of surface temperature and precipitation. J Geophys Res 113:D20,119, DOI 10.1029/2008JD10201

Holton JR (1979) An Introduction to Dynamic Meteorology, 2nd edn. Academic Press, Inc.

van den Hurk B, Klein Tank AMG, Lenderink G, et al (2006) KNMI Climate Change Scenarios 2006 for the Netherlands. Tech. rep., Koninklijk Nederlands Meteorologisch Instituut (KNMI)

Joshi MM, Gregory JM, Webb MJ, Sexton DMH, Johns TC (2008) Mechanisms for the land/sea warming contrast exhibited by simulations of climate change. J Clim 30:455–465

Kattenberg A, et al (2008) De Toestand van het Klimaat in Nederland. Tech. rep., KNMI, De Bilt, URL `http://www.knmi.nl/toestandklimaat`

Kew S, Selten F, Lenderink G, Hazeleger W (2011) Robust assessment of future changes in extreme precipitation over the rhine basin using a gcm. Hydrology and Earth System Sciences 15:1157–1166, DOI 10.5194/hess-15-1157-2011

Klein Tank AMG, Lenderink G (2009) Klimaatverandering in Nederland; Aanvullingen op de KNMI '06 scenario's. Tech. rep., KNMI, De Bilt

Klein Tank AMG, Können GP, Selten FM (2005) Signals of anthropogenic influence on european warming as seen in the trend patterns of daily temperature variance. Int J Climatol 25:1–16

Lenderink G, van Meijgaard E (2008) Increase in hourly precipitation extremes beyond expectations from temperature. Nat Geosci 1:511–514, DOI 10.1038/ngeo262

Lolkema J (2006) De Tocht der Tochten. De geschiedenis van de Elfstedentocht, 1749-2006. Steven Sterk

Lorenz EN (1963) Deterministic nonperiodic flow. J Atmos Sci 20:130–141

Masato G, Hoskins BJ, Woollings TJ (2011) Wave-breaking characteristics of midlatitude blocking. Quart J Roy Meteorol Soc DOI 10.1002/qj.990

Meehl GA, Covey C, Taylor KE, Delworth T, Stouffer RJ, Latif M, McAvaney B, Mitchell JFB (2007) The WCRP CMIP3 multimodel dataset: A new era in climate change research. Bull Amer Meteor Soc 88:1383–1394, DOI 10.1175/BAMS-88-9-1383

Meinshausen M, Smith S, Calvin K, Daniel J, Kainuma M, Lamarque JF, Matsumoto K, Montzka S, Raper S, Riahi K, Thomson A, Velders G, van Vuuren D (2011) The RCP greenhouse gas concentrations and their extensions from 1765 to 2300. Climatic Change 109:213–241, DOI 10.1007/s10584-011-0156-z, URL `http://dx.doi.org/10.1007/s10584-011-0156-z`

O'Gorman PA, Schneider T (2009) The physical basis for increases in precipitation extremes in simulations of 21st century climate change. Proc Natl Acad Sci USA 106:14,77314,777, DOI 10.1073/pnas.0907610106

van Oldenborgh GJ, Drijfhout S, van Ulden A, Haarsma R, Sterl A, Severijns C, Hazeleger W, Dijkstra H (2009) Western Europe is warming much faster than expected. Clim Past 5:1–12, DOI 10.5194/cp-5-1-2009

Pall P, Allen MR, Stone DA (2006) Testing the Clausius-Clapeyron constraint on changes in extreme precipitation under co2 warming. Clim Dyn 28:351363, DOI 10.1007/s00382-006-0180-2

Rex DR (1950) Blocking action in the middle troposphere and its effect upon regional climate. Tellus 2:169–211

Sterl A, Severijns C, Dijkstra et al H (2008) When can we expect extremely high surface temperatures? Geophys Res Lett 35:L14,703, DOI 10.1029/2008GL034071

Tibaldi S, Molteni F (1990) On the operational predictability of blocking. Tellus 42A:343–365, DOI 10.1034/j.1600-0870.1990.t01-2-00003.x

Trigo R, Trigo I, DaCamara C, Osborn TJ (2004) Climate impact of the European winter blocking episodes from the NCEP/NCAR Reanalysis. Clim Dyn 23:17–28, DOI 10.1007/s00382-004-0410-4

Uppala SM, Kallberg PW, Simmons et al AJ (2005) The ERA-40 Re-analysis. Quart J Roy Meteorol Soc 131:2961–2013, DOI 10.1256/qj.04.176

van Ulden A, van Oldenborgh GJ, van der Schrier G (2009) The construction of a central Netherlands temperature. Tech. Rep. WR 2009-03, KNMI

van Ulden AP, van Oldenborgh GJ (2006) Large-scale atmospheric circulation biases and changes in global climate model simulations and their importance for climate change in Central Europe. Atmos Chem Phys 6:863–881, DOI 10.5194/acp-6-863-2006

Visser H, Petersen A (2009) The likelihood of holding outdoor skating marathons in the Netherlands as a policy-relevant indicator of climate change. Climatic Change 93:39–54, DOI 10.1007/s10584-008-9498-6

von Storch H, Zwiers FW (2003) Statistical Analysis in Climate Research, 1st edn. Cambridge University Press

de Vries H (2007) Inzicht in opkomende depressies. Meteorologica 16:14–19

de Vries H (2011a) Cold winters and the relation to atmospheric blocking. Tech. Rep. TR324, KNMI, URL http://www.knmi.nl/bibliotheek/knmipubTR/TR324.pdf

de Vries H (2011b) Koudegolven van de toekomst. Meteorologica 20(4):20–23

de Vries H (2012a) On future western European winters, with applications to the energy sector. Tech. Rep. , to appear, KNMI

de Vries H (2012b) Winter temperatures in the Netherlands and Western Europe. Tech. Rep. , to appear, KNMI

de Vries H, van Westrhenen R (2012) Weer (g)een Elfstedentocht. Meteorologica 21(1):4–7

de Vries H, Haarsma RJ, Hazeleger W (2012a) On the future reduction of snowfall in western and central Europe. Clim Dyn in press:1–12, DOI 10.1007/s00382-012-1583-x

de Vries H, Haarsma RJ, Hazeleger W (2012b) Western European cold spells in current and future climate. Geophys Res Lett 39:L04,706, DOI 10.1029/2011GL050665

de Vries H, Woollings T, Haarsma RJ, Hazeleger W (2012c) Atmospheric blocking and its relation to jet changes in a future climate. Clim Dyn acc. minor revisions:–, DOI -

Weijenborg C, de Vries H, Haarsma RJ (2012) On the direction of Rossby wave breaking in blocking. Clim Dyn in press:1–9, DOI 10.1007/s00382-012-1332-1

Wever N (2008) Effectieve temperatuur en graaddagen: Klimatologie en klimaatscenario's

Wilks DS (2006) Statistical Methods in the Atmospheric Sciences, International Geophysics Series, vol 91, 2nd edn. Academic Press

Ybema K (2007) Wat een weer! Kroniek van het weer in Friesland, 1901-2006. Friese Pers Boekerij bv

A complete list of all KNMI-publications (1854 – present) can be found on our website

www.knmi.nl/knmi-library/knmipub_en.html

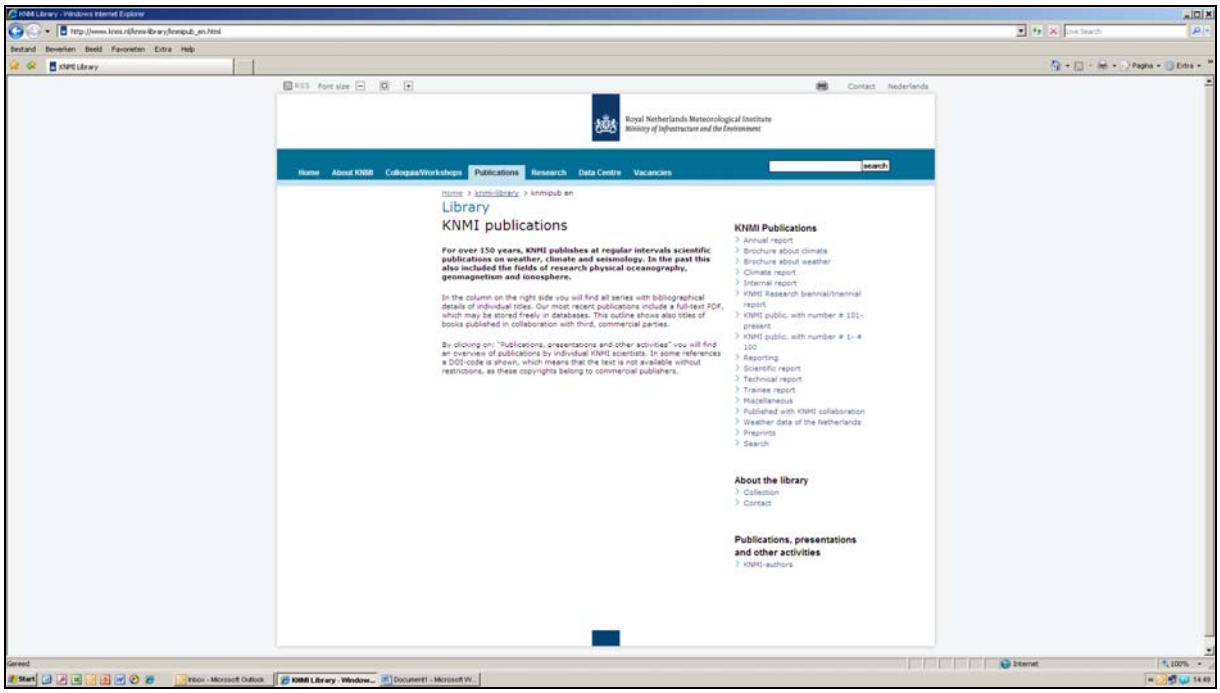

The most recent reports are available as a PDF on this site.